

Master Thesis

**Using chemical composition and grain size distribution of a palaeochannel-fill to identify Lower Rhine flood events and their origin in the catchment**

Jochem Ypma BSc

June 2014

Dept. Physical Geography  
Utrecht University

*Supervision:*

Dr. M. van der Perk

Dr. K.M. Cohen

Dr. W.H.J. Toonen

## **Abstract**

At this moment no long-term records are available that reveal the upstream origin of sediment deposited during flood events in the Rhine. Tracing flood deposits in the lower Rhine back to Rhine subcatchments would increase the ability to trace sources of pollution, of flood events, and to reconstruct geomorphological developments throughout the catchment. In this research a data set of fluvial deposits throughout the Rhine catchment was created, covering both the Lower Rhine, the Oberrhein and three main tributaries (Neckar, Main and Moselle rivers). The data set was built up by corings from the lower Rhine and its upstream subcatchments and surface samples from locations throughout the subcatchments. Grain size analysis was performed on these samples to identify flood events. A XRF scan was performed to obtain the chemical composition of the samples. Chemical composition data was used to investigate the distribution and propagation of trace elements. Grain size data and chemical composition data were combined to find a correlation between specific set of elements and grain size fractions. Based on data analysis combined with previous research, the Zr/Rb ratio was found to correlate with the sand fraction of the grain size data, and thus to act as a proxy for flood events. The Zr/Rb ratio was used to identify flood events in the chemical composition data, and to characterize the chemical composition of these flood events. The chemical composition of the corings and surface samples from the subcatchments were used to characterize the chemical composition of the subcatchments. Based on a combination of these characteristics an origin was suggested for some of the flood events. The 1671 and 1682 flood events are likely originate from the Oberrhein area. The 1726 and 1729 flood events are likely to originate from the Moselle area.

## List of figures

Figure 2-1 Overview of the study area.....	10
Figure 4-1 Overview of the Rhine River catchment .....	18
Figure 4-2 Location of coring site along the Lower Rhine: Bienener Altrhein (Bienen).....	19
Figure 4-3 Location of coring site along the Upper Rhine: Römerberg.....	20
Figure 4-4 Location of coring site along Neckar: Lauffen.....	21
Figure 4-5 Location of coring sites along Main: Sindlingen and Klein Krotzenburg.....	22
Figure 4-6 Location of coring site along Moselle: Kenn. ....	23
Figure 6-1 Depth plots of Bienener Altrhein core segments 3-10. ....	34
Figure 6-2 Basic correlation plots of Bienen 3.....	38
Figure 6-3 Basic correlation plots of Bienen 4.....	39
Figure 6-4 Basic correlation plots of Bienen 5.....	40
Figure 6-5 Basic correlation plots of Bienen 6.....	41
Figure 6-6 Basic correlation plots of Bienen 7.....	42
Figure 6-7 Basic correlation plots of Bienen 8.....	43
Figure 6-8 Basic correlation plots of Bienen 9.....	44
Figure 6-9 Basic correlation plots of Bienen 10.....	45
Figure 6-11 Correlation matrices for the Bienen cores.....	47
Figure 6-10 Graphs of the Zr and Rb counts. ....	48
Figure 6-12 Element occurrence versus Rhine kilometers.....	50

## List of Tables

Table 4-1 Overview of the sampling sites (corings) .....	25
Table 4-2 Overview of the sampling sites (surface samples) .....	25
Table 6-1 Correlation of extreme flood events. ....	36
Table 6-2 Correlation matrix for Bienen 3. Original and shifted data .....	38
Table 6-3 Correlation matrix for Bienen 4.....	39
Table 6-4 Correlation matrix for Bienen 5. Original, shifted and upper part data.....	40
Table 6-5 Correlation matrix for Bienen 6.....	41
Table 6-6 Correlation matrix for Bienen 7.....	42
Table 6-7 Correlation matrix for Bienen 8. Original and shifted data.....	43
Table 6-8 Correlation matrix for Bienen 9.....	44
Table 6-9 Correlation matrix for Bienen 10.....	45
Table 6-10 Correlation coefficients of AI with grain size (clay) classes. ....	48
Table 6-11 Occurrences of trace elements in subcatchments .....	51
Table 6-12 Selection of flood events.....	52
Table 6-13 Chemical composition of selected flood events.. ....	53
Table 6-14 Occurrence of trace elements in flood events .....	53

## List of appendices

Appendix 1 (A-H) Raw data from grain size and XRF scans (sorted by segment) .....	63
Appendix 2 Normalized counts of selected elements.....	63
Appendix 3 Sampling locations .....	63
Appendix 4 Handheld XRF elemental counts .....	63
Appendix 5 Normalized and standardized data for subcatchment cores.....	63
Appendix 6 AI standardization Bienen Cores .....	63
Appendix 7 Flood event data .....	63
Appendix 8 Correlation of grain size with Zr/Rb ratio (Bienen) .....	63
Appendix 9 Correlation of grain size with Zr/Rb ratio (Subcatchments) .....	63
Appendix 10 Standardized elemental data Bienen.....	63
Appendix 11 XRF settings.....	63
Appendix 12 Geological map of the Rhine catchment.....	64
Appendix 13 Distributive regions of the Rhine catchment .....	65

## Table of contents

Abstract .....	2
1. Introduction .....	7
2. Study area .....	10
2.1. The Rhine River .....	10
2.2. Lower Rhine .....	11
2.3. Subcatchments .....	11
3. Factors controlling sediment deposition and composition in the Rhine River .....	14
3.1. Flood events .....	14
3.2. Sediment deposition .....	14
3.3. Sediment composition .....	16
4. Fieldwork and core collection .....	17
4.1. Site selection .....	17
4.2. Sampling sites .....	18
4.3. Sample collection .....	23
5. Laboratory methods and data analysis .....	26
5.1. Laboratory methods .....	26
5.2. Data Analysis .....	29
6. Results and discussion .....	34
6.1. Identification of flood events .....	34
6.2. Correlating grain size and chemical composition data .....	37
6.3. Correction of clay content .....	47
6.4. Fingerprinting upstream catchments .....	49
6.5. Tracing flood origin .....	52
7. Conclusions and recommendations .....	55
Acknowledgements .....	58
References .....	59
Appendices .....	63

## 1. Introduction

Discharge records of the Rhine River in the Netherlands and upstream locations go back to 1900 A.D. and before. Descriptions of recent flooding (Disse & Engel, 2001) and historical records (e.g. Buisman, 2000) indicate that the origin of lower Rhine floods is highly variable, with both the High Rhine and the Middle Rhine producing peak discharges. For flood risk assessments it is important to understand the origin of flood pulses, generated throughout the catchment, because this would increase the ability to identify important regions for pollution. It has been suggested that floods in catchments affected by pollution result in the remobilization of contaminated sediment (Foulds et al., 2014). This poses a significant threat for ecology and agriculture along the floodplains. By analyzing (post-industrial revolution) deposits in up- and downstream locations along the Rhine River, pollution propagation throughout the catchment can be monitored, sources of pollution can be traced, and subsequently measures can be taken. Allocating the origin of floods is also of great social importance; resulting information can be used to research flood genesis and source areas in past and present situations. This information can be used to develop a system that predicts the peak discharge of flood events in the Lower Rhine. Moreover these data can be used to determine the most beneficial location to construction local flood reservoirs to intercept peak discharges in both downstream and upstream parts of the catchment. Besides of the above-mentioned applications, the unraveling of the origin of palaeo-floods can also be used; in the reconstruction of (long term) geomorphologic developments, research in flood sensitivity to changing land use, climate research, and in (more accurate) flood risk predictions.

A complex set of factors, including upstream geology, a large-scale catchment, varying flood parameters (discharge, duration) and floodplain storage, determine the chemical composition of flood deposits deposited along the Lower Rhine. The Upper Rhine from the Alpine region, and three main tributaries to the Middle Rhine, the Neckar, Main and Moselle Rivers, mainly determine the chemical composition of sediment transported and deposited by the downstream Rhine River. The relative discharge and sediment contribution of these tributaries during a flood event is thought to determine the chemical composition of the sediments deposited during the same flood event in the Lower Rhine region. Middelkoop (1997; 2002) found that there is a close relation between the amount of sediment transported and deposited, and the discharge and duration of a flood event; the higher the discharge, the more sediment can be transported. Previous research also indicates that the variation in grain size of flood event deposits can be used to identify single flood event layers (Middelkoop et al., 2010; Toonen et al., 2012). Other studies have correlated Lower Rhine flood event layers with historical flood events by making use of historical records (e.g. Winkels, 2011;

Aloserij, 2013; Toonen, 2013). Previous research conclude that chemical composition data can be used to acquire grain size information (e.g. Dypvyk and Harris, 2001). The use of such a geochemical proxy in small scale catchments has shown that the chemical composition of flood layers can be used to trace the upstream origin of sediment by making use of the characteristic chemical composition of tributary rivers (E.g. Passmore and Macklin, 1994; Jones et al., 2009). The same methods have, at this moment not been tested in large river systems with a complex catchment configuration and with considerable mixing of sediments (also with temporarily stored floodplain deposits (e.g. Erkens, 2009)), which may complicate traditional fingerprinting of upstream catchments. No study has yet combined these approaches and applied these on a large catchment, such as that of the Rhine River.

The main goal of this study is to find out whether we can use the relation between the grain size and the chemical composition of floodplain deposits to identify flood events and to trace Lower Rhine River flood events back to upstream Rhine subcatchments. The first objective of this study is the creation of an inventory of flood deposits found in cores from upstream and downstream locations in the Rhine catchment. To enable a catchment-wide correlation, flooding events need to be identified in a sedimentary sequence (and dated) throughout the catchment by performing grain analysis (Winkels, 2011; Aloserij, 2013; Toonen, 2013). The next objective is to find a chemical proxy that can be used to link grain size data with chemical composition data, and subsequently to identify flood events within the chemical composition data (Walling, 2005; Macklin et al., 2006). This chemical proxy will also be used to find a method to correct for the clay content in the flood deposits. The latter is needed to enable a catchment-wide comparison of cores. The next objective involves the construction of a series of fingerprints of each of the subcatchments, and a characterization of a series of flood events. Eventually, the aim is to unravel the contribution (quantitative or qualitative) of each of the subcatchment to the selected flood events.

To achieve our main goal, the following research questions are specified:

- Can flood events be identified in grain size data and chemical composition data?
- Can chemical composition data be corrected for clay content?
- Can a characteristic fingerprint be set up for individual Rhine subcatchments?
- Can the above-mentioned fingerprints be used to trace the (mixed) origin of Lower Rhine flood events?



To answer these questions we applied a series of sedimentary and statistical approaches. First an overview of the study area and its hydrologic background is provided in chapter 2. Here the local settings of the source areas are also described. Chapter 3 describes the processes that occur from the source area towards the deposition of sediment in the floodplains along the Lower Rhine. The local settings of flood depositions also are described here. Chapter 4 describes the process of core selection and present the sampling sites. Samples were collected from suitable locations in both the Lower Rhine (sedimentary sink) and the upstream subcatchments (sedimentary sources). Chapter 5 describes laboratory and analytical methods. Grain size distributions of flood layers and chemical composition data were analyzed and compared to distinguish flood layers and correlate these throughout the Rhine catchment. The latter involved a series of research steps, of which (preliminary) results are provided in the appendices.

## 2. Study area

### 2.1. The Rhine River

The Rhine River originates in the Swiss Alps where its headwaters confluence, at Lake Constance these form the Alpine Rhine or High Rhine (Fig 2-1). After the joining of the river Aare and crossing the Swiss-German national border, it is named the Upper Rhine. further downstream, the Rhine River confluent with several tributaries, of which the Neckar (at Mannheim) and the Main (at Mainz) are the most important (Fig. 2-1). In central Germany the Middle Rhine flows through the Rhenish Massif (Schiefergebirge) which is characterized by a narrow bed-rock canyon. At Koblenz the Middle Rhine is joined by the Moselle River. Downstream from Bonn the Rhine River is named the Lower Rhine. The apex of the Rhine delta is roughly located at the Dutch-German national border. A few kilometres downstream, the Rhine River splits into the Waal River and the Pannerdens Kanaal, Nederrijn, and Lek branches. At Arnhem, another distributary, the IJssel River, splits from the Nederrijn River (Fig. 2-1).

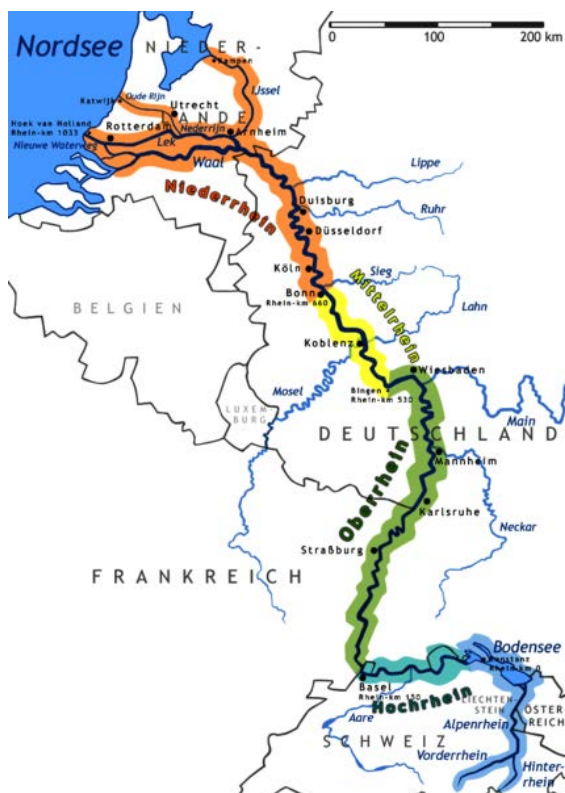


**Figure 2-1 Overview of the study area.**

Map of the course of the River Rhine, from the Swiss Alps to the North Sea. In blue the High Rhine (Hochrhein, including the Alpine Rhine), in green the Upper Rhine (Upper Rhine), in yellow the Middle Rhine (Mittelrhein), and in orange the Lower Rhine (Niederrhein) and deltaic distributaries.

The Rhine River drains approximately 185000 km<sup>2</sup> of NW-Europe and its main river channel stretches ~1320 km (Middelkoop, 1997). Its hydrological regime varies from glacial in the upstream, to pluvial in the downstream parts of the catchment. At the Lower Rhine the mean annual discharge is 2200 m<sup>3</sup>/s. Most floodplains are inundated when discharge exceeds 6000 – 7000 m<sup>3</sup>/s while largest measured floods occurred in 1926 A.D. and 1995 A.D. with discharges of ~12000 m<sup>3</sup>/s (Middelkoop, 1997). Most peak discharges occur between December and April as a results of extensive snow melt and increased precipitation. Highest magnitudes of flood discharges in the Lower Rhine occur when flood pulses from the main tributaries enter the Rhine River simultaneously.

## *2.2. Lower Rhine*

During the Holocene the Lower Rhine developed a meandering course. During the last ~3000 years the Lower Rhine has been transformed into the Rhine delta apex (Berendsen and Stouthamer, 2001). Throughout the Holocene several phases of fluvial activities have resulted in palaeo-channels and meander cut-offs of varying ages. These slack-water environments are located at lower lying areas in embanked floodplains and are characterized high sedimentation rates. Moreover, some dike breach ponds and cut-off channels are currently being filled in.

## *2.3. Subcatchments*

### *Upper Rhine*

In this report we use the name Upper Rhine for the part of the Rhine River upstream from the confluence with the Neckar. Main tributaries confluencing downstream from this point to form the Rhine River include the Neckar, Main and Moselle rivers (Figure 2-1). A large canalization project took place just after the start of the industrial revolution, during the period between 1820 and 1860 (Beeger, 1990; Herget et al, 2005).

The geology of the Upper Rhine region is characterized by the Jurassic source rocks of the Aare and Birs rivers and other tributaries in Switzerland. Both the Aare and the Birs provinces (Appendix 212) are formed by minerals from the Molasse foreland basin (Oligocenen/Miocene) and the Alps. Characterizing minerals are garnet, epidote (silicate of aluminium, iron and calcium), hornblende, staurolite and Rhine-alterites (Van Andel. 1958). The Black Forest-Vosges province, geologically characterized as granite and crystalline schists (Appendix 12) has several mineral associations of which the principles are garnet and hornblende. Furthermore, some typical minerals like augite, sillimanite and barite are found, these are derived from the rocks of the Black Forest (Eocene) and the Vosges mountains (Eocene).

### *Neckar*

The Neckar drains a watershed of about 14.000 km<sup>2</sup> of South-west Germany. It originates in the Black Forest, in the Swabian scarplands. Nearby the city of Mannheim the Neckar conflues with the Upper Rhine (428 km). From here on downstream it is called the Rhine River. In the upstream part, south of Stuttgart, the drainage area of the Neckar is densely populated and highly industrialized. Then, after passing Stuttgart it meanders through a landscape built up of Triassic and Pleistocene limestones; an area built up of carbonates (Hantke, 1993). More mineral associations from the Neckar backland are monazite (phosphate mineral containing rare earth metals), from Bohemia, garnet (Triassic) and tourmalite, zirconium silicates and rutile (titanium), from the Bunter sandstone (Triassic) of the Zorn province (13) (Van Andel, 1950). Moreover, minerals from the volcanic rocks are also found in the south-eastern part of the Neckar catchment.

In 1976 Abadian and Lippman studied heavy metals in the Upper Neckar river to determine the amount of industrial pollution. XRF analysis was used to detect elements and corresponding minerals. The occurrence of brushite was said to be a mineralogical indicator of pollution. Phosphate, one of the components of brushite, is used in fertilizers, detergents, industrial waste waters and more (Abadian, 1976). Moreover, an important industrial signal can be found back in the abundance of Cadmium. Due to the metal working industry along the tributary Enz river, high amounts of Cadmium were emitted and deposited along the Neckar. Cadmium is bound with fine grained sediment. These heavy metals emissions depleted after the 1970's (Gerbersdorf et al, 2005).

### *Main*

The Main conflues with the Rhine River near the city of Mainz (497 km). It originates from the German state of Bavaria, and before it meets the Rhine River, it flows through the industrial zone of Frankfurt am Main. The backland of the Main resembles that of the Neckar. It is also built up from Triassic and Pleistocene limestones. Specific mineral associations are monazite, garnet, tourmalite, zirconium silicates and rutile (titanium) from the Bunter sandstone (Triassic) of the Zorn province (Appendix 213) (Van Andel, 1950). In the Main region there might also be found some minerals from the eastern part of the catchment, these include augite, titanite (including rare earth metals), clinozoisite (calcium and aluminium) and (basaltic) hornblende (Van Andel 1950). These are all derived from the Bohemian, Keuper (Triassic) and Rhaetic (Triassic) massifs (Appendix 12). Moreover, aeolian deposits (loess) is found in this area which will be reflected in the chemical composition signal of the sediment coming from the Main river (Van Andel, 1950). Besides of that, there is the Staurolite province (Appendix 13), which supplies the Rhine and the Main with staurolites, derived from Mayence Basin (Oligocene).

### *Moselle*

In contrast to the other tributaries, the Moselle originates in the area west of the Upper Rhine. It confluences with the Rhine River nearby Koblenz (592 km). The Moselle originates in a Tertiary and Mesozoic carbonate area, and flows through crystalline and Palaeozoic rocks in the Vosges, where it encounters garnet, blue-green and brown hornblende (Van Andel, 1950). After that it flows through the Eifel and Hunsrück (Appendix 12) where it encounters quaternary volcanic rocks of the Rhenish Massif (Volcanic province, Appendix 13). This results in a signal of specific elements originating from volcanic minerals including augite, basaltic hornblende and titanite (Edel & Fluck, 1989; Van Andel, 1950). In the downstream part of the Moselle River, it is extremely incised into the Rhenish massive. As a result, the floodplains are small and narrow and there are no Holocene cut-off-meanders.

### 3. Factors controlling sediment deposition and composition in the Rhine River

#### 3.1. Flood events

Patterns of flooding of the Rhine River have been documented throughout the Holocene and through historical records for the past 500-100 years (Brázdil et al., 1999). The last severe floods occurred in December 1993 and January 1995, at these moments the discharge increased up to  $\sim 12000 \text{ m}^3/\text{s}$ . Only in 1926 a higher discharge ( $\sim 12600 \text{ m}^3/\text{s}$ ) has been recorded. From the 1950s onward hydraulic modelling has resulted in a design discharge with a recurrence interval of 1/1250 years. Whereas this design discharge was initially forecasted at  $15000 \text{ m}^3/\text{s}$  for the 1990s, this number has been adapted to  $16800 \text{ m}^3/\text{s}$  for the year 2100 (Silva et al., 2001). This forecast of rare events (1/1250 years) is based on a record of only 100 years. Recent research has focused on extending the discharge data set of the Lower Rhine, based on historical and sedimentary information, in order to assess current flood risk (Toonen, 2013). Contributing research mainly includes the construction of a discharge data set throughout the Rhine river catchment. Multiple analytical approaches can consequently be used to identify flood events and their characteristics.

#### 3.2. Sediment deposition

During flood events, sediment, which mainly consists of silt and clay, is deposited in the floodplain areas. Depositional processes during and after flood events are influenced by both upstream and local factors. Upstream factors include flood characteristics, including differences in flood magnitude and frequency, and the characteristics of the suspended sediment in a flood, including differences in composition, grain size, and heavy metal concentration, and are strongly interrelated (Thonon, 2006). The latter are described in section 3.3.

##### *Upstream factors*

The sediment yield of a large river as the Rhine River is controlled by several factors. First, it depends on the amount of weathering and soil erosion that takes place in the hinterland. The Rhine River catchment has different erosion characteristics in forest areas, hills with loess, and agricultural areas (for example covered with vineyards). Several models can be used to determine the amount of soil erosion (Asselman, 1997). Another factor is the sediment delivery ratio (SDR), which is the ratio between the amount of transported and eroded soil at the outlet of the catchment. Second, a large part of the flood deposits along the Lower Rhine originates from locally reworked floodplain sediment that has been eroded by lateral fluvial migration; especially bed load sediments are not transported through the entire system during a single flood event (Hoffmann et al, 2007). Moreover, the SDR varies per season, in the summer it is lower, due to the increases surface roughness by crops. In the winter there is low soil cover but the transport capacity also decreases (Walling, 1990;

Asselman, 1997). The third main factor influencing flood characteristics is climate. Climate (change) controls the probability of the duration and frequency of floods (the flooding regime). Processes such as (de)forestation, changing agriculture, and other changes in land use influence the upstream sediment supply (Hoffmann et al. 2007).

Moreover, recent river basin management projects, rehabilitation of floodplains, construction of secondary channels, and restoration projects have changed the flooding regime of the Rhine River (Herget et al. 2005; Lammersen et al., 2002; Vorogushyn and Merz, 2012). In the Upper Rhine a large canalization project took place in between 1820 and 1860, when the Count of Tulla designed a plan to improve the navigability by straightening meanders (Beeger, 1990). Recent projects try to improve the water storage capacity of the river, by giving the river more space in times of high discharges, in order to prevent downstream floods (Lammersen et al., 2002; Herget et al., 2005).

#### *Local factors*

On a local scale, the amount of sediment that is deposited and the sedimentary pattern in the floodplains is controlled by two factors; floodplain topography and flood magnitude. Floodplain topography includes (natural) elevation differences and variations in the width of the floodplain. The topography of the floodplain is important as (averaged over multiple floods of varying magnitude) the amount of sand and coarse silt decreases with increasing distance to the river channel, while the content of clay and attached organic matter is relative constant with distance (Middelkoop, 1997). Therefore it is easier to identify an extreme flood event as a rare spike of coarser material at a distal floodplain than at proximal floodplain locations. The magnitude of the flood determines both the total sedimentation and the spatial pattern of deposition. The total deposition increases with flood magnitude. However, this increase is stronger for sand; minor floods are dominated by larger accumulation of fine sediment in lower areas and depressions while major floods are dominated by sand deposits, at least close to the channel (Middelkoop, 1997).

Dike-breach ponds and cut-off meanders within the embanked floodplains are natural traps for sediment during floods; meters of sediment can accumulate at such locations (Middelkoop, 1997; Toonen et al., 2012). Especially in lower lying regions (at slackwater conditions) detailed sequences of sediment record are deposited (Middelkoop, 2000; Thonon, 2006). Deposited sediments in local aquatic environments in the floodplains are generally laminated; deposition during successive floods builds up a sequence of layers with varying coarseness. Previous research concluded that the coarseness of suspended sediment that is transported, increases in the case of a higher discharge (Middelkoop, 1997; Toonen, 2013). Depending on flood magnitude (discharge), flood duration and the amount of sediment that is available, lamination and thickness of the deposits varies between

several mm's to several cm's. The lamination is not regularly annual, but depends on the occurrence of floods roughly exceeding bank-full discharge (Middelkoop, 2011).

### *3.3. Sediment composition*

Once deposited in the floodplains, sediment (especially in the clay fraction) acts as a transport agent for contaminants, nutrients and organic material. This role of fine-grained sediment is due to the binding ability of clay minerals, that allows contaminants to chemically attach to minerals. This way contaminants can be transported to lower river reaches to be deposited in the floodplains. The amount of heavy metals that is deposited depends on the amount of sediment that is deposited and therefore an important influence is the sediment yield. Furthermore the amount of heavy metals depends on the sources and inputs of heavy metals. Heavy metals can be spread in the dissolved phase, as aerosols or attached to soil particles (Vink et al., 1999; Vink & Behrendt, 2002). A distinction between natural and anthropogenic sources can be made when background concentrations can be distinguished. This is done using the information that urban areas are the main contributors of heavy metals and that the attribution of these areas has declined over the past few decades.

Concentrations of elements and ratios of elements can be measured in order to retrieve a chemical fingerprint (Peart & Walling, 1986; Walling & Woodward, 1992; Støren et al, 2010). The chemical composition of the sediment depends on the source area of the suspended load. Each of the tributaries has a geologically and industrially distinct source area and therefore the sediment from the different sub-catchments has a varying chemical composition (Van Andel, 1950; Vink & Behrendt, 2002).

Disturbing factors, such as natural processes (Middelkoop, 2000; Thonon, 2006) and human activity (Herget et al, 2005) need to be taken into account. A range of chemical and physical processes controls the variation in metal pattern in floodplain deposits (Peart and Walling, 1986; Passmore and Macklin, 1994; Vink et al., 1999; Thonon 2006). Horizontal processes including (changes in) local floodplain topography, floodplain storage, and flow velocity can influence the chemical composition of surface samples. Besides of these horizontal processes, vertical processes can influence the chemical composition of the corings. The latter include hydraulic sorting (re-suspension), metal enrichment and biological activities. An important aspect concerning the chemical composition of sediment from the youngest centuries to millennia is pollution. The basin of the Rhine is densely populated and in the last 300 years has become heavily industrialized with the Ruhr district and agglomerations as Frankfurt am Main, Stuttgart, Mannheim and Nuremberg. Change in the use of land and the environment have their impact on the emission of heavy metals, besides of that the transport of sediment is also affected by these industrialization factors (Thonon, 2006).



## 4. Fieldwork and core collection

### 4.1. Site selection

In this study, a core from the Bienener Althrein (along the Lower Rhine), from now on called the Bienen coring, was obtained to reconstruct a detailed record of the flood events along the Lower Rhine. This core is considered the sink of all upstream eroded material. To perform analysis on source areas, subsequently two types of data were needed from all the locations in the subcatchments. At first, for each of the subcatchments a (pre-industrial) record was needed of the local flood deposits; these were obtained by performing a coring (4.1.1). To obtain a post-industrial record for the tributaries, we also needed at least one surface sample from each of the subcatchments (4.1.2).

#### 4.1.1. Cores

The cores on which this study is based were collected both from locations along the Lower Rhine, and from its upstream tributaries. As we want to perform a high resolution comparison, a location was needed that has a constant and rather stable deposition rate. To minimize the impact of grain size fluctuations caused by a varying distance to an active channel, we look for a site that is close a channel with an low migration rate. While selecting the locations of our coring sites, we need to keep in mind these needs to be able to obtain cores with a representative, high resolution, record of the local fluvial deposits. Slack-water environments seem to be the ideal locations for the coring locations along the lower Rhine and its main tributaries. Due to high sedimentation rates, cores collected in slack-water environments are assumed to have a high temporal resolution (Middelkoop, 1997). Another advantage of slack water environments is that they are currently being filled in. The latter is important to be able to make a comparison between recent fill-in the lower Rhine and the sub-catchments, as deposition rates can be calibrated (Middelkoop, 2000). An additional advantage of dike-breach ponds is that the formation date of a pond can often be obtained from historical data.

Suitable locations were selected using palaeogeographic maps (Toonen, 2013), geological maps, historical maps, Google Maps and detailed elevation models (AHN, Rijkswaterstaat, 2005). Residual channels are visible on maps as longitudinal depressions in the landscape, due to relative strong compaction of clay and peat in comparison with coarser clastic materials (Berendsen and Stouthamer, 2001). Historical maps were used to give insight in possible dike breach locations, channel diversions, canalization projects and natural displacements of river systems. The latter was used to check the lateral stability of the channel system; a channel with a low migration rate was needed to best represent the spectrum of grain size classes. In our search for coring locations we avoided areas where sedimentation was disturbed by human activities such as agricultural and industrial activities. Moreover, core samples were inspected visually for identification of bioturbation

and soil-forming processes as these could affect the chemical composition of the sediment (Middelkoop, 2000).

#### 4.1.2. Surface samples

Locations of post-industrial sample sites were determined in the field. Prerequisites for these sites included that the material samples was deposited by recent fluvial floods, and that these deposits had not been affected by any external factor with a possible influence on its chemical composition. We thus took care of pollution from industrial activities (waste, cooling water), pollution from external (natural) sources (other attributing rivers, land run-off), agricultural land use, and digging activities (commercial, recreation).

#### 4.2. Sampling sites

In this subchapter sampling sites (cores and surface samples) are presented. An overview of the catchment of the Rhine River including its tributaries sampling locations is found in Figure 4-1.



**Figure 4-1 Overview of the Rhine River catchment**

An overview of the Rhine River, its tributaries (blue) and some major adjacent cities (black) and regions (green). In red are the locations along the main tributaries from which the cores were taken. After Google maps 2011.

#### 4.2.1. Lower Rhine

Close to the Dutch-German border, in between the German towns of Emmerich am Rhein and Xanten, the small town of Bienen is located. Northeast of the present-day path of the Rhine River, two cut-off meanders are located in the subsoil. The Bienener Altrhein, the oldest, has been active from the 14<sup>th</sup> century A.D. until the Rhine River shifted its course in Western direction (Toonen, 2013). This is when the other palaeochannel, the Grietherother Altrhein, became active (16<sup>th</sup> century A.D.). The latter remained active until it was artificially cut-off in the 18<sup>th</sup> century A.D. Due to its proximity to the main channel, the Bienener Altrhein palaeochannel was periodically flood with fluvial sediment from the Rhine River. In the last few centuries, a continuous record of fluvial deposits has been built up in the Bienener Altrhein palaeochannel. A coring was performed at the Bienener Altrhein site (Winkels, 2011; Toonen, 2013).



**Figure 4-2 Location of coring site along the Lower Rhine: Bienener Altrhein (Bienen)**

*Exact location of site Bienener Altrhein (Bienen), Germany. Including present path and palaeochannels of the Rhine River. Source: Google Maps 2011. After Winkels, 2011; Aloserij, 201.*

#### 4.2.2. Tributaries

##### *Upper Rhine*

##### *Pre-industrial*

In the area around Speyer we noticed several cut-off meanders on the map (Figure 4-3). These are of different generations; first there is current Rhine channel, subsequently a first generation meander cut-offs caused by the canalization project, and then a second generation, that have been incised twice, by two new Rhine channel generations. These abandoned meander bends could be dated (relatively) using spatial cross-relations (Berendsen & Stouthamer, 2001). The second generation cut-offs originate from before the canalization project, these meander cut-offs were found at the villages

of Mechtersheim and Binshof, south and north of Speyer. We performed a coring nearby the town of Mechtersheim (Figure 4-3), this location will be referred to as Römerberg.

*Post-industrial*

Near the village of Römerberg, a recent cut-off meander is located. This has been filled up after the canalization project and therefore we took recent deposits from this location. Sampling sites along the Upper Rhine were located at 465 km, 515 km, 613 km and 655 km along the Rhine River. Exact locations of sampling sites are found in Table 3-2 and Appendix 3.

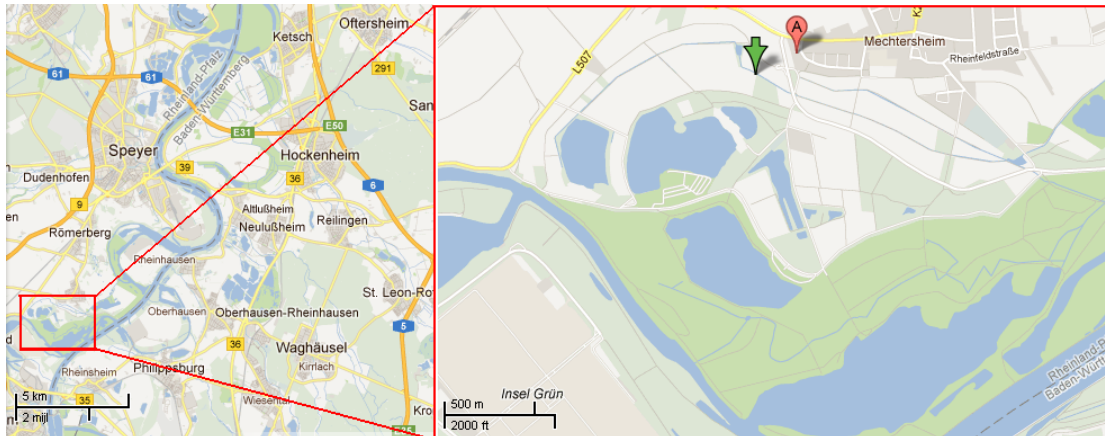


**Figure 4-3 Location of coring site along the Upper Rhine: Römerberg.**

Exact location (green arrow), Mechtersheim, Römerberg, Speyer, Germany. GPS position: N49 15 49.0 E8 23 12.2. After Google Maps 2011.

*Neckar*

*Pre-industrial*

Just to the south of the city of Heilbronn, close to the village of Lauffen am Neckar, a cut-off meander is visible on the map (Figure 4-4). This has been dated to be a Holocene cut-off, which has thus been filled in with floodplain sediment for approximately 6000 years (Hantke, 1993). At this location we performed a coring which can be used to establish a pre-industrial chemical composition signal.

*Post-industrial*

South of the location mentioned above, we found our coring location of recent deposits. Near the village of Kirchheim a river channel straightening project in the early 19<sup>th</sup> century took place. After the straightening the cut-off meanders have been filled up with material. From these post-industrial channel fills on the floodplains the post-industrial samples were collected. Sampling sites along the Neckar were located at 311 km, 410 km, and 418 km equivalent to the Rhine River. Exact locations of sampling sites are found in Table 4-2 and Appendix 3.

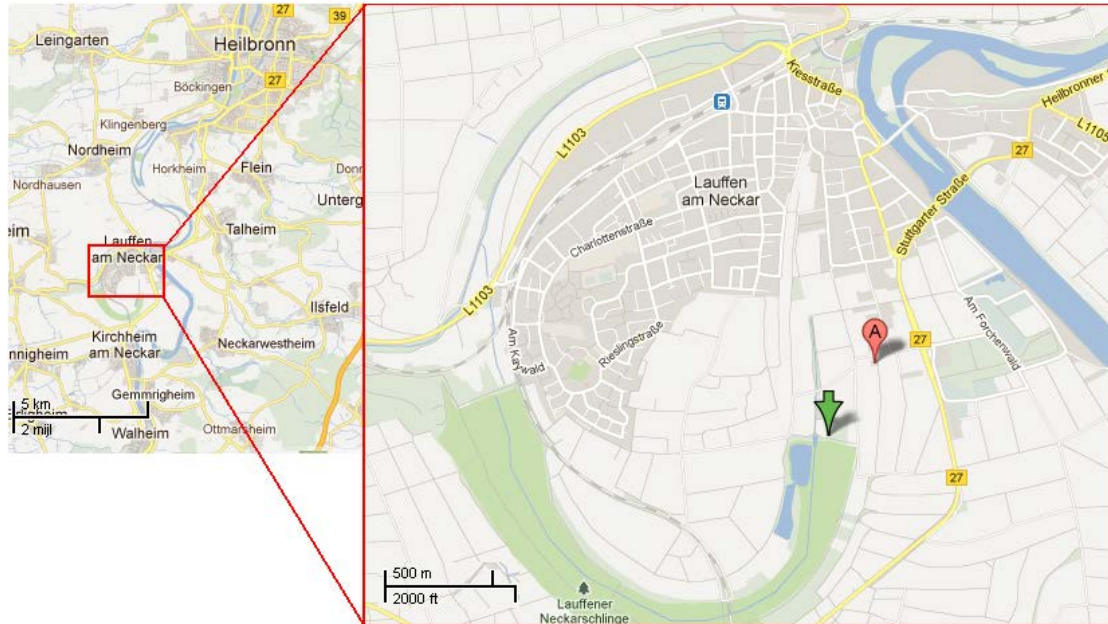


**Figure 4-4 Location of coring site along Neckar: Lauffen.**

Exact location (green arrow), Lauffen am Neckar, Heilbronn, Germany. GPS position: N49 03 45.0 E9 09 10.5. After Google Maps 2011.

*Main*

*Pre-industrial*

As the area around Frankfurt am Main is heavily industrialized, no pre-industrial floodplain deposits were found close to Frankfurt am Main. Therefore, a location had to be found upstream of the industrialized area. Around 50 km upstream of Frankfurt am Main, south of the city of Hanau, we found a palaeo meander (Figure 4-5). The meander shifted to the East, leaving behind remnants of the old meander, which are still visible in the form of a little stream near the village of Klein Krotzenburg. We also found a suitable location west of Frankfurt am Main, Sindlingen, close to Kelsterbach (Figure 4-5).

### *Post-industrial*

On the other side of the Main, nearby the village of Kelsterbach (close to the Rhine-Main Airport) we have found suitable locations to collect post-industrial samples. These were taken from a location parallel to the river stream along an old river channel. Sampling sites along the Main were located at 433 km and 476 km equivalent to the Rhine River. Exact locations of sampling sites are found in Table 4-2 and Appendix 3.

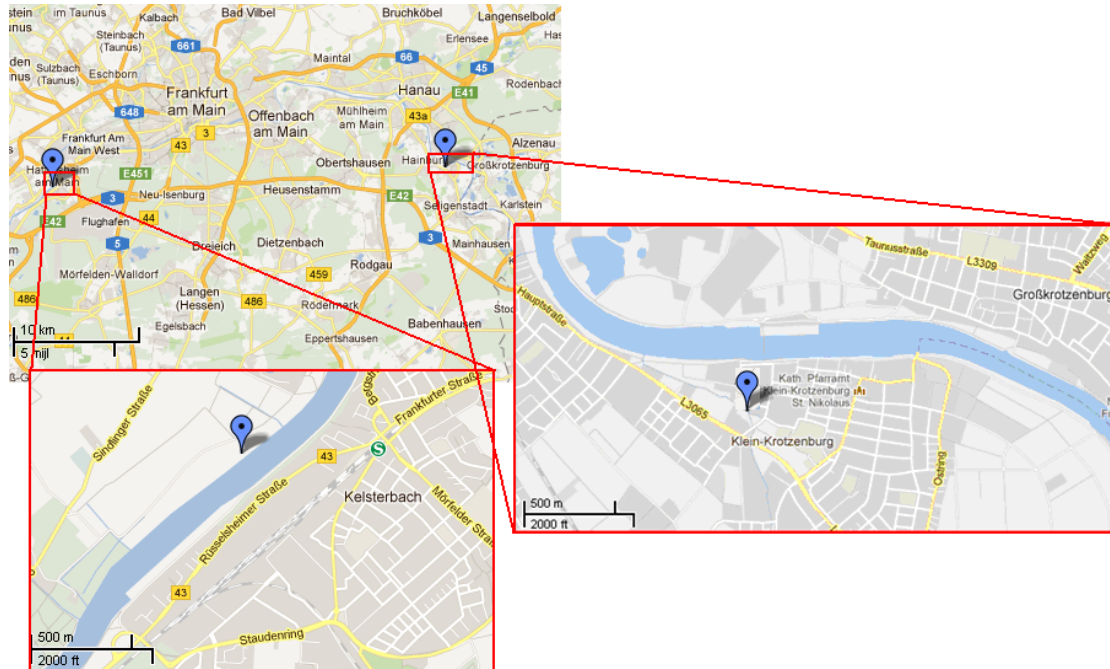


**Figure 4-5 Location of coring sites along Main: Sindlingen and Klein Krotzenburg.**

Exact locations (blue arrows), (1, left) Sindlingen, West of Frankfurt am Main, Germany. GPS Position: N50 03 45.0 E8 31 11.6. (2, right) Klein Krotzenburg, East of Frankfurt am Main, Germany. GPS position: N50 04 32.1 E8 57 33.6. After Google Maps 2011.

### *Moselle*

#### *Pre-industrial*

To be able to find a location to collect Holocene material we looked on geological maps of the Moselle area. As the chemical compositional signal should be specific for the sediment entering the Rhine River at Koblenz, a location close to Koblenz had to be found. However, the only Holocene floodplain deposits that are visible on the geological map, were found close to the city of Kenn (Figure 4-6).

#### *Post-industrial*

The floodplains along the lower part of the Moselle are confined in a bedrock valley and the river has been canalized during the last 50 years. We looked for a location close to the mouth of the main at Koblenz (in order to obtain the signal of the complete Moselle), but the possible influence of the backwater of the river Rhine was also taken into account. A location was found somewhat upstream

of Kenn. Sampling sites along the Moselle were located at 412 km and 570 km equivalent to the Rhine River. Exact locations of sampling sites are found in Table 4-2 and Appendix 3.

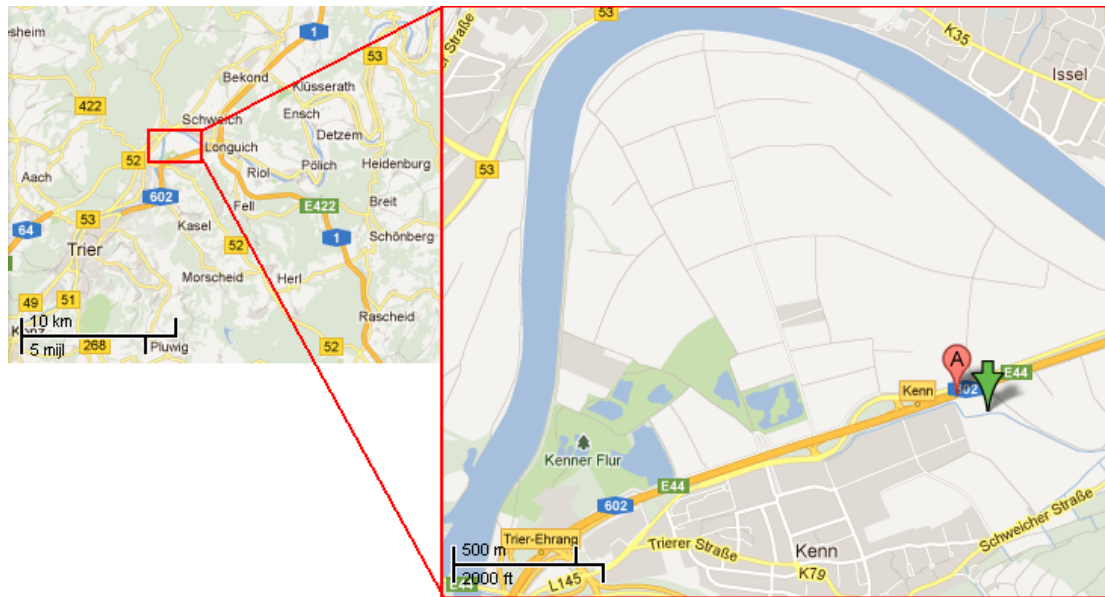


**Figure 4-6 Location of coring site along Moselle: Kenn.**

Exact location (green arrow), Kenn, North-East of Trier, Germany. GPS position: N49 48 26.3 E6 43 55.8. After Google Maps 2011.

### 4.3. Sample collection

#### 4.3.1. Corings

The cores were collected using a hand-operated corer which delivers 1 meter long segments of 4.5 cm diameter and they were collected in PVC tubes. Cores were logged in the field; sediment structure, organic matter content, colour, oxidation/reduction zone, carbonate content and plant remains were noted every ten centimetre interval. In the laboratory the core segments were divided into two halves (along the longer axis), logged in detail and photographed. The cores were sealed and packed again and stored in refrigerated storage cells to prevent oxidation of the cores. Both of the sections of each core segment were used; one for grain size analysis, and the other half was transported to the lab of the Aberystwyth University where a XRF scan was performed to retrieve chemical compositional data (chapter 5.1.2).

#### *Lower Rhine site: Bienener Altrhein (Bienen)*

In the context of his research about the infill of a cut-off meander of the Rhine River (i.e. Bienener Altrhein palaeochannel), Winkels performed a coring along the Bienener Altrhein (Table 3-1). The core segments were collected with a Bohncke modified piston corer. This coring resulted in a series

of 10 core segments, from now on called Bienen 1 to Bienen 10. In total, the depth covered over 8 meters corresponding to a maximum age of approximately 400 years (Winkels, 2011; Toonen, 2013).

#### *Pre-industrial sites*

During a fieldwork campaign (October 2011), cores have been taken at the sites presented in the previous section (Table 4-1). From each of the subcatchments, at least one core was collected with a soil corer. All of the corings resulted in a single core segment with a length of approximately one meter.

#### *4.3.2. Surface samples*

##### *Post-industrial sites*

Recent depositions are taken along the river channels of the different tributaries (Table 3-1). These samples were taken with an Edelman corer. From each catchment samples are taken from at least two different locations that are not too close to each other. At each location two samples are taken; one from a depth of 10 cm to 20 cm and one of a depth of 20 cm to 30 cm. Samples were collected in a plastic bag to transport them to the lab.

To allow further analysis, the samples were homogenised. First the bulk samples were dried at ambient room temperature and plant remnants were removed. Samples that were too moist were dried in an oven, overnight at 55 °C. Then, the bulk samples were manually grounded and pulverised in a porcelain mortar. By sieving the samples they were eventually homogenised.



**Table 4-1 Overview of the sampling sites (corings)**

Site	Location	Catchment Lower Rhine / Tributary	Date of collection (month, year)	Coring depth (cm)
Bienener Altrhein	Bienen	Lower Rhine	June, 2011	156 - 849
Römerberg	Speyer	Upper Rhine	October 2011	148 - 238
Lauffen	Heilbronn	Neckar	October 2011	100 - 190
Sindlingen	Frankfurt (west)	Main	October 2011	120 - 205
Klein Krotzenburg	Frankfurt (east)	Main	October 2011	125 - 215
Kenn	Trier	Moselle	October 2011	10 - 60

**Table 4-2 Overview of the sampling sites (surface samples)**

Site (#)	Setting	Location (exact location (GPS) in Appendix 3)	Catchment (Tributary)	Date of collection (month, year)	Coring depth (cm)
4	Levee	Kenn	Moselle	October 2011	0.10-0.30
5	Pointbar	Kenn	Moselle	October 2011	0.10-0.30
9	Levee	Klein Krotzenburg	Main	October 2011	0.10-0.30
11	Levee/floodplain (high)	Horkheim	Neckar	October 2011	0.10-0.30
12	Levee/floodplain (low)	Horkheim	Neckar	October 2011	0.10-0.30
13	Levee	Edingen/Neckarhausen	Neckar	October 2011	0.10-0.30
14	Floodplain (high)	Mannheim	Neckar	October 2011	0.10-0.30
16	Floodplain (high)	Römerberg	Upper Rhine	October 2011	0.10-0.30
17	Floodplain (low)	Römerberg	Upper Rhine	October 2011	0.10-0.30
18	Palaeochannel	Sindlingen	Main	October 2011	0.10-0.30
19	Floodplain	Rheindürkheim	Upper Rhine	October 2011	0.10-0.30
20	Levee	Rheindürkheim	Upper Rhine	October 2011	0.10-0.30
21	Levee	Ingelheim	Upper Rhine	October 2011	0.10-0.30
22	Levee	Ingelheim	Upper Rhine	October 2011	0.10-0.30
23	Floodplain	Alken	Moselle	October 2011	0.10-0.30
24	Floodplain	Alken	Moselle	October 2011	0.10-0.30
25	Floodplain	Alken	Moselle	October 2011	0.10-0.30
26	Floodplain	Andernach	Upper Rhine	October 2011	0.10-0.30
27	Floodplain (low)	Andernach	Upper Rhine	October 2011	0.10-0.30
28	Levee	Bonn	Upper Rhine	October 2011	0.10-0.30
29	Floodplain (high)	Bonn	Upper Rhine	October 2011	0.10-0.30

## 5. Laboratory methods and data analysis

### 5.1. Laboratory methods

#### 5.1.1. Grain size analysis

The cores segments referred to as Bienen 1 to Bienen 10 were collected by Winkels in July 2011 at the Bienener Altrhein location (section 4.3.1). Winkels (2011) made notes of clearly visible transitions and sandy layers within the core segments. Moreover, photographs were taken, which also show the major depositional transitions and some sandy layers could be identified. The results of this visual analysis, including pictures and notes, are found in Appendix 8 and, more extensively, in Winkels (2011).

The Bienen cores were sampled continuously at a semi-regular sample thickness of 1-2 cm's to perform grain size analysis (Winkels, 2011). The upstream cores (Kenn, Klein Krotzenburg, Lauffen, Römerberg and Sindlingen) were sampled with a regular sample thickness of 1 cm per 5 cm. The relative low average sampling resolution can be interpreted in two ways. 1) A constant grain size within the sample results in corresponding mode and average values of the measurement. 2) If the grain size within a sample is not constant (in the case of a sandy layer) mode and average value differ and (minor) sandy layers might not be detected.

Sample intervals were slightly adjusted to correspond with visual flood layering i.e. sandy layers that had been identified during visual analysis were taken into account to be able to separate specific grain size classes in a sample. This was done to avoid the out averaging of grain size results within a sample and obtain an optimal representation of the grain size class for each of the samples. However, during the sampling of the Bienen core segments, Winkels sometimes deviated from the 2 cm sampling interval border instead of sticking to the continuous sampling, without notifying this. Therefore, the exact borders of the sample interval are not always known. The post-industrial samples have been sampled from homogenized material; each sample thus represents a depth of 10 cm.

Before grain size analysis was performed all samples were pre-treated, i.e. all non-siliclastic particles that could affect grain size measurements (e.g. plant or root remains), were removed from the sample (Konert and Vandenberghe, 1997). Organic matter was removed from the samples by adding 10 ml 30% H<sub>2</sub>O<sub>2</sub> solution. All carbonates and other ions were removed from the sample by adding 5 ml of 10% HCl solution and boiling the mixture. Flocculates, caused by cohesiveness were separated by adding 300 mgs natriumpyrophosphate (Na<sub>4</sub>P<sub>2</sub>O<sub>7</sub>·10H<sub>2</sub>O).

Grain size was measured using laser diffraction analysis. This method is based on the correlation between (1) the angle of light scattered by particles under influence of a laser beam and

(2) the size distribution of these particles (Jonkers et al., 2009). Based on available time and budget, grain size analysis was performed on 2 cm resolution average.

Grain size analysis was carried out in the lab of the Vrije Universiteit in Amsterdam. Particle size distributions of suspended sediment samples in the range between 0.15  $\mu\text{m}$  and 2000  $\mu\text{m}$  were measured in 56 bins by the HELOS KR (Sympatec) Laser Particle Sizer (LPS) (Jonkers et al, 2009; Witt et al., 2010). Results of the analysis were grouped in a series of logarithmically spaced grain size distribution classes for each of the samples.

#### *5.1.2. Chemical composition analysis*

##### *XRF core scanning*

All cores were scanned at Aberystwyth University in Wales (UK) using an Itrax XRF scanner (Croudace et al, 2006). X-Ray Fluorescence (XRF) core scanning is a non-destructive characterization of sediment sequences that can be used for material from lacustrine environments (Jenkins & De Vries, 1970; Croudace et al, 2006; Richter et al, 2006). It provides high resolution information about changes in the chemical composition of a core by creating an elemental profile with a range from Aluminium ( $^{13}\text{Al}$ ) to Uranium ( $^{92}\text{U}$ ). Although the quality of elemental data resulting from the scan mainly depends on the quality of the sample, the scanner provides a detailed relative log of the chemical composition of the core.

Under the influence of incoming X-ray radiation, an electron from an inner atom shell is ejected. This results in a vacancy which is filled by an electron falling back from an outer shell. The energy difference between the inner and the outer shell is emitted as electromagnetic radiation, the latter can be detected by the XRF core scanner. Each element has a characteristic wavelength of this emitted radiation, and the amplitudes of the peaks in the detected XRF-spectrum are proportional to the concentration of the elements in the range between Aluminium ( $^{13}\text{Al}$ ) to Uranium ( $^{92}\text{U}$ ) (Croudace et al, 2006; Richter et al, 2006; Jones et al., 2009, 2010).

The XRF scanner performs a continuous XRF analysis on the surface of a split sediment core. Before inserting the core into the scanner, the surface of the core was cleaned and smoothed. Any visible cracks and holes were logged. Before the actual scan, the core was covered with micro-film to prevent desiccation (Lamb et al., 2005; Croudace et al, 2006). All cores were scanned using a molybdenum tube set, the preset voltage was 60 kV and the current varied between 40 mA and 50 mA. Based on available time and budget the scan resolution was either 500  $\mu\text{m}$  or 1000  $\mu\text{m}$ . For the all the Bienen cores, we used a XRF exposure time of 200 ms and a dwelling time of 30 s. Specific (optimal) XRF scan settings varied per core and are reported in Appendix 11. As starting and ending points of the measurements were put in manually, minor shifts in the depth output of the scanned core segments could occur.

### *Handheld XRF surface samples scanning*

To identify the chemical composition of the surface samples, we used a handheld XRF scanning device. Although this device, provided by and operated at the Aberystwyth University, performs a scan on fewer elements, measures the concentration of several elements in the bulk samples. The handheld XRF scan detects the following elements; Sb, Sn, Cd, Ag, Sr, Rb, Pb, Se, As, Hg, Zn, Cu, Ni, Co, Fe, Mn and Cr. The output of the scan is an elemental count for each of these elements in parts per million (ppm). Cores were scanned by hand, applying a scanning time of at least 100 seconds to ensure all elements were detected and to minimize the error percentage of the scans. As these error percentages are relatively stable for each of the elements, a mean error percentage was calculated to determine the usability of the elements. Moreover, the duration of the scan is listed for each of the scans.

## 5.2. Data Analysis

In order to answer our research questions, a series of analytical steps was performed on the data obtained by grain size analysis and chemical composition analysis (Fig. 5-1). First, the grain size data were combined with historical data to identify flood events in the grain size data. Chemical composition data were normalized, to filter all scan-specific variations, and bulked, to equalize the resolution with that of the grain size data. The normalized and bulked data were combined with previous research to obtain element ratios that were usable to acquire information on grain size. This chemical proxy was consequently used for the first objective; i.e. to identify flood events in grain size data and chemical composition data.

Moreover, the chemical proxy was used to correspond the grain size data set with the chemical composition data set. Subsequently, the correlation of aluminium ( $^{13}\text{Al}$ ) with the clay fraction was tested for its suitability as corrector for the clay content. Also, a series of correlation matrices were set up to acquire information for possible application of additional statistical methods.

Chemical composition data from the subcatchments (cores and surface samples) were used to setup characteristic fingerprints for each of the subcatchments. Also, the chemical proxy was used to obtain the chemical composition of the selected flood deposits from the chemical composition data set. Subsequently the results of the previous objectives were combined to trace the (mixed) origin of Lower Rhine flood events.

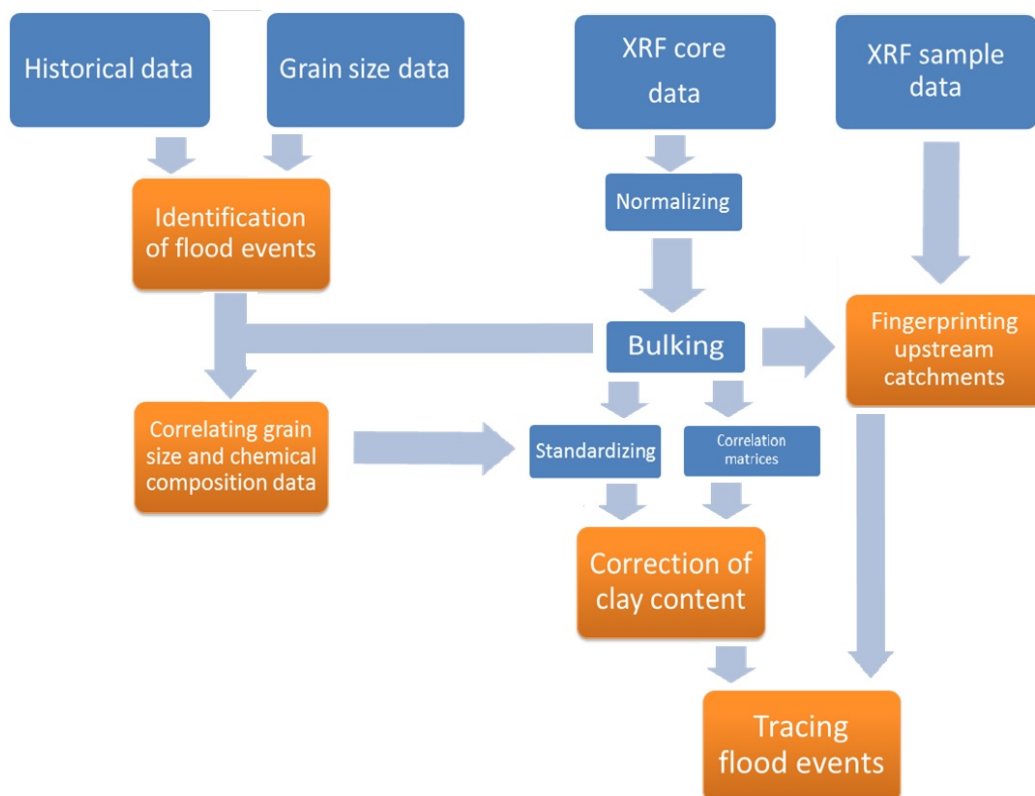


Figure 5-1. Schematic overview of analytical methods used in this study.

### *5.2.1. Grain size data*

The distribution classes resulting from the analysis were bulked to five classes, representing the sand fraction (63 - 2000  $\mu\text{m}$ ), the silt fraction (8 - 63  $\mu\text{m}$ ), and the clay fraction (subdivided into three classes, < 2  $\mu\text{m}$ , < 4  $\mu\text{m}$ , and < 8  $\mu\text{m}$ ). In addition, the 95<sup>th</sup> percentile (P95) value was calculated for each of the samples (Aloserij, 2013; Toonen, 2013). To enable analysis of the grain size data, grain size distributions of each of the samples were combined to assemble a continuous grain size depth profile. Due to human interference close to the sample location (the construction of a sluice and input of coarse-grained sands), the data retrieved from the upper part of the coring (Bienen 1 and Bienen 2) were not used in this analysis (Winkels, 2011; Aloserij, 2013). Furthermore, because separate core segments might have shrunk or expanded (due to compaction by drilling, transport or storage) causing discontinuities in the sample depth, sample depths were converted to real depth to form a continuous record of all the Bienen cores. In this conversion, it was assumed that the maximum depth of individual core segments resemble true depth, and that the core record was continuous. This way the length of (some) core segments was extended or reduced to fit the contiguous core segment, i.e. the real depth of the deepest point of the contiguous core segment.

From these data flood events were identified from peaks in the sandy grain size classes and higher P95 values. Subsequently, previous theses were used to verify these identified flood events in order to date the flood events. Toonen (2013) used historic sources to identify flood events. However, these data can be incomplete (due to varying source material) and the source of flood events is mostly not known. Aloserij (2013) verified whether these flood events had an upstream origin instead of being caused by local impacts (i.e. the collapse of ice dams or failure of river embankments). This was done by comparing two lower Rhine cores and identifying identical flood events in both cores (Aloserij, 2013). Only the most extreme floods were selected as these events are easier to recognize in distal floodplains, based on the fact that the coarse material and the amount of coarse material in these floods is relatively high.

### *5.2.2. Chemical composition data*

#### *Normalizing elemental data*

The XRF core scanner provides counts for each of the elements. The amount of scattering is measured for each sampling point and each element in terms of coherent and incoherent scattering; to account for changes in water content and sediment density, this count-to-scatter ratio is calculated (personal communication with Rassner). To filter the scattering, measurement results had to be normalized by dividing elemental counts by the sum of the corresponding coherent and incoherent counts of molybdenum (a molybdenum tube set was used, see section 4.1.3).

### *Bulking XRF data*

To compare grain size data with chemical composition data (see section 4.2.3), the data have to be uniform in resolution. This is not the case for the data resulting from the different analytical methods; the resolution of the grain size data is 1 cm to 5 cm while the resolution of the chemical composition data is 500  $\mu\text{m}$  or 1000  $\mu\text{m}$ . To set up a combined data set throughout the depth of the cores, the chemical composition data was bulked (continuously) by averaging a consecutive series of chemical composition data points to obtain a resolution that matches with the resolution of the grain size data.

### *5.2.3. Correlating grain size data and chemical composition data*

#### *Chemical proxy for grain size*

Previous literature indicates that there are some elements that correlate with certain classes of the grain size of sediment. Previous research indicates that the Zr/Rb ratio can be exploited to acquire information on grain size (Dypvyk and Harris, 2001; Kylander et al., 2011). Zirconium (Zr) is an element that is associated with the relatively coarse grained fraction of sediments (Dypvyk and Harris, 2001). Consequently, the Zr counts can be used as an indicator of the abundance of relatively coarse grained sediment. Rubidium (Rb) on the other hand, shows a positive correlation with fine grained sediments (Dypvyk and Harris, 2001). Rb is normally associated with claystones and siltstones. Therefore Rb can be used as an indicator of the amount of fine grained sediment. Other ratios of elements that can be used to acquire grain size information are the Zr/Ti ratio (Oldfield et al., 2003) and some ratios based on Al, which is supposed to correlate with fine grained sediment and several elements that correlate well with coarse grained sediment (i.e. Si/Al, Ti/Al, and Zr/Al) (Calvert et al., 1996; Schneider et al., 1997; Calvert et al., 2001).

#### *Correlating grain size and chemical composition*

After normalizing, bulking and standardizing the chemical composition data were used to calculate the Zr/Rb ratio and other ratios (Zr/Ti, Si/Al, Ti/Al and Zr/Al). For each of the core segments, these ratios were compared with different cumulative grain size classes. For all of these classes the correlation coefficients were calculated. In some cases, results from the grain size analysis and ratios showed similar patterns, although the exact position of the peaks were slightly shifted. In these cases the correlation was improved by applying a minor shift to the depths of the chemical proxy ratio. Subsequently correlation coefficients were calculated for the corrected (i.e. shifted) matched depths.

#### 5.2.4. Correction of the clay content

##### *Correlation matrices*

Set of elements that are associated with each other, can be used as an indicator for changes in grain size. To quantify the strength of association between sets of elements, correlation matrices were constructed using the data analysis tool of Microsoft Excel 2010. Sets of elements that are associated well, can be used in statistical methods (linear regression, principal component analysis) to unravel the contribution of a component. Although the XRF scans were standardized, XRF scan settings vary per core segment (due to varying settings). Therefore a separate correlation matrix was constructed for each of the core segments. We made a selection of ten elements of interest for this research, including Si, K, Ca, Ti, Mn, Fe, Rb, Sr, Zr and Pb.

##### *Al-standardizing chemical composition data*

To correct the chemical composition data for the variation in clay content, the correlation of  $^{13}\text{Al}$  with the clay fraction was tested. Correlation coefficients of  $^{13}\text{Al}$  were calculated with the clayey grain size classes ( $< 2 \mu\text{m}$ ,  $< 4 \mu\text{m}$ , and  $< 8 \mu\text{m}$ ). Correcting the elemental counts for the clay content was done by dividing the elemental count of each sampling point by the corresponding  $^{13}\text{Al}$  count. We applied the same standardizing method on the subcatchment cores, to enable a comparison between the elemental counts of all core segments.

#### 5.2.5. Characterizing subcatchments

The next part of the analysis involved the determination of the chemical composition of the subcatchments. The normalized and standardized elemental data of the upstream cores were used to find the chemical characteristics of each of the subcatchment source areas. The elements of the post-industrial samples that exceeded the average error percentage 15 %, were excluded. For each element a catchment-propagation graph was constructed to create a visual overview of the occurrence of these elements throughout the catchment.

Subsequently the data of the cores and the surface samples were used to set up a characteristic fingerprint for each of the subcatchments. To enable a combination of these two data sets, a set of elements was selected that was detected in both the cores and the surface samples. Elements that are sensitive to horizontal or vertical displacements and soil conditions were excluded from this selection. The remaining set of elements was used to identify the origin (source area) of certain downstream (flood event) depositions (i.e. fingerprinting). For each subcatchment a fingerprint was constructed by averaging the elemental occurrence in the pre-industrial core (i.e. throughout depth), and averaging the elemental occurrence of the surface samples.



To be able to use a set of fingerprints to provide information on the relative contribution of potential sediment sources to the sediment deposited of an downstream river, there are three main requirements (Walling et al, 1993);

1. Fingerprints should reflect environmental control and are capable of discriminating potential sediment sources.
2. The selection of fingerprints needs to be statistically tested to confirm that individual sediment sources can be distinguished by their fingerprint(s).
3. A system needs to be developed that is capable of comparing the composition of downstream deposited sediment with the fingerprints of potential upstream sources. This system should also be able to provide an estimate of the relative contributions of those sources.

#### *5.2.6. Tracing flood origin*

By linking the peaks in grain size data with flood events, we identified the flood events in the grain size data (5.2.1). Taking into account the shifts that were needed to fit the grain size data with the chemical composition data, the chemical proxy was used to identify the flood events within the chemical composition data (5.2.3). These correlations were used to determine the chemical composition of the flood events. In this process we have only used the flood events that were dated to the same year at which we had identified peaks in our proxy abundance plots. As a consequence, we have only used those of the floods that were recognized with the chemical proxy data.

## 6. Results and discussion

### 6.1. Identification of flood events

Figure 5-1 provides plots of the cumulative silt and sand fraction and the P95 plotted against the converted (real) depth for each of the core segments. Appendix 1 provides the raw grain size data and raw XRF data for each of the Bienener Althrein core segments. Below, the processed grain size data are discussed for each of the core segments. Based on the percentage of the sandy fraction, or based on an excessive sum of the silt and sand fraction, layers were identified as a sandy layers. The relative low grain size sampling resolution (4.1.2) and in some cases the unnoticed varying sampling interval borders (4.1.2), can cause some sandy layers (flood events) to remain unidentified.

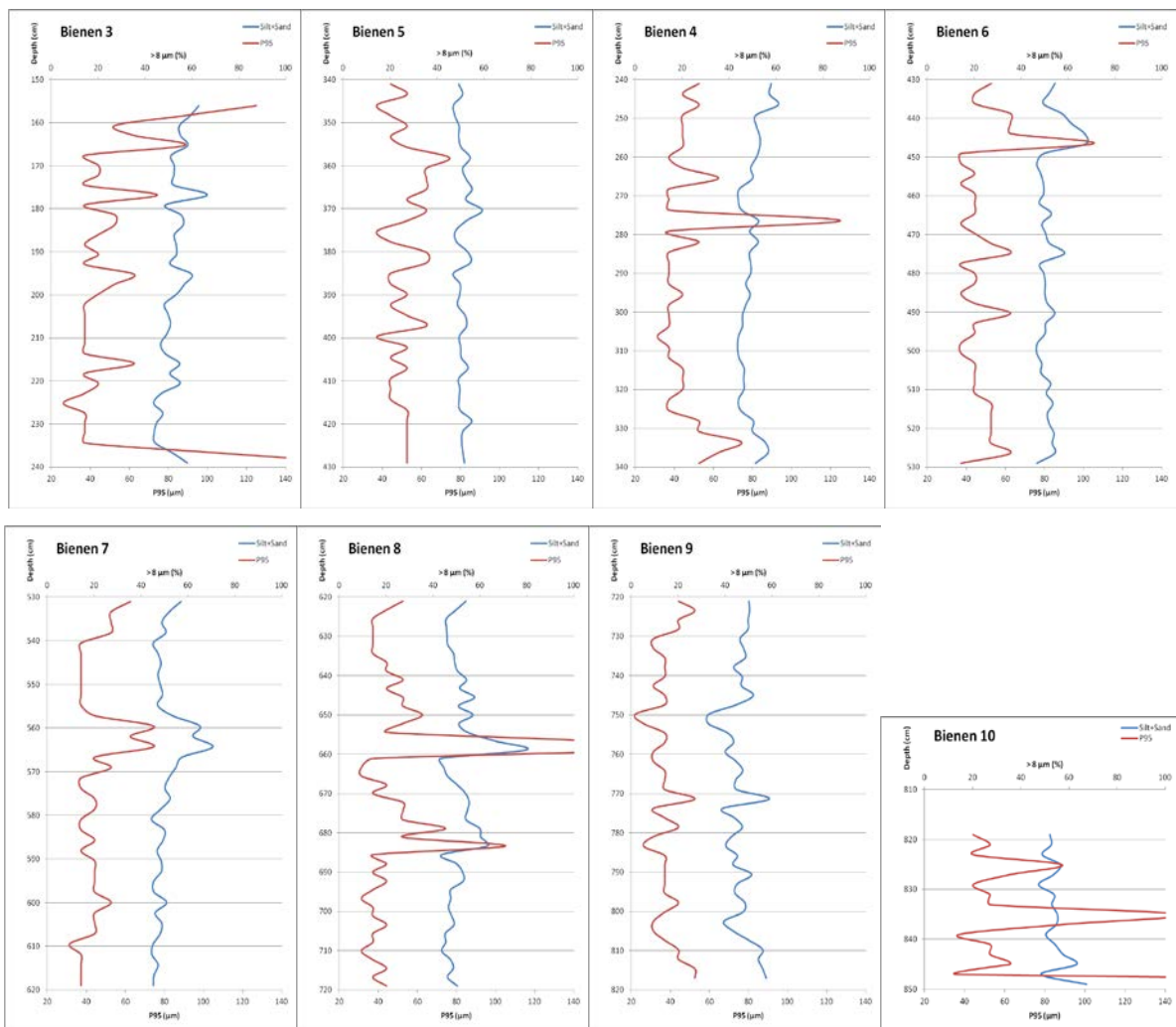


Figure 6-1 Depth plots of Bienener Althrein core segments 3-10.

Vertical axis represents depth (cm) throughout the core. Horizontal axis represents silt+sand fraction (% , upper axis, blue) and P95 ( $\mu\text{m}$ , lower axis, red).

### *Bienen 3*

The original depth of Bienen 3 was 167 cm to 239 cm, we converted these to a real depth of 156 cm to 239 cm. Due to a partial collapse of the coring hole, the sandy upper part (3-4 cm) is not representative. Sandy layers were found at 165 cm, 177 cm, 184 cm, 195 cm, 198 cm, 216 cm, 221 cm and 239 cm.

### *Bienen 4*

The original depth of 267 cm to 339 cm was converted to a real depth of 241 cm to 339 cm. Sandy layers were found at 246 cm, 266 cm, 276 cm, 282 cm, 320 cm. Moreover, two areas were identified as sandy, the first in between 298 cm and 304 cm and the other at the bottom of the core, from 331 cm to 339 cm.

### *Bienen 5*

The original depth of 357 cm to 429 cm was converted to a real depth of 341 cm to 357 cm. Sandy layers were found at 370 cm, 383 cm and 429 cm.

### *Bienen 6*

The original depth of 453 cm to 529 cm was converted to a real depth of 431 cm to 529 cm. We found a relative high average percentage of the sand fraction compared to the other cores. Sandy layers were distinguished at 444 cm to 446 cm, 465 cm, 475 cm, 490 cm and 526 cm.

### *Bienen 7*

The original depth of 545 cm to 619 cm was converted to a real depth of 531 cm to 619 cm. Sandy layers could be distinguished and were found at 560 cm, 564 cm, 576 cm, 600 cm.

### *Bienen 8*

The original depth of 631 cm to 719 cm was converted to a real depth of 621 cm to 719 cm. Sandy layers were found at 645 cm, 650 cm, 659 cm and between 679 cm and 683 cm.

### *Bienen 9*

The original depth of 737 cm to 817 cm was converted to a real depth of 721 cm to 817 cm. We found a relative low average percentage of the sand fraction compared to the other cores. Sandy layers were distinguished at 745 cm, 771 cm, 791 cm and 810 cm.

### *Bienen 10*

The Bienen 10 core was not converted as the original and real depth corresponded, i.e. they were both 819 cm to 849 cm. We found a relative high average percentage of the sand fraction compared to the other cores. No real sandy layers were distinguished, but grain size increased with depth. At the bottom of the core grain size increased rapidly due to coarser sands on which the coring ended.

### 6.1.1. Selected flood events

The results from Aloserij (2013) were used to link extreme flood events (known from historical flood data) with peaks in the grain size data. Ten major flood events were selected (based on grain size data) from the Bienener Altrhein core segments. Table 6-1 provides an overview of these flood events, their corresponding (cumulative) grain size classes (including sand and silt + sand) and the dates of these flood events.

**Table 6-1 Correlation of extreme flood events.**

Extreme flood events (based on historical flood data) were correlated with grain size data throughout depth (based on Aloserij, 2013).

Depth (real, cm)	Sand (%)	Silt + Sand (%)	Historical flood data (year A.D.)
156	15.13	62.92	1882/1883
239	15.75	57.95	1850
276	13.69	52.53	1845
446	12.63	67.90	1784
560	7.83	65.04	1729
564	8.48	70.58	1726
659	50.39	79.71	1682
683	16.32	63.03	1671
825	8.48	56.36	1608
835	9.21	55.17	1602

### 6.1.2. Upstream Rhine cores

Appendix 9 provides the results of the upstream Rhine cores. The sampling resolution of the upstream Rhine cores was 5 cm, which does not allow us to analyze these data in detail. Due to varying floodplain settings (e.g. distance to active river channel) and different core depths average sand fractions varied per subcatchment core. In the Upper Rhine core (Römerberg, 148-238 cm) the sand fraction varies between 40 to 60 percent. The sand fraction remains stable throughout the core, sandy areas were identified around 150 cm, 185 cm and 230 cm. In the Neckar core (Lauffen, 100-190 cm) the sand fraction varies between 70 to 90 percent. The sand fraction increases with depth, a sandy area was identified around 125 cm. In the first Main core (Sindlingen, 120-205 cm) the sand fraction varies between 60 to 80 percent. The sand fraction remains stable throughout the core, a sandy area was identified around 170 cm. In the other Main core (Klein Krotzenburg, 125-215 cm) the sand fraction varies between 50 to 80 percent. The sand fraction remains stable throughout the core, sandy areas were identified around 135 cm, 150 cm and 160 cm. In the Moselle core (Kenn, 10-

60 cm) the sand fraction varies between 40 to 60 percent. The sand fraction decreases with depth, a sandy area was identified around 15 cm.

### *6.1.3. Discussion*

A series of flood events was identified throughout the Bienen coring. However probably not all sandy layers were detected during visual and grain size analysis. Limiting factors as the relative low grain size sampling resolution and unnotified varying sampling interval borders might have caused some minor sandy layers to remain undetected. However, the major sandy layers were identified. The focus of this study is not on the construction of a detailed framework of flood events, in the next part of this research the major sandy layers are used to find a relation with chemical composition data.

## *6.2. Correlating grain size and chemical composition data*

### *6.2.1. Normalized chemical composition data*

Appendix 1 (raw data) and Appendix 2 (selected elements) provide the normalized elemental data for each of the Bienen core segments. These data include the normalized elemental counts at each depth, for the elemental range between Al and Pb. Zr counts vary between 0.040 and 0.060 for all the Bienen core segments and remain stable. Peaks in the Zr counts were identified at 179 cm, 184 cm and 232 cm (Bienen 3), 405 cm (Bienen 5), 441 and 446 cm (Bienen 6), 585 cm (Bienen 7), 663 cm, 674 cm and 681 cm (Bienen 8), 750 cm, 771 cm, and 810 cm (Bienen 9), and 829 cm and 845 cm (Bienen 10). Rb counts vary between 0.030 and 0.040 and remain stable. No peaks were identified in the Rb counts. The continuous record of the combined Bienen core segments does not show any trends. The records of the elemental counts of the combined Bienen core segments are not continuous, each of the separate core segments can be identified in the plots of most of the elemental counts.

### *6.2.2. Chemical proxy for grain size*

Appendix 1 provides comparative data for each of the proposed chemical proxies. For each of the Bienen core segments an overview is given of the correlation coefficients (Zr/Rb, Si/Al, Ti/Al, Zr/Al, and Zr/Ti) with varying grain size classes (> 8  $\mu\text{m}$ , > 16  $\mu\text{m}$ , > 32  $\mu\text{m}$ , and > 64  $\mu\text{m}$ ). In some cases a (partial) shift was needed to correlate the grain size data with the chemical composition data. Correlation coefficients were highest (overall > 0.7) with the Zr/Rb ratio in each of the core segments. In most cases there also was a mediocre correlation coefficient (0.3-0.6) with the Zr/Ti ratio. The other proposed chemical proxies had low correlation coefficients with grain size classes and are therefore not usable as a proxy. Due to its high correlation coefficient with particular grain size classes, the Zr/Rb ratio is the most suitable chemical proxy.

### 6.2.3. Bienen core segments

Appendix 8 provides the comparative data for the Bienen core segments, i.e. the combined plots of the Zr/Rb ratio and the grain size fractions.

#### Bienen 3

The basis plots of Bienen 3 core segment (Figure 6-2) of the Zr/Rb ratio and the > 8 µm grain size class look similar; peak areas do correspond and the overall trend throughout depth is similar. However when we take a closer look, we find that although the peak show a similar pattern, they are not at the exact same position. The first grain size peak, at 165 cm, has no corresponding Zr/Rb ratio peak. The pattern of the grain size peaks at 177 cm, 184 cm and 195 cm have a corresponding pattern in the Zr/Rb ratio plot. However, these peaks are slightly shifted. The same goes for the grain size peaks at 216 cm and 221 cm, this pattern of peaks, although slightly shifted, is also found in the Zr/Rb ratio plot. The Zr/Rb ratio peak at 233 cm is not found in the grain size plot.

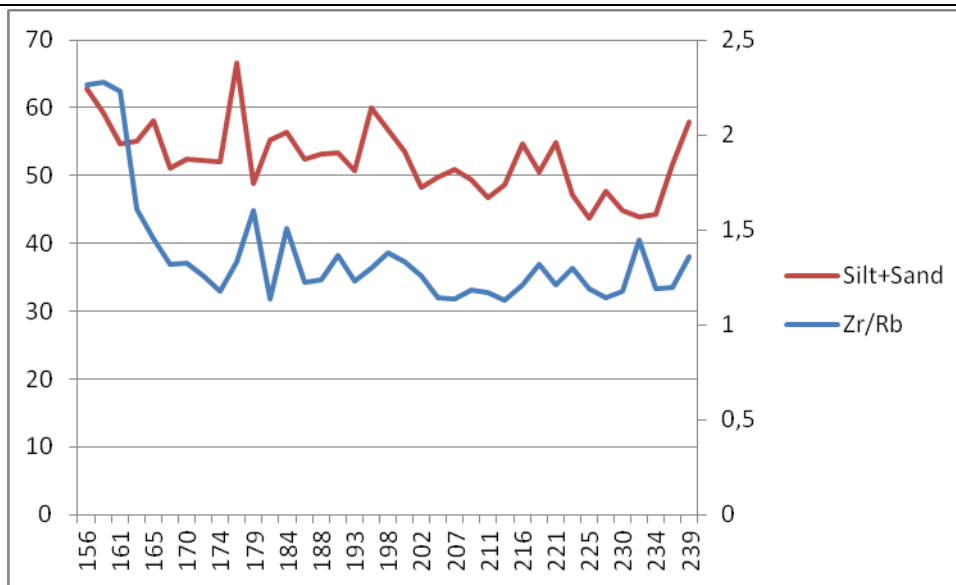


**Figure 6-2 Basic correlation plots of Bienen 3**

Horizontal axis represents depth (cm), vertical axis represents Silt+Sand (%) and Zr/Rb ratio.

Although the distribution of peaks in both the grain size and the Zr/Rb ratio plots show a similar pattern, the exact position of the peaks are slightly shifted. Therefore all data points were shifted to a new depth, that of 1 cm less deep than the original depth.

**Table 6-2 Correlation matrix for Bienen 3. Original and shifted data.**

	>8µm	>16µm	>32µm	>64µm
Original	0,461224	0,539429	0,578639	0,539442
Shifted	0,644679	0,723982	0,805674	0,834349

Table 6-2 shows the correlation matrix of the different grain size fractions with the Zr/Rb ratio for the shifted data. Although the correlation of the Zr/Rb ratio goes best ( $r = 0.83$ ) with the coarsest class ( $> 64 \mu\text{m}$ ), there is a good correlation with all the selected fraction classes. The correlations increase with increasing particle size.

*Bienen 4*

The basic plots of the Bienen 4 core segment (Figure 6-3) show a similar pattern. Although the peak in the upper part of the core does not correspond, the same trend is visible in both plots. In the bottom of the core (310 cm – 339 cm) the two plots do correspond. The grain size peaks at 246 cm, 276 cm and 282 cm are not found in the Zr/Rb ratio plot. The Zr/Rb ratio peaks at 252 cm and 268 cm are not visible in the grain size plot. The bottom part shows a similar pattern in both of the plots. Overall there is a similar trend, the plots do not correspond well in the upper part whereas they do correspond in the bottom part of the core. Relative to each other, there is no shift that can be applied in order to improve the fit of the two plots.

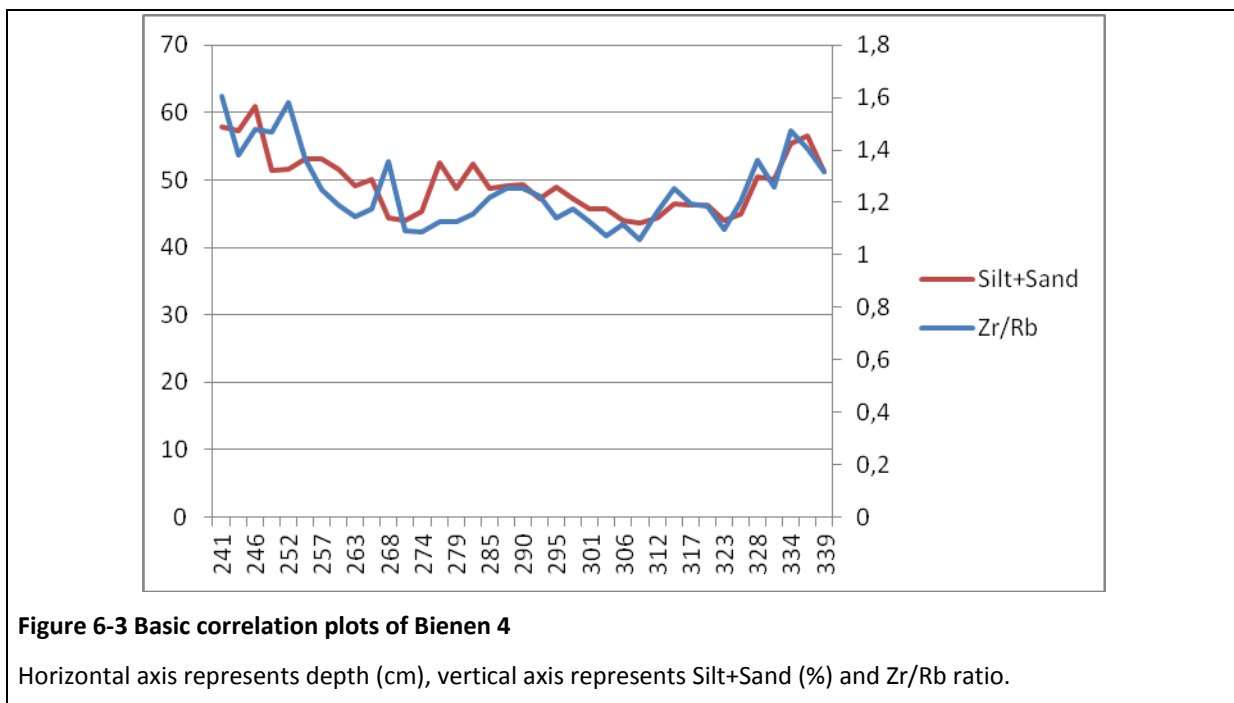


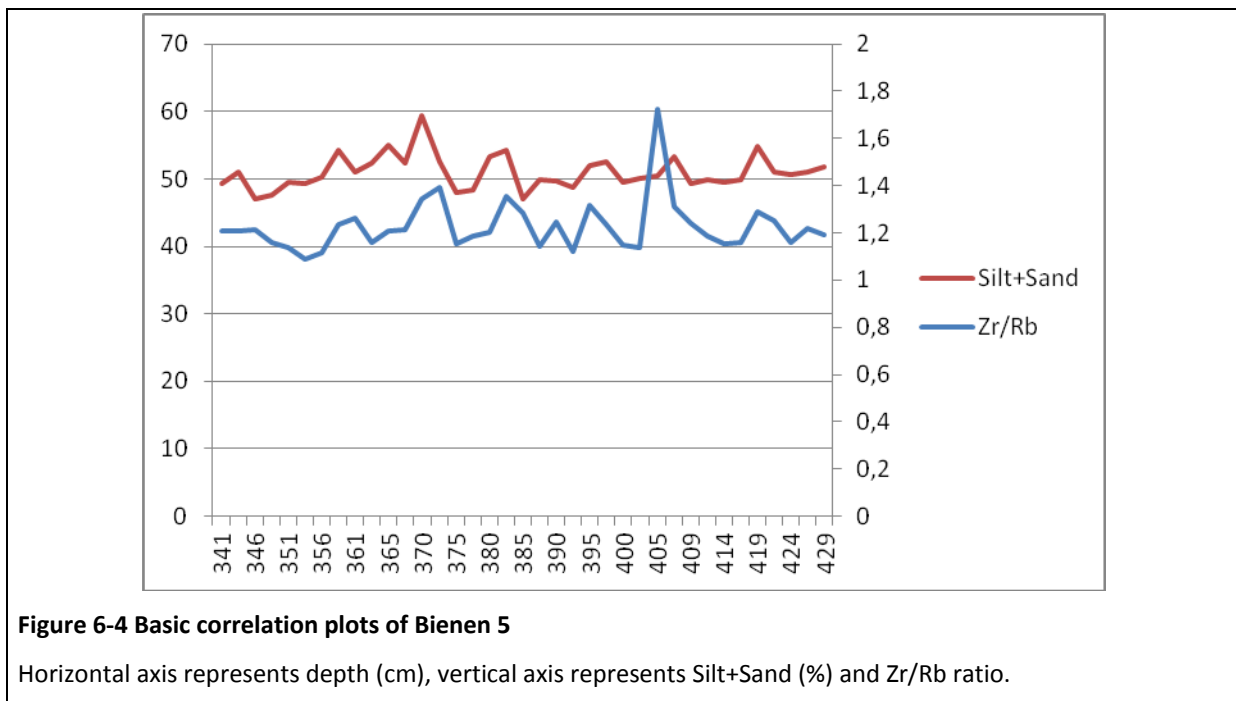
**Table 6-3 Correlation matrix for Bienen 4.**

	>8um	>16um	>32um	>64um
Original	0,717176	0,700221	0,553047	0,110655

Table 6-3 shows the correlation matrix of the different grain size fractions with the Zr/Rb ratio. The correlation of the Zr/Rb ratio with the class > 8 µm is good ( $r = 0.72$ ). However, the correlation with the coarsest particle size class (> 64 µm) is rather weak ( $r = 0.11$ ).

#### Bienen 5

The basic plots of the Bienen 5 core segment (Figure 6-4) show a similar pattern, except for the extreme Zr/Rb ratio peak at 405 cm which is not visible in the grain size plot. The upper part of the Bienen 5 core shows a similar pattern for both of the plots. Peaks in the grain size data at 358 cm, 370 cm and 383 cm, have their equivalents in the Zr/Rb ratio plot. The extreme Zr/Rb ratio peak at 405 cm is not visible in the grain size plot. The correlations decrease with increasing particle size.



Although the distribution of peaks in both the grain size and the Zr/Rb ratio plots show a similar pattern, the exact position of the peaks are slightly shifted in the upper part of the core segment. For this part (341 cm – 385 cm) a shift of the Zr/Rb ratio data would fit the peak areas of the plots. For this part we recalibrated the Zr/Rb ratio data; these data points are allocated to a new depth, that of 1 cm less deep than the original depth. However, the lower part still does not fit well. This is probably due to the Zr/Rb ratio peak at 405 cm which lacks in the grain size plot.

**Table 6-4 Correlation matrix for Bienen 5.** Original, shifted and upper part data.

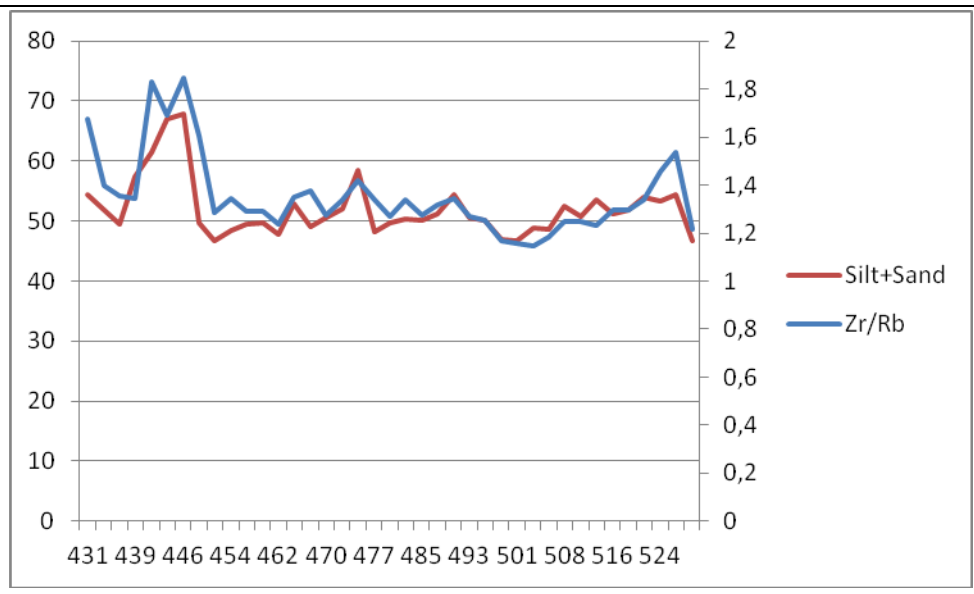
	>8µm	>16µm	>32µm	>64µm
Original	0,322911	0,323142	0,276425	0,197411
Shifted	0,319491	0,310755	0,323192	0,361464
Upper part (shifted)	0,731762	0,703849	0,692514	0,581068



Table 6-4 shows the correlation matrix of the different grain size fractions with the Zr/Rb ratio for the shifted data. The correlation values are only based on the upper part of the core segment (341 cm – 385 cm). Although the correlation of the Zr/Rb ratio with the class > 8 μm is good (r = 0.73), there also is a good correlation with the > 16 μm and > 32 μm classes. In the lower part of the core segment, the correlations are weak. The original correlations are weak (r < 0.33) and decrease with increasing particle size for the original. The correlations for the Upper part remain stable (variation < 0.05) with varying particle size.

*Bienen 6*

The basic plots of the Bienen 6 core segment (Figure 6-5) show a similar pattern. An equal trend is visible in both plots and the peak areas of the two plots do correspond well. The grain size peak area around 446 cm corresponds with the peak area in the Zr/Rb ratio plot. Moreover, the other peaks (around 465 cm, 475 cm, and 490 cm) are found at equal depths in both of the plots. The only area that corresponds less perfectly between the two plots, is the bottom 5 cms. No shift was needed to improve the fit of the two plots.



**Figure 6-5 Basic correlation plots of Bienen 6**

Horizontal axis represents depth (cm), vertical axis represents Silt+Sand (%) and Zr/Rb ratio.

**Table 6-5 Correlation matrix for Bienen 6.**

	>8um	>16um	>32um	>64um
Original	0,786676	0,759489	0,73804	0,696085

Table 6-5 shows the correlation matrix of the different grain size fractions with the Zr/Rb ratio. The correlation of the Zr/Rb ratio goes best ( $r = 0.79$ ) with the class  $> 8 \mu\text{m}$ . The correlation with the  $> 16 \mu\text{m}$  class and the  $> 32 \mu\text{m}$  class are also quite good ( $r = 0.76$  and  $r = 0.74$ ). The correlations decrease with increasing particle size.

#### Bienen 7

The basic plots of the Bienen 7 core segment (Figure 6-6) of the Zr/Rb ratio and the  $> 8 \mu\text{m}$  class look similar; peak areas are corresponding and the overall trend throughout depth is similar. All peaks are found in both the grain size and the Zr/Rb ratio plots, although sometimes minor shifts are visible. No shift was applied to improve the fit of the two plots.

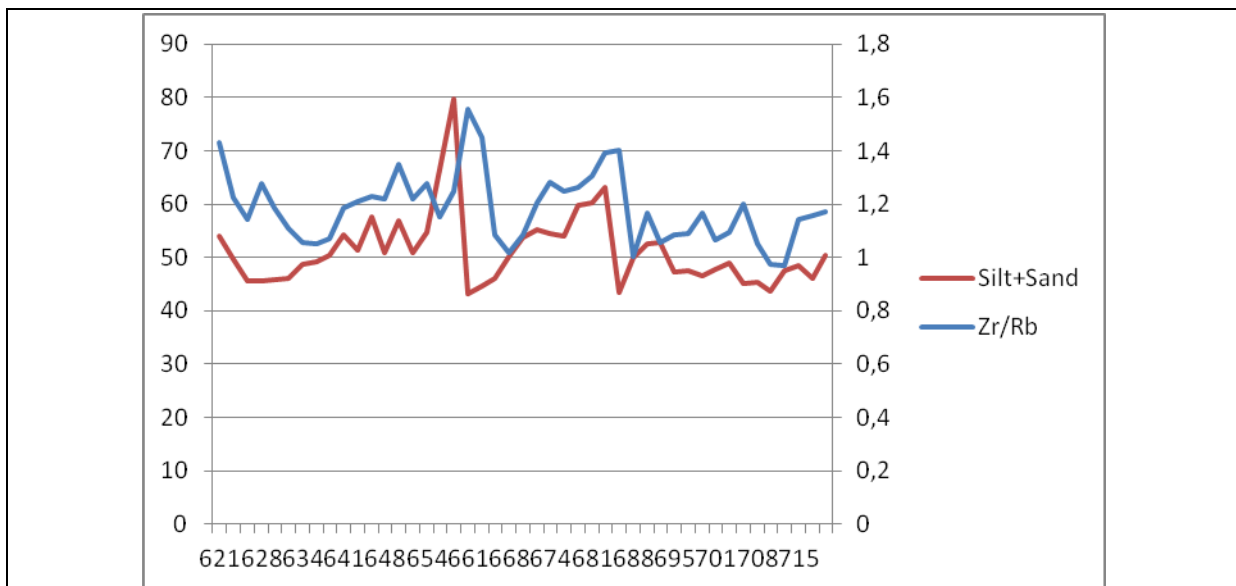


**Figure 6-6 Basic correlation plots of Bienen 7**

Horizontal axis represents depth (cm), vertical axis represents Silt+Sand (%) and Zr/Rb ratio.

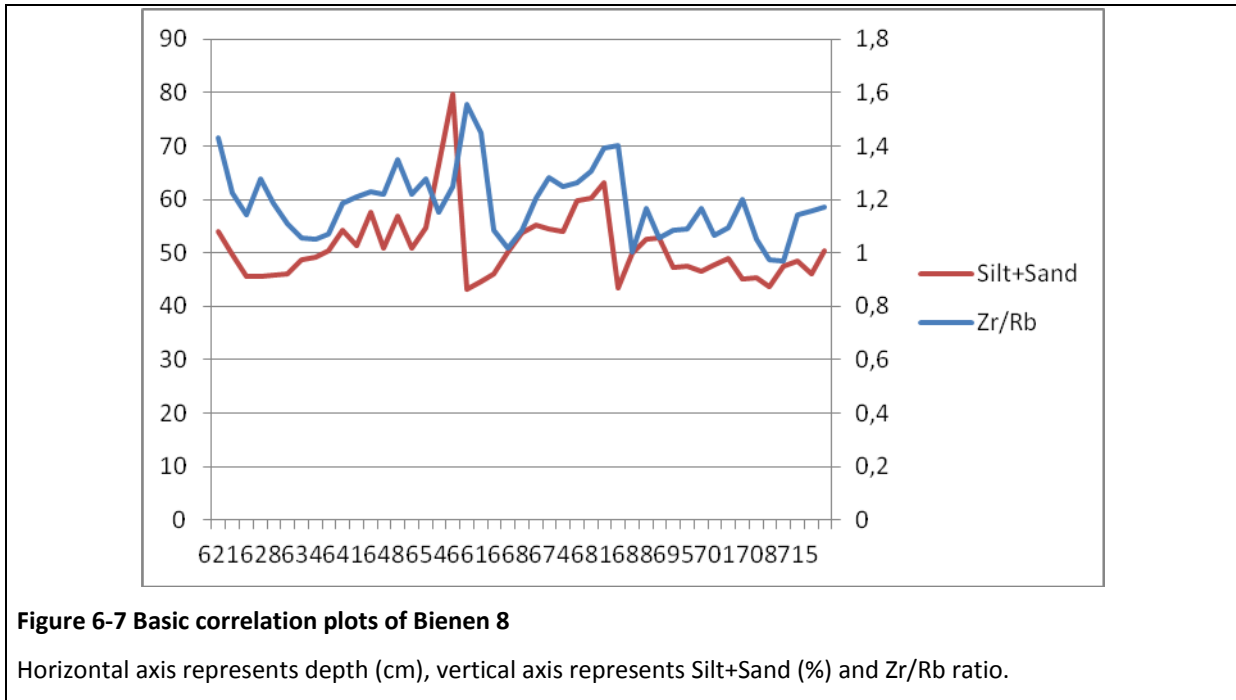
**Table 6-6 Correlation matrix for Bienen 7.**

	>8um	>16um	>32um	>64um
Original	0,888924	0,918979	0,898392	0,847635

Table 6-6 shows the correlation matrix of the different grain size fractions with the Zr/Rb ratio. The correlation of the Zr/Rb ratio goes best ( $r = 0.92$ ) with the class  $> 16 \mu\text{m}$ . The correlation with the  $> 8 \mu\text{m}$  class and the  $> 32 \mu\text{m}$  class is also good ( $r = 0.89$  and  $r = 0.90$ ). The correlations slightly decrease with increasing particle size.

*Bienen 8*

The basis plots of the Bienen 8 core segment (Figure 6-7) of the Zr/Rb ratio and the > 8 µm class show a similar overall trend and pattern of peak areas throughout depth. However, none of the peak areas are at the exact same depth, they are all shifted. The two major grain size peaks, at 659 cm and at 683 cm both correspond with a slightly shifted Zr/Rb ratio peak. The same shift can be applied to the general pattern of grain size peaks to fit the corresponding Zr/Rb ratio plot.



A shift was applied to fit the peak area of the plots. Therefore we recalibrated the Zr/Rb ratio data; all data points are allocated to a new depth, that of 1 cm less deep than the original depth.

**Table 6-7 Correlation matrix for Bienen 8.** Original and shifted data.

	>8µm	>16µm	>32µm	>64µm
Original	0,19721	0,242569	0,227442	0,154496
Shifted	0,667298	0,706786	0,676712	0,581338

Table 5-6 shows the correlation matrix of the different grain size fractions with the Zr/Rb ratio after we performed the recalibration. The correlation of the Zr/Rb ratio goes best ( $r = 0.71$ ) with the class > 16 µm. The correlations decrease with increasing particle size.

*Bienen 9*

The basic plots of the Bienen 9 core segment (Figure 6-8) show a similar pattern, although some grain size peak areas (at 745 cm and 791 cm) are dislocated (shifted). The grain size peak at 771 cm and the majority of the minor peaks do correspond quite well with the Zr/Rb ratio plot. However, the Zr/Rb ratio peak at 783 cm does not have its equivalent in the grain size plot.

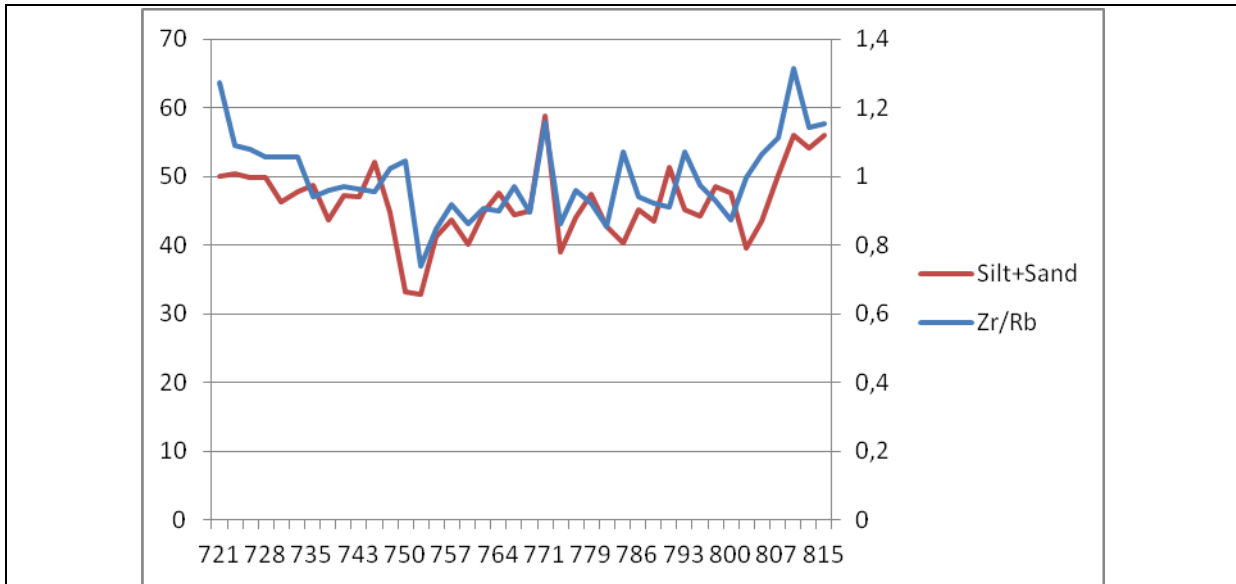


**Figure 6-8 Basic correlation plots of Bienen 9**

Horizontal axis represents depth (cm), vertical axis represents Silt+Sand (%) and Zr/Rb ratio.

**Table 6-8 Correlation matrix for Bienen 9.**

	>8um	>16um	>32um	>64um
Original	0,601645	0,630126	0,599367	0,4238

Figure 6-8 shows the correlation matrix of the different grain size fractions with the Zr/Rb ratio after we performed the shift. Although there is no outstanding correlation, the Zr/Rb ratio correlates best ( $r = 0.63$ ) with the class  $> 16 \mu\text{m}$ . The correlations decrease with increasing particle size.

*Bienen 10*

The basic plots of the Bienen 10 core segment (Figure 6-9) show a similar trend, but the plots of both grain size and the Zr/Rb ratio do not correspond. No equivalent peak areas are visible. One major peak (829 cm) in the Zr/Rb plot does not have an equivalent in the grain size plot. At 845 cm there is a peak in both of the plots. No shift could be used to improve the fit of the two plots.

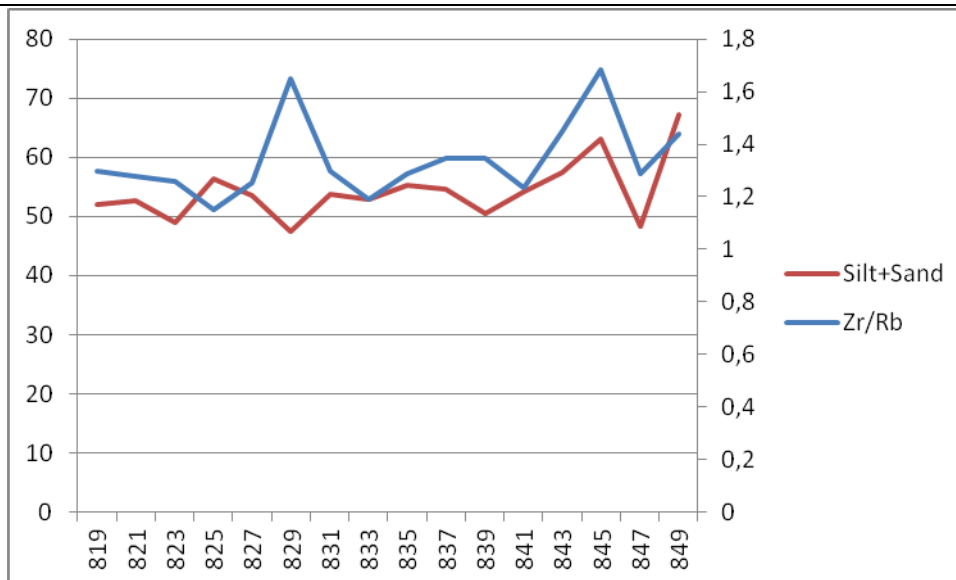


**Figure 6-9 Basic correlation plots of Bienen 10**

Horizontal axis represents depth (cm), vertical axis represents Silt+Sand (%) and Zr/Rb ratio.

**Table 6-9 Correlation matrix for Bienen 10.**

	>8um	>16um	>32um	>64um
Original	0,28399	0,274286	0,218542	0,13276

Table 6-9 shows the correlation matrix of the different grain size fractions with the Zr/Rb ratio. The correlations are weak ( $r < 0.28$ ) and decrease with increasing particle size.

#### 6.2.4. Upstream Rhine cores

Appendix 9 provides the combined grain size data and elemental data for the upstream cores. For none of the upstream cores, a good correlation between grain size and Zr/Rb ratio was found.

#### 6.2.5. Discussion

The normalized data show that the elemental counts for each of the Bienen core segments are not continuous. Variations in scan results are caused by the different settings under which each of the core segments were scanned. To set up a relation between the grain size data and the chemical composition data, the separate core segments were consequently used to calculate correlation coefficients. Different chemical proxies were tested for their correlation with the sandy grain size classes ( $> 8 \mu\text{m}$ ,  $> 16 \mu\text{m}$ ,  $> 32 \mu\text{m}$ , and  $> 64 \mu\text{m}$ ). The correlation coefficients for the Bienen core segments shows that the Zr/Rb ratio best correlates with the grain size fractions.

Subsequently, the Zr/Rb ratio were correlated with the different grain size fractions by means of plotting the graphs and calculating the correlation coefficients. For some core segments (Bienen 4, Bienen 6, Bienen 7, and Bienen 9), a relation was clearly detectable. For core segments

Bienen 3, Bienen 5, and Bienen 8 the correlation coefficients were increased by shifting the chemical composition data. The shifts were needed to correct for shrinking of the core segments, that might have occurred during transport and storage, or as a result of desiccation or scan settings. After the shifts were applied, good correlation coefficients were also obtained for the remaining core segments.

The resulting correlation coefficients show that in general the Zr/Rb ratio is a good indicator for the sandy grain size fraction. A quantified correlation was set up for each of the core segments. Highest correlations were found with the grain size classes  $> 8 \mu\text{m}$ ,  $> 16 \mu\text{m}$  for most of the Bienen core segments (Bienen 4 - Bienen 10). Although the Zr/Rb ratio is correlated with the sandy class ( $> 63 \mu\text{m}$ ), a better relation is obtained when the silty grain size fraction is included in the correlation. Correlations coefficients vary per core segment, therefore a statistical relationship significant for the continuous Bienen coring could not be set up.

Anomalies occur between the plots of the silt and sand grain size fractions and the Zr/Rb plots; some peaks in the Zr/Rb plots are not visible in the grain size data. Possible explanations for these anomalies include the grain size sampling strategy (5.1.1) and the fact that small sandy layers could not be identified as these do not stand out in the grain size average (see 6.1.3). However, the corresponding peaks in both data sets represented some of the major sandy layers and could thus be used to match the data sets.

Making use of the Zr/Rb ratio as a chemical proxy for grain size, and taking into account the shifts that were performed, the flood events (detected in the grain size data) were also identified in the chemical composition data. For the upstream cores, no strong relations were found between grain size data and chemical composition data. This could be explained by the relative low sampling resolution on grain size (and, after bulking) chemical composition data; minor layers could not stand out in averages and were thus not reflected in the plots. As a result, no flood events were identified in the upstream cores.

### 6.3. Correction of clay content

#### 6.3.1. Correlation matrices

Appendix 1 provides the correlation matrices representing the intercorrelation of elements for each of the core segments based on the non-bulked normalized data as well as the bulked normalized data. Although the first version (non-bulked) has a higher resolution, the correlation of elements is better shown in the bulked version. Therefore, we find the latter in the tables below (Figure 6-11), in which strong correlations are highlighted in orange. Elements Si, Ti and K are strongly correlated in most of the core segments. This group of elements also correlate quite well with elements Fe and Rb. Other correlations include Mn and Fe, and Ca and Sr. However these correlations were not strong in all core segments, i.e. they are not continuous throughout depth.

Bienen 3	Si	K	Ca	Ti	Mn	Fe	Rb	Sr	Zr	Pb
Si	1,000									
K	0,938	1,000								
Ca	0,758	0,814	1,000							
Ti	0,953	0,992	0,775	1,000						
Mn	0,737	0,769	0,730	0,764	1,000					
Fe	0,890	0,980	0,771	0,974	0,826	1,000				
Rb	0,876	0,959	0,685	0,956	0,653	0,945	1,000			
Sr	0,560	0,589	0,898	0,538	0,564	0,535	0,466	1,000		
Zr	-0,223	-0,495	-0,480	-0,428	-0,384	-0,574	-0,494	-0,348	1,000	
Pb	0,246	0,146	0,070	0,201	0,205	0,111	0,107	0,043	0,483	1,000

Bienen 4	Si	K	Ca	Ti	Mn	Fe	Rb	Sr	Zr	Pb
Si	1,000									
K	0,885	1,000								
Ca	0,070	0,009	1,000							
Ti	0,889	0,976	-0,053	1,000						
Mn	0,450	0,427	0,048	0,466	1,000					
Fe	0,660	0,876	0,071	0,832	0,606	1,000				
Rb	0,729	0,889	-0,137	0,860	0,168	0,729	1,000			
Sr	0,206	0,050	0,565	0,032	0,277	0,192	-0,239	1,000		
Zr	0,185	-0,114	-0,274	0,026	0,002	-0,413	-0,101	-0,106	1,000	
Pb	0,255	0,130	-0,535	0,277	0,288	-0,049	0,116	-0,326	0,611	1,000

Bienen 5	Si	K	Ca	Ti	Mn	Fe	Rb	Sr	Zr	Pb
Si	1,000									
K	0,723	1,000								
Ca	-0,066	-0,338	1,000							
Ti	0,721	0,920	-0,476	1,000						
Mn	0,138	0,014	0,418	-0,005	1,000					
Fe	0,431	0,645	-0,229	0,678	0,564	1,000				
Rb	0,444	0,692	-0,610	0,746	-0,212	0,435	1,000			
Sr	-0,128	-0,443	0,764	-0,459	0,367	-0,349	-0,588	1,000		
Zr	0,389	-0,051	0,128	0,135	-0,132	-0,302	-0,038	0,303	1,000	
Pb	0,100	0,287	-0,254	0,324	0,130	0,369	0,367	-0,253	-0,235	1,000

Bienen 6	Si	K	Ca	Ti	Mn	Fe	Rb	Sr	Zr	Pb
Si	1,000									
K	0,862	1,000								
Ca	0,056	-0,209	1,000							
Ti	0,800	0,974	-0,321	1,000						
Mn	0,148	0,398	-0,068	0,342	1,000					
Fe	0,692	0,924	-0,166	0,895	0,622	1,000				
Rb	0,549	0,797	-0,127	0,823	0,224	0,768	1,000			
Sr	0,368	0,328	0,059	0,298	0,240	0,272	0,048	1,000		
Zr	0,075	-0,130	-0,121	-0,009	-0,578	-0,364	-0,070	0,142	1,000	
Pb	0,426	0,574	-0,398	0,653	0,150	0,475	0,524	0,220	0,232	1,000

Bienen 7	Si	K	Ca	Ti	Mn	Fe	Rb	Sr	Zr	Pb
Si	1,000									
K	0,489	1,000								
Ca	0,356	0,071	1,000							
Ti	0,611	0,888	-0,007	1,000						
Mn	-0,258	0,134	0,328	-0,009	1,000					
Fe	-0,134	0,687	0,024	0,486	0,640	1,000				
Rb	0,108	0,718	-0,572	0,615	-0,084	0,544	1,000			
Sr	0,499	0,031	0,916	0,035	0,093	-0,148	-0,537	1,000		
Zr	0,468	-0,371	0,106	-0,012	-0,453	-0,754	-0,442	0,330	1,000	
Pb	-0,107	0,107	-0,285	0,078	-0,016	0,101	0,218	-0,300	-0,138	1,000

Bienen 8	Si	K	Ca	Ti	Mn	Fe	Rb	Sr	Zr	Pb
Si	1,000									
K	0,142	1,000								
Ca	0,102	-0,151	1,000							
Ti	-0,119	0,935	-0,174	1,000						
Mn	-0,045	0,530	0,105	0,515	1,000					
Fe	-0,256	0,814	-0,138	0,886	0,708	1,000				
Rb	-0,188	0,688	-0,335	0,735	0,259	0,716	1,000			
Sr	0,371	0,132	0,555	-0,010	0,228	-0,107	-0,359	1,000		
Zr	0,186	0,006	0,343	0,055	-0,286	-0,225	-0,334	0,435	1,000	
Pb	0,104	0,201	-0,192	0,190	0,048	0,122	0,205	-0,222	-0,018	1,000

Bienen 9	Si	K	Ca	Ti	Mn	Fe	Rb	Sr	Zr	Pb
Si	1,000									
K	0,614	1,000								
Ca	0,723	0,449	1,000							
Ti	0,790	0,957	0,333	1,000						
Mn	0,479	0,579	0,257	0,643	1,000					
Fe	0,663	0,933	0,327	0,923	0,757	1,000				
Rb	0,741	0,963	0,402	0,949	0,589	0,936	1,000			
Sr	0,859	0,731	0,879	0,665	0,423	0,638	0,740	1,000		
Zr	0,756	0,537	0,460	0,632	0,334	0,396	0,573	0,635	1,000	
Pb	0,388	0,382	0,057	0,497	0,377	0,366	0,361	0,201	0,531	1,000

Bienen 10	Si	K	Ca	Ti	Mn	Fe	Rb	Sr	Zr	Pb
Si	1,000									
K	0,384	1,000								
Ca	0,111	0,069	1,000							
Ti	0,108	0,817	-0,467	1,000						
Mn	-0,307	0,268	0,100	0,240	1,000					
Fe	-0,311	0,576	-0,027	0,596	0,867	1,000				
Rb	-0,040	0,645	-0,596	0,936	0,028	0,425	1,000			
Sr	-0,150	0,011	0,933	-0,419	0,005	-0,034	-0,460	1,000		
Zr	0,293	0,176	-0,637	0,502	-0,537	-0,323	0,636	-0,535	1,000	
Pb	-0,164	0,380	-0,293	0,464	-0,005	0,217	0,556	-0,202	0,167	1,000

Figure 6-10 Correlation matrices for the Bienen cores

These correlation matrices show the intercorrelation of the selected elements of each of the Bienen cores (bulked). Elements that correlate well are highlighted (orange). Appendix 1 provides the raw data.

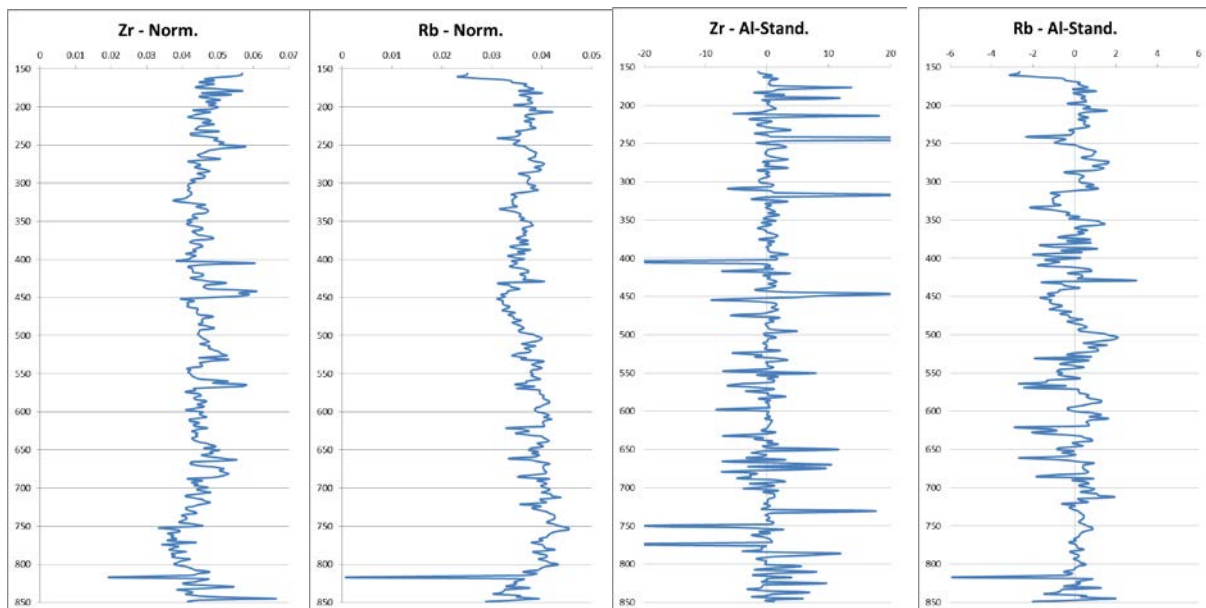
### 6.3.2. Al-standardized elemental data

Table 6-10 provides the correlation coefficients for  $^{13}\text{Al}$  with the clayey grain size classes ( $< 2 \mu\text{m}$ ,  $< 4 \mu\text{m}$ , and  $< 8 \mu\text{m}$ )(Appendix 6 provides raw data). Although  $^{13}\text{Al}$  does not correlate very well with any of the clayey grain size classes, the highest correlation coefficient is that with the class smaller than  $8 \mu\text{m}$ . Therefore  $^{13}\text{Al}$  is used as an indicator for the clay content and subsequently it was used to correct the chemical composition correct for the clay content.

**Table 6-10 Correlation coefficients of Al with grain size (clay) classes.**

Bienen Core segments	Grain size: clay classes		
	$< 2 \mu\text{m}$	$< 4 \mu\text{m}$	$< 8 \mu\text{m}$
3	0.0120	-0.0189	-0.0300
4	-0.1563	-0.2107	-0.2259
5	0.0637	-0.1222	-0.2004
6	-0.1568	-0.0942	-0.0289
7	0.0383	0.1553	0.2345
8	0.2598	0.2234	0.1714
9	0.1496	0.0905	0.0080
10	-0.0601	0.0041	0.0259
Bienen total:	0.1705	0.21800	0.2137

Figure 6-12 provides the plots of the Zr and Rb counts, corrected by the clay content (i.e. standardized by the Al content), merged to a continuous record of the coring. Appendix 2 provides the raw data of other elemental counts standardized by the Al content (Appendix 5 for the subcatchment cores). The plots are mainly characterized by the amount of Al counts, as we have learned the Zr and Rb counts remain relatively stable in each of the subcatchment cores.



**Figure 6-11 Graphs of the Zr and Rb counts.**

Plots of element occurrences of Zr and Rb. Left: normalized counts. Right: standardized by Al counts.



### *6.3.3. Discussion*

In this section two methods were applied in order to correct the chemical composition data for clay content. First, correlation matrices for the selected elements for each Bienen core segment indicated that there were no groups of elements that were associated with each other, throughout the Bienen core. Therefore, it was not possible to use such a group of elements in additional statistical methods that can be applied to correct for the clay content (Kylander et al., 2011). Second, the chemical proxy (6.2.2) was used to find the correlation coefficient of Al with the clayey grain size classes. Although Al does not correlate well with any of the clayey grain size classes, we did use Al to standardize the chemical composition data. No other indicator for the clay content was found, and to be able to trace the origin of flood, the chemical composition of flood events has to be corrected for the clay content.

## *6.4. Fingerprinting upstream catchments*

### *6.4.1. Handheld XRF data*

Appendix 4 provides the data resulting from the handheld XRF scans. Six elements remain usable for further research, these include Sr, Rb, Pb, Zn, Fe and Mn (i.e. these do not exceed 15% error margin). Elemental occurrence at all locations were plotted on a Rhine kilometers axis and were sorted by subcatchment area.

Figure 6-12 shows the occurrence of the selected elements six elements, Sr, Rb, Pb, Zn, Fe and Mn. The occurrence of Pb shows an interesting trend. The amount of Pb present in the Moselle samples is relatively high compared to the other regions, although there are some variations per location. When the Moselle conflues with the Rhine the amount of Pb present in the Rhine (at 613 km) instantly increases. However, further downstream the amount of Pb decreases. The amount of Pb is influenced by pollution; especially in the catchment of the Moselle the impact of pollution is represented well by an increased occurrence of Pb. The same trend is found in the Zn plots; the amount of Zn in the Moselle is relatively high causing an increase of the Zn level in the Rhine after its confluences with the Moselle. For Zn, we see the same effect (to a lesser extent) after the Main confluences with the Rhine. This might also be due to pollution. The Rb rates remain quite constant throughout the Rhine River course, but the amount of Zr seems to be relatively high in the Upper Rhine while it is relatively low in all of the tributaries. The amount of Zr in the Rhine decreases with Rhine kilometers. The amount of Fe and Mn is too dependent on soil conditions to make any conclusions about changes in presence throughout the Rhine catchment.

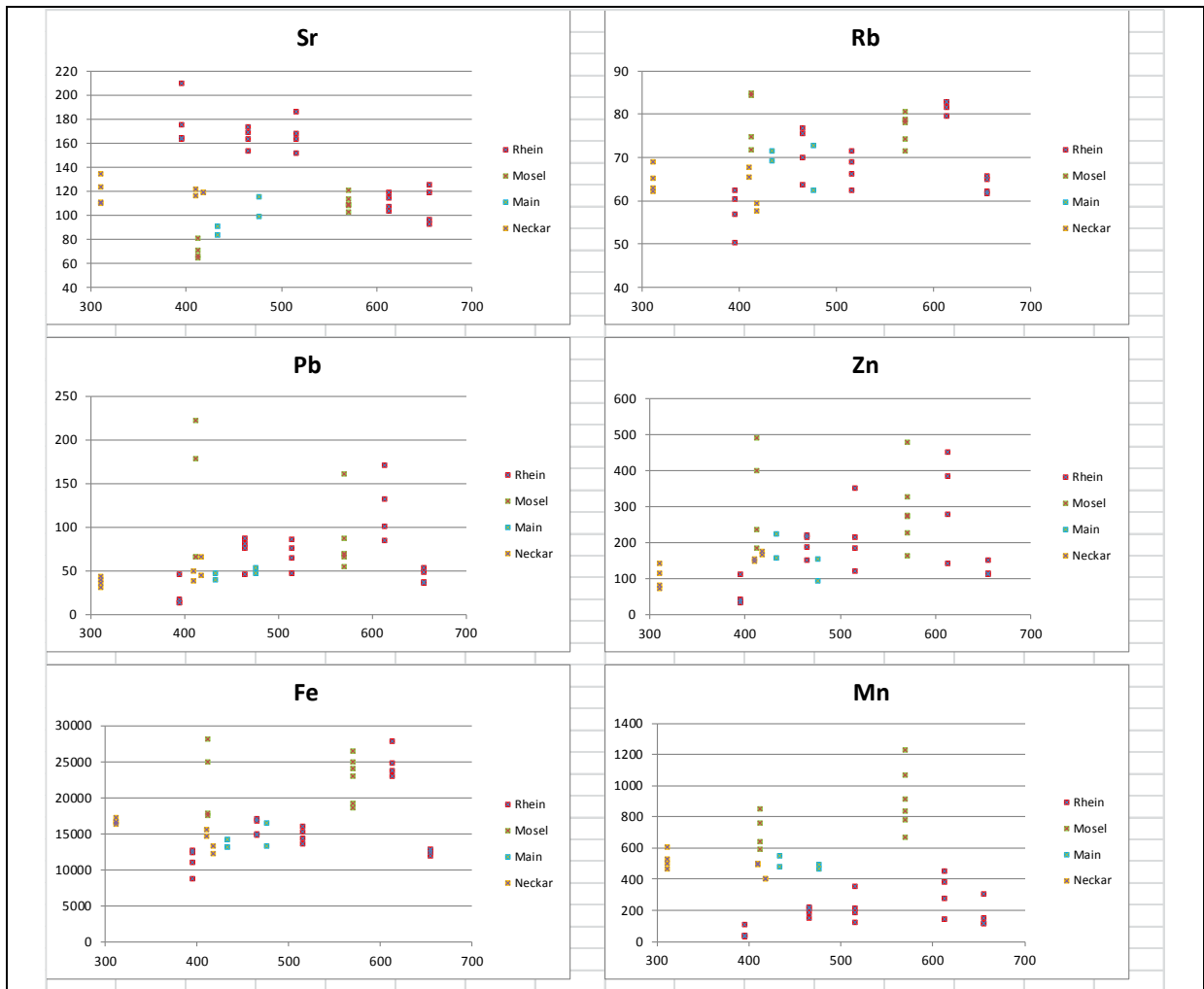


**Figure 6-12 Element occurrence versus Rhine kilometers**

Graphs representing the occurrence of the selected six elements (Sr, Rb, Pb, Zn, Fe and Mn) versus Rhine kilometers. In red is the Rhine River (Rhein), green the Moselle River, blue the Main River and yellow the Neckar River. On the vertical axis are the occurrences (in ppm) of the elements, on the horizontal axis are the Rhine kilometers. For the tributaries, this axis represents the relative Rhine kilometers.

#### 6.4.2. Characterizing subcatchments

The tables in 5 provide the characteristic elemental composition for each of the subcatchments. The first part is the data obtained from the XRF scan of the pre-industrial cores (Appendix 5), the second part is the data obtained from the handheld XRF scan performed on the post-industrial samples (Appendix 4 and Appendix 5). Fe and Mn were excluded from the fingerprint (section 6.4.3). Table 6-11 provides the occurrences of the remaining set of elements, which includes Sr, Rb, Pb and Zn.

**Table 6-11 Occurrences of trace elements in subcatchments**

Occurrences of trace elements, grouped per subcatchment, sampling location and sampling method. Pre-industrial cores are in normalized and Al-standardized elemental counts, post-industrial surface samples are in ppm. Raw data are provided in Appendix 5.

Subcatchment	XRF data used	Standardized (Al) element counts			
		Sr	Rb	Pb	Zn
Upper Rhine	Romerberg	413.8	119.3	10.6	33
	<i>Surface samples</i>	145,8	68,3	65,6	179,5
Neckar	Lauffen	212.3	84.7	5.8	18.2
	<i>Surface samples</i>	119,4	63,7	43,2	132,0
Main	Sindlingen	204.8	143.9	29	61.8
	Klein Krotzenburg	109.5	128.4	8.3	29.6
	<i>Surface samples</i>	97,7	69,0	46,4	157,4
Moselle	Kenn	90.5	135.4	16.6	78.7
	<i>Surface samples</i>	94,7	77,7	103,6	305,1

Based on the results shown in figure 6-11 the following remarks can be made:

- The most upstream subcatchments (Upper Rhine and Neckar) are characterized by a relative high amount of Sr, while the amounts of both Zn and Pb are low to average.
- The amount of Zn increases in downstream direction. Whereas Zn counts are low in the Upper Rhine and Neckar, they are high in the Main and Moselle catchments.
- When we compare the two cores from the Main; we see that the downstream core (Sindlingen) is characterized by much higher amounts of both Pb and Zn. Note that Sindlingen is located downstream of Frankfurt am Main while Klein Krotzenburg is located upstream of this industrialized area.
- The Moselle catchment is characterized by a low amount of Sr and average to high amount Rb. More important are the high amounts of Pb and Zn.

#### 6.4.3. Discussion

To construct a fingerprint for each of the subcatchments, a series of requirements should be satisfied. In this study corings and surface samples were used to determine the chemical composition of floodplain depositions. The interpretation of changes in these chemical composition data solely as a result of changes of the chemical composition of sediment (as deposited in the floodplain) and/or as a results of varying grain size, would be an oversimplification. As stated in chapter 3, the complex patterns caused by both horizontal and vertical processes, might have influenced the results of the chemical composition analysis in the study. By carefully selecting suitable sampling sites, and by using multiple surface samples from each subcatchment, the influence of these processes was

minimized. This way the set of elements do reflect the environmental control. However, the resulting set of elements can barely be regarded a fingerprint as it consists of only 4 trace elements making it hard to be discriminating potential sources.

Although on a Rhine River catchment scale the different source area are only subcatchments, in fact the catchment of these area are enormous. Therefore, the composition of material transported by the tributaries may differ per flooding event. Within each subcatchment another layer of tributaries determines the composition of material that is transported to the point of confluence with the Rhine. This might explain the variation and inconsistency of the composition of a series of floods from a subcatchment. Subsequently it is impossible to set up a fingerprint that is characteristic for a subcatchment.

Lacking a set of fingerprints meeting the criteria (5.2.5), a set of elements was selected that is present in all core material and thus reflects a chemical signal of both the pre- and post-industrial composition. This set of elements, including Sr, Rb, Pb and Zn, represents the chemical composition of the source areas and subsequently, it can be used to correlate with the (characteristic) chemical composition of flood events.

## 6.5. Tracing flood origin

### 6.5.1. Characterizing flood events

Six of the floods that were identified in the grain size data (section 6.1) were also identified in the chemical composition data. Table 6-12 shows this subselection of cross-correlated flood events. Note that one of the flood events could not be identified in the chemical composition data. The data of the 1850 A.D. flood event (239 cm) were lost in the shifting process (section 6.2), as this layer was at the bottom of the Bienen 3 core segment. Table 6-11 provides the chemical composition data (selected elements) of the remaining five flood events (Appendix 7 provides raw data).

**Table 6-12 Selection of flood events..**

Depth (cm)	Core (#)	Flood event (year A.D.)	Sand (%)	Silt+Sand (%)	Zr/Rb
446	Bienen 6	1784	12,63	67,9	1,846883
560	Bienen 7	1729	7,83	65,04	1,42952
564	Bienen 7	1726	8,48	70,58	1,673995
659	Bienen 8	1682	50,39	79,71	1,555375
683	Bienen 8	1671	16,32	63,03	1,400364

**Table 6-13 Chemical composition of selected flood events.** Appendix 7 provides raw data.

Depth (cm) Flood event (year A.D.)		Standardized (Al) element counts.										
		Si	K	Ca	Ti	Mn	Fe	Rb	Sr	Zr	Pb	Zn
446	1784	12,9	142,7	553,5	152,5	95,1	5932,1	135,8	190,9	250,8	15,1	36,5
560	1729	12,6	117,7	314,5	100,7	128,3	4819,8	77,2	87,1	84,5	5,7	21,0
564	1726	19,1	174,0	318,5	159,9	157,9	6868,8	118,1	121,7	133,3	11,2	35,6
659	1682	28,0	296,9	1443,0	249,4	291,3	10020,9	197,2	343,8	306,7	21,0	51,3
683	1671	23,8	276,5	1130,4	243,6	318,9	11027,5	195,4	309,9	273,6	17,0	51,8

When we take a closer look at table 6-13, the following remarks can be made. The 1784 flood event has average occurrences of Sr, Rb and Zn. The flood events from the years 1729 and 1726 show a similar pattern: both have relatively low Sr occurrence and relatively high Zn occurrence. Rb occurrences are average for these flood events. The last two flood events (1682 and 1671) both have a relatively high Sr occurrence, Rb and Zn occurrences are average.

**Table 6-14 Occurrence of trace elements in flood events**

Occurrence of trace elements in percentage for each of the historical flood events that we could correlate with the elemental data using the Zr/Rb ratio.

Depth (cm)	Corresponding flood event (year A.D.)	Elemental counts (normalized, Al-standardized)			
		Sr	Rb	Pb	Zn
446	1784	190,9	135,8	15,1	36,5
560	1729	87,1	77,2	5,7	21,0
564	1726	121,7	118,1	11,2	35,6
659	1682	343,8	197,2	21,0	51,3
683	1671	309,9	195,4	17,0	51,8

### 6.5.2. Allocating flood origins

When we compare the characteristic catchment compositions (table 5-12) with the characteristic flood composition (table 6-14) the following conclusions can be drawn concerning the allocation of flood origins:

- The combination of high values for Sr with low values for Pb and Zn, suggests that both the 1671 and the 1682 floods have an origin high upstream in the Rhine catchment; the sediment is likely to be deposited during floods originating from the Upper Rhine and Neckar.
- The combination of low Sr values and high Zn values suggest that both the 1726 and the 1729 floods are mainly composed by Moselle sediment; this sediment is likely to be deposited by a flood consisting of a high discharge from the Moselle catchment.

### 6.5.3. Discussion

Making use of a chemical proxy, the chemical compositions of the selected flood events (6.1 and 6.2) were obtained. These data were compared to the specific chemical composition of each of the subcatchments, which was reflected in the occurrences of a selected set of elements. Subsequently an attempt was made to allocate each of the flood events to one of the subcatchments. As no real fingerprints were set up, this comparison was based on the occurrences of a set of only four elements. These sets of elements were not sufficient to make any distinct remarks about the chemical composition of the flood events, only some minor variations were detected (6.4).

The selected trace elements could not characterize the flood events, as the variations of presence in the flood events were too low. Moreover, in some cases an inconsistent amount of these elements were present when the standardized with the normalized data are compared. The latter is due to the standardization method that was used (6.3).

It was thus not possible to quantitatively locate the flood origins. Consequently, it was not possible to unravel the mixed contribution of the subcatchment to each of the floods. However, some remarks were made about the (partial) contribution of tributaries to the flood events. Although a system was developed in which the composition of downstream deposited sediment was compared with “fingerprints” of upstream source areas, both the downstream flood signal, and the upstream source area signals, could not be characterized distinctively. Therefore this system was not able to provide an estimate of the relative contributions of the source areas (subcatchments).

However, the chemical composition of sediment deposited during flood events along the Lower Rhine, is not only built up by its main tributaries. Although the Upper Rhine, Neckar, Main and Moselle largely determine the chemical composition of the sediment, there also a series of minor tributaries that confluence with the Rhine River on its way downstream. These tributaries dilute the Rhine discharge and can therefore cause additional variations in flood deposits along the Lower Rhine.

## 7. Conclusions and recommendations

Making use of historical sources and grain size analysis on the Bienener Altrhein palaeo-fill, a series of major flood events was identified. Together with knowledge obtained from previous research, the chemical composition of this core was used to set up a proxy for grain size. Analysis of the Bienener Altrhein coring has shown that Zr/Rb is a suitable proxy for grain size in flood plain sediments. When looking at the separate Bienen core segments and taking into account minor shifts, most of the peaks in the grain size data had a corresponding peak area in the Zr/Rb ratio data. These correlations were recorded in correlation coefficients, resulting in a qualitative relationship per core segments. However, to set up a qualitative relation for the whole core, instead of for the separate Bienen segments, a standardization method needs to be found to correct for the varying settings for each of the core segments.

In this study it is proved that chemical composition data can be used to derive grain size peaks from (and flood events, Winkels, 2011; Aloserij, 2013). This relationship was quantified by means of the Zr/Rb ratio as proxy. Combined with previous research (Aloserij, 2011; Toonen, 2013) Zr/Rb profiles can be used to reconstruct a history of flood events at flood plain sites with high resolution deposits (slack water environments). However, a more detailed (higher resolution) grain size analysis needs to be performed to detect all (minor) sandy layers and create a continuous flood record in the data set. Moreover, better results can be obtained by improving the sampling method.

No adequate method was found to standardize the data for clay content. By correcting the chemical composition for clay content, all cores can be filtered by the clayey grain size fractions, enabling a comparison between downstream and upstream flood deposits. Two methods were applied in order to find a way to correct for the clay content. First, the construction of correlation matrices did not result in any group of elements that clustered throughout the Bienen core. The other method, involved the correlation of Al with the clayey grain size fractions and use this relation to correct for the clay content. Although, the relation of Al with clay, qualified with correlation coefficients, was not good, we have used this standardization method. A better standardization method, is of vital importance for the succeeding of the second part of this research. Therefore, additional research is needed to set up an adequate standardization method.

The next part of this research included the characterization of the subcatchments. Based on the corings and surface samples, we characterized each of the subcatchments. Although there were some minor differences in the chemical composition of the different subcatchment, it was not possible to set up characteristic fingerprints for the subcatchments. However, based on set of

elements that occurred in both the cores and the surface samples, some remarks were made regarding the characteristics of the subcatchments. The Upper Rhine and the Neckar are characterized by a high amount of Sr and low to average amounts of Zn and Pb. Moreover, sediment deposited by the Moselle is characterized by a low amount of Sr and high amounts of Pb and Zn.

Making use of the Zr/Rb ratio as a proxy, selected flood events were detected in the normalized and standardized (i.e. corrected for the clay content) chemical composition data. Although the variation of presence of these elements in the flood events was not high, a few remarks could be made regarding the characterization of these flood events. The flood events from the years 1729 and 1726 both have relatively low Sr occurrence, while the two flood events from the years 1682 and 1671 both have a relatively high Sr occurrence.

The combination of the characterizations of the subcatchments and the floods have led to the following suggestions: (1) the 1671 and 1682 floods are likely to have an origin in the Upper Rhine and Neckar catchments (due to high Sr values combined with low Pb and Zn values), and (2) the 1726 and 1729 floods are likely to originate from the Moselle catchment (due to the combination of low Sr values and high Zn values). Whereas we aimed for a quantitative calculation of the contribution to floods from each of the subcatchments, we can conclude that for now only a qualitative contribution can (partially) be obtained.

An additional conclusion can be made regarding pollution, which specifically had its effect on the sediment transported by the Moselle. Pb (and Zn) occurrences in the Moselle are higher than in the other tributaries. These results were found in the data from the cores and in the handheld XRF data. The coring performed at the Sindlingen location, downstream of Frankfurt am Main, has higher amounts of Pb and Zn compared to the coring upstream of Frankfurt am Main (Klein Krotzenburg); the pollution from the industrialized area around the city of Frankfurt is thus reflected in the chemical composition of floodplain deposits.

This study was performed in the floodplains of the Lower Rhine and its tributaries in the Netherlands and Germany. The research area is therefore focused on a moderate to long meandering river with a mixed load and its tributaries, while previous studies on a similar topic (based on the infill of cut-off meanders) were performed on a much smaller scale (Peart and Walling, 1986; Passmore and Macklin, 1994). The results of this study, i.e. the relation between the Zr/Rb ratio and grain size and the (quantitative) relation used to allocate flood origin, have yet to be applied in other study areas. Different results might be expected for sedimentary environments with another drainage basin, climate settings, river valley morphology and sediment transported.



A last recommendation for further research includes the investigation of historic sources. Besides of the historic sources describing flood events in the Rhine River, flood propagation throughout the Rhine catchment should be mapped. Analysis of historic sources from each of the tributaries can be used to map flood events throughout the subcatchments. Combining flood propagation of each of the subcatchments in a model, will create an overview of flood propagation throughout the Rhine catchment.

## **Acknowledgements**

Facilities for grain size analysis were provided by the Vrije Universiteit Amsterdam (NL), thanks go out to Maarten Prins who helped us operating the grain size scanning device. Facilities for XRF analysis were provided by the Aberystwyth University (Wales, UK). I want to thank Sarah Rassner and Simon Foulds for helping us to understand and operate both XRF devices. Special thanks go out to Mark Macklin, as we could stay at his house during our visit at Aberystwyth.

I would like to thank Hans Middelkoop, Marcel van der Perk and Willem Toonen who accompanied me during the fieldwork in Germany. I also want to thank Willem Toonen (again) and Joost Aloserij with their help during my data collection in the Netherlands. Regarding these field trips, thanks also go out to Chris Roosendaal and Hans van Aken, who helped me preparing the necessary equipment.

I am grateful to Marcel van der Perk and Kim Cohen for their supervision and assistance during the preparation and writing of this thesis. Special thanks also go out for again Willem Toonen, he not only supported me writing the report and performing the research, I also had a great time with Willem during our trips to Germany, Wales, Amsterdam and at our own Utrecht University. Besides of their constructive comments of on earlier versions of this report, I also want to thank Marcel, Kim and Willem for the patience that they have had with me finishing this report.

My thanks also go out to the numerous people that have accompanied me during the writing stage of this thesis. I have spent hours, days, weeks, months and years in the GIS room with my co-students; without numerous coffee breaks with Marijn, Martijn, Niek, and especially Jonathan and Rik, I would probably still be there. Moreover I thank my friends; Bart, Bas, Bruno, Evelien, Jesse, Jonathan, Marlous, Martijn, Rik, Tristan and my family for their support during the last two and half years. Thank you!

## References

- Abadian, H., Lippmann, F. (1976) X-ray determination of brushite ( $\text{CaHPO}_4 \cdot 2\text{H}_2\text{O}$ ) suspended in the water of the Neckar River, West Germany. *Environmental Geology*, Vol. 1, No. 5, pp. 313-316
- Aloserij, L.H.J. (2013) Historical floods of the Rhine river, reconstructed from the sedimentary fills of a dike breach pond and abandoned channels: application for recalculation of the design discharge. MSc thesis, Faculty of Geosciences, Dept. of Physical Geography, Utrecht University.
- Asselman, N.E.M. (1997), Suspended sediment in the River Rhine – The impact of climate change on erosion, transport and deposition. Utrecht: Koninklijk Nederlands Aardrijkskundig Genootschap/faculteit Geowetenschappen, Universiteit Utrecht (Netherlands Geographical Studies, Vol. 234)
- Beeger, H. (1990), Upper Rhine Correction from Tulla to the Present Day (Staustufen, Polder, und Kein Ende. Die Ausbaumassnahmen am Oberrhein von Tulla Bis Heute). *Mitteilungen der Pollichia*, Vol. 77, pp 55-72.
- Berendsen, H.J.A., Stouthamer, E. (2001) Palaeogeographic development of the Rhine-Meuse delta. Assen: Van Gorcum, 270 pp.
- Berner, Z.A., Bleeck-Schmidt, S., Stüben, D., Neumann, T., Fuchs, M., Lehmann, M. (2012) Floodplain deposits: A geochemical archive of flood history – A case study on the River Rhine, Germany. *Applied Geochemistry*, Vol. 27, pp. 543-561.
- Brázdil, R., Demarée, G.R., Deutsch, M., Garnier, E., Kiss, A., Luterbacher, J., Macdonald, N., Rohr, C., Dobrovolný, P., Kolář, P., Chromá, K. (2009), European floods during the winter 1783/1784: scenarios of an extreme event during the 'Little Ice Age'. *Theoretical and applied climatology*, Vol. 100, pp. 163-189.
- Buhl, D., Neuser, R.D., Richter, D.K., Riedel, D., Roberts, B., Strauss, H., Veizer, J. (1991) Nature and Nurture: Environmental Isotope Story of the River Rhine. *Naturwissenschaften*, Vol. 78, pp. 337-346
- Calvert, S.E., Bustin, R.M., Ingall, E.D. (1996) Influence of water column anoxia and sediment supply on the burial and preservation of organic carbon in marine shales. *Geochimica et Cosmochimica Acta*, Vol. 60, pp. 1577-1593.
- Calvert, S.E., Pedersen, T.F., Karlin, R.E. (2001) Geochemical and isotopic evidence for post-glacial palaeoceanographic changes in Saanich Inlet, British Columbia. *Marine Geology*, Vol. 174, pp. 287-305.
- Chapron, E., Arnaud, F., Noël, H., Revel, M., Desmet, M., Perderau, L. (2005), Rhone river flood deposits in Lake Le Bourget: a proxy for Holocene environmental changes in the NW Alps, France. *Boreas*, Vol. 34, pp. 404-416.
- Christophersen, N., Hooper, R.P., (1992) Multivariate analysis of stream water chemical data: The use of principal components analysis for the end-member mixing problem. *Water Resources Research*, Vol. 28, No. 1, pp. 99-107
- Croudace, I.W., Rindby, A., Rothwell, R.G. (2006), ITRAX: description and evaluation of a new multi-function X-ray core scanner. *Geological Society, Special publications*, Vol. 267, pp. 51-63.
- Disse, M., Engel, H. (2001), Flood events in the Rhine Basin: Genesis, Influences and Mitigation. *Natural Hazards*, Vol. 23, No. 2-3, pp. 271-290.

- Dypvyk, H., Harris, N.B. (2001) Geochemical facies analysis of fine-grained siliclastics using Th/U, Zr/Rb and (Zr + Rb)/Sr ratios. *Geochemical geology*, Vol. 181, pp. 131-146.
- Edel, J.B., Fluck, P. (1989), The upper Rhenish Shield basement (Vosges, Upper Rhinegraben and Schwarzwald): Main structural features deduced from magnetic, gravimetric and geological data. *Tectonophysics*, Vol. 169, No. 4, pp. 303-316.
- Erkens, G. (2009) Sediment dynamics in the Rhine catchment: quantification of fluvial response to climate change and human impact. *Netherlands Geographical Studies*, Vol. 388, 278 pp.
- Foulds, S.A., Brewer, P.A., Macklin, M.G., Haresign, W., Betson, R.E., Rassner, S.M.E. (2014) Flood-related contamination in catchments affected by historical metal mining: An unexpected and emerging hazard of climate change. *Science of the Total Environment*, Vols. 476-477, pp. 165-180.
- Frings, R.M. (2007) From gravel to sand. Downstream fining of bed sediments in the lower river Rhine. PhD thesis, Utrecht University, *Netherlands Geographical Studies*, Vol. 368, 220 pp.
- Gerbersdorf, S.U., Jancke, T., Westrich, B. (2005), Physico-chemical and biological sediment properties determining erosion resistance of contaminated riverine sediments – Temporal and vertical pattern at the Lauffen reservoir/River Neckar, Germany. *Limnologica – Ecology and Management of Inland Waters*, Vol. 25, No. 3, pp. 132-144
- Hantke, R. (1993) *Flussgeschichte Mitteleuropas: Skizzen zu einer Erd-, Vegetations- und klimageschichte der letzten 40 Millionen Jahre*. Ferdinand Enke Verlag Stuttgart.
- Herget, J., Bremer, E., Coch, T., Dix, A., Eggenstein, G., Ewald, K. (2005) Engineering impact on river channels in the river Rhine catchment. *Erdkunde*, Vol. 59, pp. 294-319.
- Hoffmann, T., Erkens, G., Cohen, K.M., Houben, P., Seidel, J., Dikau, R. (2007) Holocene floodplain sediment storage and hillslope erosion within the Rhine catchment. *The Holocene*, Vol. 17, pp. 105-118.
- Jenkins, R., De Vries, J.L. (1970), *Practical X-ray spectrometry*. Macmillan, London
- Jones, A.F., Brewer, P.A., Macklin, M.G. (2009), Geomorphological and sedimentological evidence for variations in Holocene flooding in Welsh river catchments. *Global and planetary Change*, Vol. 70, pp. 92-107.
- Jones, A.F., Lewin, J., Macklin, M.G. (2010), Flood series data for the later Holocene: Available approaches, potential and limitations from UK alluvial sediments. *The Holocene*, Vol. 20, pp. 1123-1135.
- Jones, A.F., Macklin, M.G., Brewer, P.A. (2012) A geochemical record of flooding on the upper River Severn, UK, during the last 3750 years. *Geomorphology*, Vol. 179, pp. 89-105.
- Jonkers, L., Prins, M.A., Brummer, G.J., Konert, M., Lougheed, B.C., (2009), Experimental insights into laser diffraction particle sizing of fine-grained sediments for use in palaeoceanography. *Sedimentology*, Vol. 56, No. 7, pp. 2192-2206.
- Konert, M., Vandenberghe, J. (1997) Comparison of laser grain size analysis with pipette and sieve analysis: a solution for the under-estimation of the clay fraction. *Sedimentology*, Vol. 4, pp. 115-124.
- Kylander, M.E., Ampel, L., Wohlfarth, B., Veres, D. (2011) High-resolution x-ray fluorescence core scanning analysis of Les Echets (France) sedimentary sequence: new insights from chemical proxies. *Journal of Quaternary Science*, Vol.26, pp. 109-117
- Lamb, H., Davies, S., Kelly, D., (2005), Using the Itrax XRF core scanner at Aberystwyth, pp. 6.

- Lammersen, R., Engel, H., Langemheen, van de, W., Buiteveld, H. (2002) Impact of river training and retention measures on flood peaks along the Rhine. *Journal of hydrology*, Vol. 267, pp. 115-124.
- Macklin, M.G., Benito, G., Gregory, K.J., Johnstone, E., Lewin, J., Michczyńska, D.J., Soja, R., Starkel, L., Thorndycraft, V.R. (2006), Past hydrological events reflected in the Holocene fluvial record of Europe, *Catena*, Vol. 66, pp. 145-154.
- Middelkoop, H. (1997), Embanked floodplains in the Netherlands: Geomorphological evolution over various time scales. Utrecht: Koninklijk Nederlands Aardrijkskundig Genootschap/faculteit Geowetenschappen, Universiteit Utrecht (Netherlands Geographical Studies, Vol. 224)
- Middelkoop, H. (2000), Heavy-metal pollution of the Rhine and Meuse floodplains in the Netherlands. *Netherlands Journal of Geosciences*, Vol. 79, No. 4, pp. 411-428.
- Middelkoop, H. (2002), Reconstructing floodplain sedimentation rates from heavy metal profiles by inverse modeling. *Hydrological processes*, Vol. 16, No. 1, pp. 47-64.
- Middelkoop, H., Erkens, G., Van der Perk, M. (2010), The Rhine delta – a record of sediment trapping over time scales from millennia to decades. *Soils Sediments*, Vol. 10, pp. 628-639.
- Oldfield, F., Wake, R. Boyle, J., Jones, R., Nolan, S., Gibbs, Z., Appleby, P., Fisher, E., Wolff, G. (2003) the Late-Holocene history of Gormire Lake (NE England) and its catchment: a multiproxy reconstruction of past human impact. *The Holocene*, Vol. 13, pp. 677-690.
- Passmore, D.G., Macklin, M.G. (1994) Provenance of fine-grained alluvium and late Holocene land-use change in the Tyne basin, northern England. *Geomorphology*, Vol. 9, pp. 127-142
- Peart, M.R., Walling, D.E. (1986), Fingerprinting sediment source: the example of a drainage basin in Devon, UK. *Drainage basin sediment delivery*, IAHS no. 159, pp. 41-55.
- Richter, T.O., Van Der Gaast, S., Koster, B., Vaars, A., Gieles, R., De Stigter, H., De Haas, H., Van Weering, T.C.E. (2006), The Avaatech XRF Core Scanner: technical description and applications to NE Atlantic sediments. *Geological Society, London, Special Publications*, Vol. 267, pp. 39-50.
- Rijkswaterstaat (2005) Actueel Hoogtebestand Nederland (AHN). Rijkswaterstaat, Adviesdienst Geo-informatie en ICT, Delft.
- Silva, W., Klijn, F., Dijkman, J.P.M. (2001) Room for the Rhine branches in the Netherlands; What the research taught us. RIZA report, Vol. 031, 162 pp.
- Schneider, R.R., Price, B., Müller, P.J., Kroon, D., Alexander, I. (1997) Monsoon related variations in Zaire (Congo) sediment load and influence of fluvial silicate supply on marine productivity in the east equatorial Atlantic during the last 200,000 years. *Paleoceanography*, Vol. 12, pp. 463-481.
- Støren, E.N., Dahl, S.O., Nesje, A., Paasche, Ø. (2010), Identifying the sedimentary imprint of high-frequency Holocene River floods in lake sediments: development and application of a new method. *Quaternary Science Reviews*, Vol. 29, pp. 3021-3033.
- Syvitski, J.P.M., (1991), *Principles, Methods, and Application of Particle Size Analysis*. Cambridge University Press, Cambridge, 388 pp.
- Toonen, W.H.J., Kleinhans, M., Cohen, K. (2012), Sedimentary architecture of abandoned channel fills. *Earth Surface Processes and Landforms, Special Issue Paper*, 42 pp.

- Toonen, W.H.J. (2013) A Holocene flood record of the Lower Rhine. Utrecht studies in Earth Sciences, Volume 041, 204 pp.
- Thonon, I. (2006) Deposition of sediment and associated heavy metals on floodplains. Nederlandse Geografische studies/Netherlands Geographical Studies, Vol. 337, 174 pp.
- Van Andel, T.H. (1950) Provenance, transport and deposition of rhine sediments: a heavy mineral study on river sands from the drainage area of the Rhine catchment. Wageningen, Dissertation Groningen University, 129 pp.
- Van Andel, T.H. (1958) A defense of the term alterite. Journal of Sedimentary Petrology, Vol. 28, No. 2, pp. 234-235.
- Vink, R.J., Behrendt, H., Salomons, W. (1999), Point and diffuse source analysis of heavy metals in the Elbe drainage area: Comparing heavy metal emissions with transport River loads. Hydrobiologia, Vol. 410, pp. 307-314.
- Vink, R., Behrendt, H. (2002), Heavy metal transport in large river systems: heavy metals emissions and loads in the Rhine and Elbe river basins. Hydrological Processes Vol. 16, pp. 3227-3244.
- Vorogushyn, S., Merz, B. (2012) What drives flood trends along the Rhine River: climate or river training? Hydrology and Earth System Sciences Discussions, Vol. 9, pp. 13537-13567.
- Walling, D.E., Woodward, J.C. (1992), Use of radiometric fingerprints to derive information on suspended sediment sources. Erosion and Sediment transport Monitoring Programmes in River Basins, IAHS no. 210, pp. 153-164.
- Walling, D.E., Woodward, J.C., Nicholas, A.P. (1993), A multi-parameter approach to fingerprinting suspended-sediment sources. Tracers in Hydrology, IAHS Publ. no. 215, pp. 329-337.
- Walling, D.E. (2005), Tracing suspended sediment sources in catchments and river systems. Science of the Total Environment, Vol. 344, pp. 159-184.
- Winkels, T.G. (2011) Flood reconstruction of sub-recent floods, based on the sedimentary record of the Bienener Altrhein. BSc thesis, Faculty of Geosciences, Dept. of Physical Geography, Utrecht University.
- Witt, W. Stübinger, T., List, J., (2010) Laser diffraction for particle size analysis at absolute precision. Sympactec GmbH, System-Partikel-Technik. 4 pp.

## **Appendices**

**Appendix 1 (A-H) Raw data from grain size and XRF scans (sorted by segment)**

**Appendix 2 Normalized counts of selected elements**

**Appendix 3 Sampling locations**

**Appendix 4 Handheld XRF elemental counts**

**Appendix 5 Normalized and standardized data for subcatchment cores**

**Appendix 6 Al standardization Bienen Cores**

**Appendix 7 Flood event data**

**Appendix 8 Correlation of grain size with Zr/Rb ratio (Bienen)**

**Appendix 9 Correlation of grain size with Zr/Rb ratio (Subcatchments)**

**Appendix 10 Standardized elemental data Bienen**

**Appendix 11 XRF settings**

Appendix 1 - Bienen 10 B

Depth	Real depth	%Clay	%Very Fine	%Fine Silt	%Coarse	%Very Fine	%Fine Sand	%Middle	%Coarse	%Very Coarse	Sand	Original				Shifted graph											
												>8um	>16um	>32um	>64um	Zr/Rb	Si/Al	Ti/Al	Zr/Al	Zr/Ti	Zr/Rb	Si/Al	Ti/Al	Zr/Al	Zr/Ti		
819	819	47.93	20.74	19.09	9.79	2.04	0.41	0	0	0	47.93	49.62	2.45	52.07	31.33	12.24	2.45	1.298183	32.2657	235.343	235.4541	1.000472	1.276342	15.42523	108.8621	110.7734	1.017556
821	821	47.37	20.22	19.16	9.63	2.75	0.87	0	0	0	47.37	49.01	3.62	52.63	32.41	13.25	3.62	1.276342	15.42523	108.8621	110.7734	1.017556	1.259673	16.88146	125.462	122.8967	0.979553
823	823	51.08	22.25	17.09	7.26	1.94	0.38	0	0	0	51.08	46.6	2.32	48.92	26.67	9.58	2.32	1.259673	16.88146	125.462	122.8967	0.979553	1.148672	18.2129	135.2645	126.7097	0.936755
825	825	43.64	18.79	17.91	11.18	4.43	2.49	1.55	0	0	43.64	47.88	8.48	56.35	37.56	19.65	8.48	1.148672	18.2129	135.2645	126.7097	0.936755	1.252195	17.71703	117.1923	114.8132	0.979699
827	827	46.44	18.85	18.09	11.49	4	1.1	0.03	0	0	46.44	48.43	5.13	53.56	34.71	16.62	5.13	1.252195	17.71703	117.1923	114.8132	0.979699	1.650056	25.01639	153.2295	250.0601	1.631932
829	829	52.6	19.89	16.63	7.91	2.55	0.43	0	0	0	52.6	44.42	2.98	47.41	27.52	10.89	2.98	1.650056	25.01639	153.2295	250.0601	1.631932	1.297267	23.209	161.6238	165.4244	1.023515
831	831	46.18	18.75	19.88	12.17	2.91	0.11	0	0	0	46.18	50.8	3.02	53.82	35.07	15.19	3.02	1.297267	23.209	161.6238	165.4244	1.023515	1.187727	18.72619	116.0446	112.9613	0.97343
833	833	47.1	19.77	18.79	10.85	3.32	0.18	0	0	0	47.1	49.4	3.5	52.91	33.14	14.35	3.5	1.187727	18.72619	116.0446	112.9613	0.97343	1.285529	25.292	154.92	162.424	1.048438
835	835	44.84	18.92	16.48	10.55	3.59	1.64	3.83	0.14	0	44.84	45.96	9.21	55.15	36.23	19.75	9.21	1.285529	25.292	154.92	162.424	1.048438	1.344235	21.34146	122.1433	134.8293	1.103861
837	837	45.29	20.49	16.95	9.65	3.02	1.33	3.08	0.19	0	45.29	47.09	7.62	54.71	34.22	17.27	7.62	1.344235	21.34146	122.1433	134.8293	1.103861	1.348158	24.54579	126.0916	144.2381	1.143915
839	839	49.62	21.93	18.29	8.64	1.52	0.01	0	0	0	49.62	48.86	1.53	50.39	28.46	10.17	1.53	1.348158	24.54579	126.0916	144.2381	1.143915	1.232656	15.46953	102.4492	102.7946	1.003371
841	841	45.81	19.34	18.99	11.82	3.63	0.41	0	0	0	45.81	50.15	4.04	54.19	34.85	15.86	4.04	1.232656	15.46953	102.4492	102.7946	1.003371	1.449206	24.16054	145.796	168.2776	1.154199
843	843	42.45	19.86	20.51	13.1	3.77	0.32	0	0	0	42.45	53.46	4.09	57.56	37.7	17.19	4.09	1.449206	24.16054	145.796	168.2776	1.154199	1.682148	23.30435	150.3288	185.6168	1.234739
845	845	36.93	18.43	22.21	17.04	5.01	0.38	0	0	0	36.93	57.68	5.4	63.07	44.64	22.43	5.4	1.682148	23.30435	150.3288	185.6168	1.234739	1.289475	17.80046	104.5092	105.6009	1.010446
847	847	51.59	22.57	16.85	7.14	1.65	0.21	0	0	0	51.59	46.55	1.86	48.42	25.85	9	1.86	1.289475	17.80046	104.5092	105.6009	1.010446	1.438752	30.23396	110.7094	146.0415	1.319142
849	849	32.78	14.11	12.35	7.82	3.38	2.44	12.71	14.05	0.36	32.78	34.28	32.94	67.22	53.11	40.76	32.94	1.438752	30.23396	110.7094	146.0415	1.319142					

		>8um	>16um	>32um	>64um
Original	Original	0.28399	0.274286	0.218542	0.13276
Shifted		0.221663	0.226339	0.236918	0.132516

	Original					Shifted				
	Zr/Rb	Si/Al	Ti/Al	Zr/Al	Zr/Ti	Zr/Rb	Si/Al	Ti/Al	Zr/Al	Zr/Ti
>8um	0.28399	0.352758	-0.05605	-0.00959	0.133732	0.221663	-0.18845	-0.20324	-0.07548	0.009488
>16um	0.274286	0.3675	-0.05816	0.017674	0.182604	0.226339	-0.17165	-0.10618	-0.00532	0.028711
>32um	0.218542	0.399188	-0.13576	-0.01443	0.241181	0.236918	-0.07363	-0.05624	0.055359	0.087992
>64um	0.13276	0.411224	-0.20095	-0.04766	0.27932	0.132516	0.041891	-0.01523	0.061863	0.09155













Appendix 1 - Bienen 7 B

Depth	Real depth	%Clay	%Very Fine	%Fine Silt	%Coarse S	%Very Fine	%Fine San	%Middle	C%	Coarse S	%Very Coarse	Sand	Clay	Silt	Sand	>8um	>16um	>32um	>64um	reversed Original				
																				Zr/Rb	Si/Al	Ti/Al	Zr/Al	Zr/Ti
545	531	43.03	19.14	19.57	13.31	4.44	0.51	0	0	0	43.03	52.03	4.95	56.97	37.83	18.26	4.95	1.476632	22.01515	146.3232	208.0859	1.422097		
547	533	48.06	20.2	17.19	10.2	3.9	0.44	0	0	0	48.06	47.59	4.35	51.93	31.73	14.54	4.35	1.188998	24	169.9226	150.6465	0.886556		
549	536	51.14	20.12	15.98	9.07	3.3	0.4	0	0	0	51.14	45.17	3.69	48.87	28.75	12.77	3.69	1.153813	15.53314	118.268	115.7205	0.97846		
551	538	49.46	20.22	16.71	9.84	3.41	0.36	0	0	0	49.46	46.77	3.77	50.54	30.32	13.61	3.77	1.195206	18.71071	143.6071	138.55	0.964785		
553	541	54.84	23.51	14.56	5.54	1.36	0.19	0	0	0	54.84	43.61	1.55	45.16	21.65	7.09	1.55	1.159216	11.69583	86.49375	79.46667	0.918756		
555	543	52.79	22.81	16.62	6.29	1.21	0.27	0	0	0	52.79	45.72	1.48	47.2	24.39	7.77	1.48	1.036847	14.82308	114.4077	90.69487	0.792734		
557	545	51.51	21.46	17.27	7.57	1.79	0.4	0	0	0	51.51	46.3	2.18	48.49	27.03	9.76	2.18	1.110693	18.95156	146.7024	126.6574	0.863363		
559	548	52.81	21.58	16.7	7	1.57	0.34	0	0	0	52.81	45.28	1.91	47.19	25.61	8.91	1.91	1.103164	23.68644	177.6356	152.0169	0.85578		
561	550	51.85	25.29	15.39	5.67	1.47	0.33	0	0	0	51.85	46.35	1.8	48.15	22.86	7.47	1.8	1.108722	14.5288	109.4476	95.14398	0.86931		
563	552	50.88	22.09	17.71	7.44	1.53	0.34	0	0	0	50.88	47.24	1.87	49.11	27.02	9.31	1.87	1.12649	16.27005	122.393	102.607	0.83834		
565	555	52.96	21.92	15.86	7.04	1.84	0.38	0	0	0	52.96	44.82	2.22	47.04	25.12	9.26	2.22	1.121668	18.58571	157.5071	133.6107	0.848284		
567	557	46.65	21.43	19.65	9.57	2.27	0.43	0	0	0	46.65	50.65	2.71	53.35	31.92	12.27	2.71	1.146752	14.13095	109.5095	93.02619	0.84948		
569	560	34.95	16.47	21.86	18.88	6.97	0.86	0	0	0	34.95	57.21	7.83	65.04	48.57	26.71	7.83	1.42952	21.85401	157.8212	161.1496	1.02109		
571	562	37.85	17.65	21.82	16.68	5.41	0.58	0	0	0	37.85	56.16	5.99	62.14	44.49	22.67	5.99	1.318132	19.1761	136.2358	128.3396	0.94204		
573	564	29.43	15.56	24.19	22.35	7.84	0.64	0	0	0	29.43	62.1	8.48	70.58	55.02	30.83	8.48	1.673995	19.49072	111.5358	126.6574	1.128112		
575	567	42.6	20.5	21.9	12.29	2.25	0.45	0	0	0	42.6	54.7	2.71	57.39	36.89	14.99	2.71	1.460346	17.0989	131.3929	130.2115	0.991009		
577	569	45.23	23.41	18.07	9.17	3.23	0.89	0	0	0	45.23	50.66	4.11	54.77	31.36	13.29	4.11	1.236536	15.32827	121.5532	109.845	0.903678		
579	571	48.21	26.09	17.19	6.33	1.95	0.22	0	0	0	48.21	49.62	2.17	51.78	25.69	8.5	2.17	1.10522	16.70755	136.4528	117.327	0.859836		
581	574	49.83	26.87	16.11	5.09	1.45	0.64	0	0	0	49.83	48.07	2.09	50.16	23.29	7.18	2.09	1.033475	23.06608	187.978	148.3789	0.789342		
583	576	47.69	26.04	16.53	7.13	2.35	0.26	0	0	0	47.69	49.7	2.62	52.31	26.27	9.74	2.62	1.123313	17.7623	123.6585	103.4645	0.836695		
585	579	51.61	21.09	16.64	8.33	2.1	0.22	0	0	0	51.61	46.07	2.32	48.38	27.29	10.65	2.32	1.121932	18.73375	141.2724	119.5882	0.846508		
587	581	55.57	21.14	15	6.32	1.54	0.44	0	0	0	55.57	42.46	1.97	44.44	23.3	8.3	1.97	1.081368	14.12366	119.4812	99.10215	0.829437		
589	583	50.07	27.69	15.52	5.44	1.22	0.06	0	0	0	50.07	48.65	1.28	49.93	22.24	6.72	1.28	1.073478	17.78931	143.8585	116.2327	0.807966		
591	586	50.63	22.74	16.21	8.2	2.14	0.08	0	0	0	50.63	47.15	2.22	49.37	26.63	10.42	2.22	1.128898	19.12541	159.8911	133.3366	0.833922		
593	588	53.17	22.26	15.79	7.07	1.66	0.06	0	0	0	53.17	45.12	1.72	46.84	24.58	8.79	1.72	1.103875	15.44	117.86	97.5025	0.827274		
595	590	51.48	24.61	14.75	6.82	2.02	0.31	0	0	0	51.48	46.19	2.33	48.51	23.9	9.15	2.33	1.095042	12.58391	100.6552	84.49195	0.83942		
597	593	51.33	21	15.96	8.62	2.66	0.42	0	0	0	51.33	45.58	3.09	48.66	27.66	11.7	3.09	1.16029	15.64266	118.9972	107.7784	0.905722		
599	595	54.7	20.2	14.72	8.13	2.21	0.03	0	0	0	54.7	43.05	2.24	45.29	25.09	10.37	2.24	1.132616	16.33125	126.6188	113.5625	0.896885		
601	598	54.48	19.83	14.59	8.08	2.68	0.34	0	0	0	54.48	42.5	3.02	45.52	25.69	11.1	3.02	1.062157	14.79634	110.5849	93.56136	0.846059		
603	600	49.11	19.48	16.82	11.28	3.25	0.06	0	0	0	49.11	47.58	3.31	50.89	31.41	14.59	3.31	1.170151	17.36607	127.6101	114.7619	0.899317		
605	602	54.03	20.97	15.23	7.94	1.8	0.02	0	0	0	54.03	44.14	1.82	45.96	24.99	9.76	1.82	1.100756	17.14245	128.6154	107.7863	0.838052		
607	605	51.18	21.56	16.11	8.9	2.23	0.03	0	0	0	51.18	46.57	2.25	48.83	27.27	11.16	2.25	1.100713	15.81313	116.404	96.67929	0.830549		
609	607	51.85	20.69	15.35	9.4	2.67	0.05	0	0	0	51.85	45.43	2.72	48.16	27.47	12.12	2.72	1.153869	23.63504	166.4781	141.1131	0.847638		
611	609	54.86	25.06	13.87	5.17	1.03	0.01	0	0	0	54.86	44.1	1.04	45.14	20.08	6.21	1.04	1.003601	14.41667	104.3148	82.57639	0.791607		
613	612	55.41	21.89	14.66	6.54	1.45	0.05	0	0	0	55.41	43.09	1.51	44.59	22.7	8.04	1.51	1.039903	14.52798	108.4599	86.67883	0.799179		
615	614	52.78	23.79	14.94	6.76	1.69	0.03	0	0	0	52.78	45.49	1.73	47.21	23.42	8.48	1.73	1.113963	15.88298	117.4681	99.1516	0.844073		
617	617	54.5	21.58	15.25	6.39	1.85	0.43	0	0	0	54.5	43.22	2.28	45.5	23.92	8.67	2.28	1.070454	16.4322	125.435	102.6215	0.818124		
619	619	54.75	21.53	15.01	6.72	1.83	0.15	0	0	0	54.75	43.26	1.99	45.24	23.71	8.7	1.99	1.083377	13.90431	106.2368	89.40191	0.841534		

Original Original >8um >16um >32um >64um  
0.888924 0.918979 0.898392 0.847635

	Original				
	Zr/Rb	Si/Al	Ti/Al	Zr/Al	Zr/Ti
>8um	0.888924	0.404022	0.179432	0.490025	0.623926
>16um	0.918979	0.409592	0.15759	0.507835	0.676282
>32um	0.898392	0.404882	0.137977	0.496107	0.680155
>64um	0.847635	0.419218	0.168177	0.514968	0.673439







Appendix 1 - Bienen 6 A

Depth	Real depth %Clay	%Very Fine %Silt %Coarse %Very Fine %Fine San %Middle C %Coarse %Very Coarse Sand										P95		
		< 8 #m	8-16 #m	16-32 #m	32-63 #m	63-125 #m	125-250 #m	250-500 #m	500-1000 #m	1000-2000 #m	Clay			
453	431	45.58	20.26	18.49	11.01	4.06	0.6	0	0	0	45.58	49.76	4.67	52.6
455	434	48.14	20.92	18.31	9.4	2.9	0.33	0	0	0	48.14	48.63	3.23	44.2
457	436	50.56	23.25	15.94	7.63	2.21	0.41	0	0	0	50.56	46.82	2.62	44.2
459	439	42.64	19.8	19.3	13.28	4.58	0.4	0	0	0	42.64	52.38	4.98	62.5
461	441	38.54	18.68	21.54	15.71	5.12	0.42	0	0	0	38.54	55.92	5.53	62.5
463	444	32.97	17.76	23.39	19.45	6.02	0.41	0	0	0	32.97	60.6	6.43	62.5
465	446	32.1	16.35	22.03	16.89	9.22	3.4	0.01	0	0	32.1	55.27	12.63	105
467	449	50.31	22.59	17.24	7.72	1.73	0.41	0	0	0	50.31	47.55	2.14	37.2
469	452	53.25	22.85	15.53	6.2	1.77	0.39	0	0	0	53.25	44.59	2.16	37.2
471	454	51.66	21.41	16.67	7.55	2.14	0.58	0	0	0	51.66	45.63	2.71	44.2
473	457	50.51	26.04	15.64	5.92	1.55	0.35	0	0	0	50.51	47.6	1.89	37.2
475	459	50.34	22.69	16.74	7.65	2.12	0.45	0	0	0	50.34	47.09	2.57	44.2
477	462	52.18	21.28	16.36	7.83	2.08	0.28	0	0	0	52.18	45.47	2.35	44.2
479	465	47.09	21.73	19.16	9.24	2.27	0.5	0	0	0	47.09	50.14	2.77	44.2
481	467	51.02	24.45	16.27	6.47	1.47	0.33	0	0	0	51.02	47.18	1.8	37.2
483	470	49.51	20.72	17.77	9.38	2.43	0.19	0	0	0	49.51	47.88	2.61	44.2
485	472	47.87	19.95	17.66	11.04	3.36	0.12	0	0	0	47.87	48.65	3.48	52.6
487	475	41.55	18.62	19.14	14.75	5.62	0.32	0	0	0	41.55	52.51	5.94	62.5
489	477	51.73	22.39	16.43	7.3	1.84	0.31	0	0	0	51.73	46.12	2.16	37.2
491	480	50.29	21.83	17.42	8.25	2.08	0.14	0	0	0	50.29	47.49	2.22	44.2
493	483	49.7	22.82	17.53	7.74	1.87	0.33	0	0	0	49.7	48.1	2.2	44.2
495	485	49.88	24.22	16.61	7.03	1.93	0.33	0	0	0	49.88	47.86	2.26	37.2
497	488	48.8	21.07	17.44	9.39	2.96	0.34	0	0	0	48.8	47.9	3.3	44.2
499	490	45.64	20.32	17.77	10.75	4.91	0.62	0	0	0	45.64	48.83	5.53	62.5
501	493	49.47	22.79	16.18	8.39	2.91	0.27	0	0	0	49.47	47.35	3.18	44.2
503	495	49.76	21.25	16.98	8.84	2.77	0.4	0	0	0	49.76	47.07	3.17	44.2
505	498	53.05	22.14	15.69	6.88	1.87	0.37	0	0	0	53.05	44.71	2.24	37.2
507	501	53.3	21.91	16.33	6.52	1.58	0.35	0	0	0	53.3	44.77	1.93	37.2
509	503	51.24	21.25	16.7	8.01	2.41	0.39	0	0	0	51.24	45.96	2.8	44.2
511	506	51.46	21.96	16.05	7.71	2.34	0.47	0	0	0	51.46	45.73	2.82	44.2
513	508	47.47	21.52	17.81	10.26	2.87	0.08	0	0	0	47.47	49.58	2.95	44.2
515	511	49.22	20.88	17.27	9.22	2.84	0.56	0	0	0	49.22	47.37	3.4	44.2
517	514	46.47	20.19	17.78	10.95	3.97	0.64	0	0	0	46.47	48.93	4.6	52.6
519	516	48.71	21.06	17.16	9.43	3.12	0.52	0	0	0	48.71	47.65	3.64	52.6
521	519	48.1	21.07	17.32	9.63	3.27	0.61	0	0	0	48.1	48.01	3.88	52.6
523	521	45.98	20.68	17.99	11.1	3.89	0.35	0	0	0	45.98	49.77	4.24	52.6
525	524	46.69	20.62	17.38	10.71	4.13	0.47	0	0	0	46.69	48.71	4.59	52.6
527	526	45.67	19.36	16.68	12.34	4.52	0.44	0	0	0	45.67	49.37	4.96	62.5
529	529	53.27	21.65	17.17	7.05	1.68	0.17	0	0	0	53.27	44.87	1.86	37.2

		Al	Si	P	S	Cl	Ar	K	Ca	Sc	Ti	V	Cr	Mn	Fe	Co	Ni	Cu	Zn	Ga	As
453	431	0.000279	0.000998	0.000265	0.007913	5.34E-05	0.009093	0.014534	0.168878	0.000127	0.017125	0.000936	0.001548	0.020865	1.005977	0.01161	0.000577	0.000269	0.005404	0.001193	0.003309
455	434	0.000186	0.002436	0.000236	0.038046	0.000108	0.007102	0.022147	0.557835	0.000173	0.021617	0.000887	0.00171	0.032802	1.375094	0.015651	0.000488	8.17E-05	0.006521	0.000863	0.003828
457	436	0.000212	0.00261	0.000119	0.03055	0	0.006014	0.034659	0.204641	3.48E-05	0.032393	0.001489	0.002297	0.037024	1.750361	0.017066	0.000906	0.000103	0.008885	0.001927	0.004358
459	439	0.000283	0.00287	8.85E-05	0.002322	7.08E-05	0.005296	0.037627	0.185191	0	0.03622	0.001425	0.002653	0.036562	1.871509	0.017924	0.00079	0.000159	0.009828	0.002228	0.003369
461	441	0.00012	0.00291	0.000177	0.001176	0	0.006274	0.034294	0.157416	9.33E-06	0.036475	0.000321	0.002399	0.028115	1.573688	0.014499	0.000944	0.00021	0.008655	0.002214	0.00219
463	444	0.000283	0.002566	2.1E-05	0.001097	1.78E-05	0.006464	0.033061	0.151002	1.94E-05	0.035643	0.000965	0.0025	0.031111	1.549826	0.015627	0.000816	0.000692	0.008613	0.002031	0.002584
465	446	0.000234	0.003033	7.22E-05	0.000918	0	0.00665	0.033441	0.129732	4.01E-05	0.035742	0.001201	0.002506	0.022297	1.390508	0.013276	0.01006	0.000634	0.008559	0.001602	0.00223
467	449	0.000234	0.003046	0.000102	0.001243	0	0.006019	0.035315	0.161835	4.93E-05	0.03294	0.001409	0.00237	0.032283	1.531051	0.014605	0.001207	0.000265	0.008121	0.002261	0.003305
469	452	0.00018	0.002438	0.000104	0.004209	0	0.006027	0.033294	0.225212	6.89E-05	0.031288	0.0011	0.002352	0.059377	1.808266	0.017656	0.000828	0.000212	0.008813	0.001141	0.004618
471	454	0.000232	0.002369	3.34E-05	0.001093	0	0.007028	0.034127	0.179882	2.99E-05	0.033055	0.001061	0.002275	0.049009	1.722095	0.016257	0.000964	0.000175	0.009137	0.001215	0.003692
473	457	0.000327	0.001976	0.000101	0.001171	9.48E-05	0.006845	0.031359	0.168759	5.22E-05	0.030685	0.001597	0.002314	0.052807	1.72602	0.016218	0.000806	0.000182	0.008623	0.002031	0.003324
475	459	0.000168	0.001818	7.86E-05	0.001105	0.0003	0.006793	0.031397	0.169077	3.69E-05	0.030767	0.001034	0.002426	0.08172	1.747327	0.016355	0.000903	0.00054	0.008186	0.00109	0.004548
477	462	0.000165	0.001666	8.72E-05	0.001174	6.46E-05	0.005966	0.030805	0.158572	1.61E-05	0.030708	0.001348	0.001824	0.083613	1.796201	0.015323	0.000315	0.000253	0.008365	0.001595	0.004296
479	465	0.000164	0.001494	0.001017	0.001877	9.47E-05	0.005627	0.027067	0.136505	8.52E-05	0.028847	0.001175	0.001994	0.03922	1.477465	0.014688	0.000857	0.000305	0.008783	0.001073	0.00252
481	467	0.0002	0.00141	0.000139	0.003722	0	0.006389	0.025166	0.17086	8.48E-05	0.026673	0.001333	0.002031	0.033427	1.461418	0.013436	0.000622	0.000206	0.00777	0.001464	0.003362
483	470	0.00016	0.001975	0.000109	0.001434	1.9E-05	0.006409	0.032568	0.133882	5.08E-05	0.033591	0.001442	0.002171	0.044242	1.836048	0.016512	0.00052	0.000321	0.008589	0.001075	0.004973
485	472	0.000276	0.002456	7.14E-05	0.001527	1.9E-05	0.006506	0.03372	0.144366	7.61E-05	0.034057	0.001239	0.002574	0.031278	1.821808	0.015711	0.000844	0.000281	0.009514	0.001216	0.003393
487	475	0.000221	0.002546	7.49E-05	0.001507	7.97E-06	0.007159	0.032388	0.147868	7.97E-06	0.033648	0.001313	0.002508	0.035374	1.651799	0.015702	0.000854	0.000481	0.009004	0.001913	0.002684
489	477	0.000216	0.002604	6.46E-05	0.001199	4.96E-05	0.006952	0.033535	0.140169	1.44E-05	0.033034	0.001436	0.002839	0.04291	1.687294	0.016405	0.001145	0.000334	0.008373	0.001871	0.003449
491	480	0.000138	0.002699	6.02E-05	0.001563	0	0.006463	0.038764	0.151637	3.01E-05	0.037771	0.001731	0.002818	0.049686	1.894144	0.017102	0.000873	0.000729	0.010455	0.002081	0.004891
493	483	0.000204	0.003178	5.7E-05	0.002127	1.11E-05	0.006264	0.039335	0.174767	0	0.037837	0.001417	0.0026	0.053499	1.840842	0.017057	0.000798	0.000242	0.008913	0.002185	0.003233
495	485	0.000423	0.00332	0.000109	0.001596	0.0006	0.006127	0.043044	0.145874	0	0.04071	0.001825	0.002746	0.062914	2.106777	0.019191	0.000377	0.000426	0.00978	0.002035	0.003266
497	488	0.000214	0.003568	5.76E-05	0.000816	1.28E-05	0.005297	0.047412	0.188156	8.96E-05	0.042076	0.001558	0.003188	0.039775	1.973269	0.018526	0.001011	0.001062	0.011123	0.002306	0.003922
499	490	0.000381	0.003591	7.33E-05	0.001152	5.89E-05	0.005972	0.046258	0.193741	3.35E-05	0.041625	0.001698	0.002891	0.043888	1.966444	0.018885	0.000881	0.000325	0.009714	0.002597	0.00288
501	493	0.00014	0.003767	0.000109	0.001																

Appendix 1 - Bienen 5 B

Depth	Real depth	%Clay	%Very Fine	%Fine Silt	%Coarse	%Very Fine	%Fine Sand	%Middle	%Coarse	%Very Coarse	Sand	Original				Shifted Graph											
												Zr/Rb	Si/Al	Ti/Al	Zr/Al	Zr/Ti	Zr/Rb	Si/Al	Ti/Al	Zr/Al	Zr/Ti						
	< 8 μm	8-16 μm	16-32 μm	32-63 μm	63-125 μm	125-250 μm	250-500 μm	500-1000 μm	1000-2000 μm	Clay	Silt	Sand	>8um	>16um	>32um	>64um	Zr/Rb	Si/Al	Ti/Al	Zr/Al	Zr/Ti						
357	341	50.74	20.26	16.53	9.28	3.09	0.12	0	0	0	50.74	46.06	3.2	49.28	29.02	12.49	3.2	1.209674	27.95862	207.1172	212.8276	1.027571	1.207495	20.42387	152.6749	142.5391	0.933612
359	343	49.06	20.34	17.16	9.92	3.37	0.15	0	0	0	49.06	47.42	3.52	50.94	30.6	13.44	3.52	1.207495	20.42387	152.6749	142.5391	0.933612	1.214384	14.49485	105.9768	105.1005	0.991731
361	346	52.89	21.19	16.46	7.42	1.92	0.12	0	0	0	52.89	45.07	2.04	47.11	25.92	9.46	2.04	1.214384	14.49485	105.9768	105.1005	0.991731	1.159693	15.1493	113.5014	102.6704	0.904574
363	348	52.34	20.55	16.36	8.04	2.39	0.31	0	0	0	52.34	44.95	2.7	47.65	27.1	10.74	2.7	1.159693	15.1493	113.5014	102.6704	0.904574	1.135805	20.01172	161.8125	145.5117	0.899261
365	351	50.56	20.42	16.75	8.85	3.1	0.32	0	0	0	50.56	46.02	3.41	49.44	29.02	12.27	3.41	1.135805	20.01172	161.8125	145.5117	0.899261	1.089273	14.92073	130.3994	111.0793	0.851839
367	353	50.74	21.14	17.15	8.31	2.34	0.32	0	0	0	50.74	46.6	2.66	49.26	28.12	10.97	2.66	1.089273	14.92073	130.3994	111.0793	0.851839	1.115834	21.02917	178.6792	156.8583	0.877877
369	356	49.7	20.48	16.99	9.31	3.22	0.3	0	0	0	49.7	46.78	3.51	50.3	29.82	12.83	3.51	1.115834	21.02917	178.6792	156.8583	0.877877	1.237924	23.31933	184.5882	174.979	0.947942
371	358	45.82	19.02	16.85	11.11	5.75	1.45	0	0	0	45.82	46.98	7.19	54.18	35.16	18.31	7.19	1.237924	23.31933	184.5882	174.979	0.947942	1.264256	21.97308	153.6192	154.5115	1.005809
373	361	48.99	19.54	16.41	9.92	4.16	0.98	0	0	0	48.99	45.87	5.14	51.01	31.47	15.06	5.14	1.264256	21.97308	153.6192	154.5115	1.005809	1.158997	15.23324	126.1749	110.3615	0.874671
375	363	47.64	19.45	16.64	10.35	4.2	1.58	0.14	0	0	47.64	46.43	5.92	52.36	32.91	16.27	5.92	1.158997	15.23324	126.1749	110.3615	0.874671	1.206359	18.79355	138.4806	124.971	0.902444
377	365	45.02	19.39	18.34	12.12	4.59	0.55	0	0	0	45.02	49.84	5.14	54.99	35.6	17.26	5.14	1.206359	18.79355	138.4806	124.971	0.902444	1.214395	20.68641	154.5226	138.4495	0.895982
379	368	47.69	20.18	17.88	10.21	3.58	0.46	0	0	0	47.69	48.27	4.04	52.31	32.13	14.25	4.04	1.214395	20.68641	154.5226	138.4495	0.895982	1.343456	18.48366	132.9673	135.4608	1.018752
381	370	40.71	17.82	18.93	15.57	6.29	0.69	0	0	0	40.71	52.31	6.98	59.3	41.48	22.55	6.98	1.343456	18.48366	132.9673	135.4608	1.018752	1.390087	17.58286	116.2686	126.5257	1.088219
383	373	47.48	20.52	18.17	10.22	3.21	0.4	0	0	0	47.48	48.91	3.61	52.52	32	13.83	3.61	1.390087	17.58286	116.2686	126.5257	1.088219	1.15601	18.58966	146.9793	131.0517	0.891634
385	375	52.11	21.71	16.92	7.72	1.54	0.01	0	0	0	52.11	46.34	1.55	47.9	26.19	9.27	1.55	1.15601	18.58966	146.9793	131.0517	0.891634	1.187209	19.70782	159.5638	149.7984	0.938799
387	378	51.62	20.86	16.43	8.15	2.49	0.45	0	0	0	51.62	45.44	2.94	48.38	27.52	11.09	2.94	1.187209	19.70782	159.5638	149.7984	0.938799	1.202469	16.14763	106.532	107.6964	1.01093
389	380	46.72	19.52	17.06	11.54	4.76	0.41	0	0	0	46.72	48.12	5.17	53.29	33.77	16.71	5.17	1.202469	16.14763	106.532	107.6964	1.01093	1.355241	17.94576	119.7492	127.4983	1.064712
391	383	45.79	18.81	18.01	12.27	4.21	0.92	0	0	0	45.79	49.09	5.12	54.22	35.41	17.4	5.12	1.355241	17.94576	119.7492	127.4983	1.064712	1.282906	19.02024	131.8826	149.004	1.129823
393	385	53.02	21.49	14.97	6.88	2.63	1.01	0	0	0	53.02	43.34	3.64	46.98	25.49	10.52	3.64	1.282906	19.02024	131.8826	149.004	1.129823	1.143311	24.94975	214.8191	195.1558	0.908466
395	387	50.11	20.55	17.02	8.77	2.96	0.59	0	0	0	50.11	46.34	3.55	49.89	29.34	12.32	3.55	1.143311	24.94975	214.8191	195.1558	0.908466	1.245141	19.8412	162.6438	163.867	1.007521
397	390	50.28	19.71	16.9	9.4	3.21	0.5	0	0	0	50.28	46.01	3.71	49.72	30.01	13.11	3.71	1.245141	19.8412	162.6438	163.867	1.007521	1.123378	22	180.0571	174.7762	0.970671
399	392	51.23	21.74	15.72	8.64	2.53	0.13	0	0	0	51.23	46.1	2.67	48.76	27.02	11.3	2.67	1.123378	22	180.0571	174.7762	0.970671	1.314298	16.11355	133.8352	140.8755	1.052604
401	395	47.99	21.56	17.14	9.51	3.24	0.56	0	0	0	47.99	48.21	3.8	52.01	30.45	13.31	3.8	1.314298	16.11355	133.8352	140.8755	1.052604	1.233094	16.25862	155.944	167.8017	1.076039
403	397	47.41	20.46	17.57	9.55	3.55	1.46	0	0	0	47.41	47.58	5.02	52.59	32.13	14.56	5.02	1.233094	16.25862	155.944	167.8017	1.076039	1.147404	17.81008	150.1318	145.876	0.971653
405	400	50.45	21.82	17.81	8.04	1.75	0.13	0	0	0	50.45	47.67	1.87	49.55	27.73	9.92	1.87	1.147404	17.81008	150.1318	145.876	0.971653	1.355241	20.04265	167.1611	158.7536	0.949704
407	402	49.89	20.86	16.75	7.96	2.9	1.62	0.03	0	0	49.89	45.56	4.55	50.12	29.26	12.51	4.55	1.135415	20.04265	167.1611	158.7536	0.949704	1.724387	19.41729	144.5188	198.4925	1.373472
409	405	49.6	20.81	17.69	8.83	2.64	0.42	0	0	0	49.6	47.33	3.06	50.39	29.58	11.89	3.06	1.724387	19.41729	144.5188	198.4925	1.373472	1.310461	18.47692	131.1462	151.3885	1.154349
411	407	46.76	19.22	17.75	11.36	4.19	0.72	0	0	0	46.76	48.33	4.91	53.24	34.02	16.27	4.91	1.310461	18.47692	131.1462	151.3885	1.154349	1.238813	22.12435	178.5492	186.0466	1.041991
413	409	50.76	20.43	16.78	8.53	2.88	0.62	0	0	0	50.76	45.75	3.49	49.24	28.81	12.03	3.49	1.238813	22.12435	178.5492	186.0466	1.041991	1.188719	14.52924	112.652	115.9766	1.029512
415	412	50.19	22.73	16.59	7.8	2.2	0.49	0	0	0	50.19	47.12	2.69	49.81	27.08	10.49	2.69	1.188719	14.52924	112.652	115.9766	1.029512	1.154966	19.33721	152.4884	150.7364	0.988511
417	414	50.6	21.11	17.25	8.95	2.06	0.03	0	0	0	50.6	47.31	2.1	49.4	28.29	11.04	2.1	1.154966	19.33721	152.4884	150.7364	0.988511	1.156567	17.08127	137.8657	136.5689	0.990594
419	417	50.21	20.86	16.5	8.58	3.04	0.81	0	0	0	50.21	45.94	3.85	49.79	28.93	12.43	3.85	1.156567	17.08127	137.8657	136.5689	0.990594	1.286926	20.99298	143.5088	142.6456	0.993985
421	419	45.21	19.86	18.56	11.64	4.21	0.53	0	0	0	45.21	50.06	4.74	54.8	34.94	16.38	4.74	1.286926	20.99298	143.5088	142.6456	0.993985	1.250047	24.09649	174.5789	174.9956	1.002387
423	422	48.89	20.8	17.33	9.26	3.29	0.44	0	0	0	48.89	47.38	3.73	51.12	30.32	12.99	3.73	1.250047	24.09649	174.5789	174.9956	1.002387	1.157522	26.58571	189.2762	174.1905	0.920298
425	424	49.41	20.8	16.75	8.88	3.5	0.66	0	0	0	49.41	46.43	4.16	50.59	29.79	13.04	4.16	1.157522	26.58571	189.2762	174.1905	0.920298	1.220151	16.95641	110.2821	96.69231	0.876773
427	427	48.93	21.7	15.99	8.88	3.66	0.84	0	0	0	48.93	46.57	4.5	51.07	29.37	13.38	4.5	1.220151	16.95641	110.2821	96.69231	0.876773	1.190826	21.90671	141.7085	127.9913	0.903201
429	429	48.29	22.62	15.94	8.37	3.85	0.93	0	0	0	48.29	46.93	4.78	51.71	29.09	13.15	4.78	1.190826	21.90671	141.7085	127.9913	0.903201					

		>8um	>16um	>32um	>64um
Original	Original	0.322911	0.323142	0.276425	0.197411
Shifted	Upper part	0.319491	0.310755	0.323192	0.361464
	part 2	0.731762	0.703849	0.692514	0.581068
	part 1	-0.05433	-0.02547		0.262926

	Original Zr/Rb	Si/Al	Ti/Al	Zr/Al	Zr/Ti	Shifted				
						Zr/Rb	Si/Al	Ti/Al	Zr/Al	Zr/Ti
>8um	0.322911	-0.00287	-0.14744	-0.10094	0.089799	0.319491	0.088393	-0.12957	0.00648	0.238375
>16um	0.323142	0.032624	-0.09852	-0.04975	0.099016	0.310755	0.070914	-0.14974	-0.02315	0.220627
>32um	0.276425	0.061952	-0.08964	-0.05782	0.063247	0.323192	0.07			

Appendix 1 - Bienen 5 A

Depth	Real depth %Clay < 8 µm	AVG										StDEV	P95	
		%Very Fine	%Fine Silt	%Coarse %Very Fine	%Fine Sand	%Middle	%Coarse %Very Coarse	Sand	Clay	Silt	Clay			
357	341	50.74	20.26	16.53	9.28	3.09	0.12	0	0	0	50.74	46.06	3.2	44.2
359	343	49.06	20.34	17.16	9.92	3.37	0.15	0	0	0	49.06	47.42	3.52	52.6
361	346	52.89	21.19	16.46	7.42	1.92	0.12	0	0	0	52.89	45.07	2.04	37.2
363	348	52.34	20.55	16.36	8.04	2.39	0.31	0	0	0	52.34	44.95	2.7	44.2
365	351	50.56	20.42	16.75	8.85	3.1	0.32	0	0	0	50.56	46.02	3.41	52.6
367	353	50.74	21.14	17.15	8.31	2.34	0.32	0	0	0	50.74	46.6	2.66	44.2
369	356	49.7	20.48	16.99	9.31	3.22	0.3	0	0	0	49.7	46.78	3.51	52.6
371	358	45.82	19.02	16.85	11.11	5.75	1.45	0	0	0	45.82	46.98	7.19	74.3
373	361	48.99	19.54	16.41	9.92	4.16	0.98	0	0	0	48.99	45.87	5.14	62.5
375	363	47.64	19.45	16.64	10.35	4.2	1.58	0.14	0	0	47.64	46.43	5.92	62.5
377	365	45.02	19.39	18.34	12.12	4.59	0.55	0	0	0	45.02	49.84	5.14	62.5
379	368	47.69	20.18	17.88	10.21	3.58	0.46	0	0	0	47.69	48.27	4.04	52.6
381	370	40.71	17.82	18.93	15.57	6.29	0.69	0	0	0	40.71	52.31	6.98	62.5
383	373	47.48	20.52	18.17	10.22	3.21	0.4	0	0	0	47.48	48.91	3.61	52.6
385	375	52.11	21.71	16.92	7.72	1.54	0.01	0	0	0	52.11	46.34	1.55	37.2
387	378	51.62	20.86	16.43	8.15	2.49	0.45	0	0	0	51.62	45.44	2.94	44.2
389	380	46.72	19.52	17.06	11.54	4.76	0.41	0	0	0	46.72	48.12	5.17	62.5
391	383	45.79	18.81	18.01	12.27	4.21	0.92	0	0	0	45.79	49.09	5.12	62.5
393	385	53.02	21.49	14.97	6.88	2.63	1.01	0	0	0	53.02	43.34	3.64	44.2
395	387	50.11	20.55	17.02	8.77	2.96	0.59	0	0	0	50.11	46.34	3.55	44.2
397	390	50.28	19.71	16.9	9.4	3.21	0.15	0	0	0	50.28	46.01	3.71	52.6
399	392	51.23	21.74	15.72	8.64	2.53	0.13	0	0	0	51.23	46.1	2.67	44.2
401	395	47.99	21.56	17.14	9.51	3.24	0.56	0	0	0	47.99	48.21	3.8	52.6
403	397	47.41	20.46	17.57	9.55	3.55	1.46	0	0	0	47.41	47.58	5.02	62.5
405	400	50.45	21.82	17.81	8.04	1.75	0.13	0	0	0	50.45	47.67	1.87	37.2
407	402	49.89	20.86	16.75	7.96	2.9	1.62	0.03	0	0	49.89	45.56	4.55	52.6
409	405	49.6	20.81	17.69	8.83	2.64	0.42	0	0	0	49.6	47.33	3.06	44.2
411	407	46.76	19.22	17.75	11.36	4.19	0.72	0	0	0	46.76	48.33	4.91	52.6
413	409	50.76	20.43	16.78	8.53	2.88	0.62	0	0	0	50.76	45.75	3.49	44.2
415	412	50.19	22.73	16.59	7.8	2.2	0.49	0	0	0	50.19	47.12	2.69	44.2
417	414	50.6	21.11	17.25	8.95	2.06	0.03	0	0	0	50.6	47.31	2.1	44.2
419	417	50.21	20.86	16.5	8.58	3.04	0.81	0	0	0	50.21	45.94	3.85	52.6
421	419	45.21	19.86	18.56	11.64	4.21	0.53	0	0	0	45.21	50.06	4.74	52.6
423	422	48.89	20.8	17.33	9.26	3.29	0.44	0	0	0	48.89	47.38	3.73	52.6
425	424	49.41	20.8	16.75	8.88	3.5	0.66	0	0	0	49.41	46.43	4.16	52.6
427	427	48.93	21.7	15.99	8.88	3.66	0.84	0	0	0	48.93	46.57	4.5	52.6
429	429	48.29	22.62	15.94	8.37	3.85	0.93	0	0	0	48.29	46.93	4.78	52.6

357	341	Al	Si	P	S	Cl	Ar	K	Ca	Sc	Ti	V	Cr	Mn	Fe	Co	Ni	Cu	Zn	Ga	As
359	343	0.000203	0.005682	7.57E-05	0.003274	2.38E-05	0.006157	0.05144	0.231043	6.59E-05	0.042093	0.001816	0.002692	0.043898	1.970676	0.019196	0.0009	6.87E-05	0.010141	0.001793	0.004293
361	346	0.000301	0.006148	5.45E-05	0.002013	4.95E-06	0.002325	0.054411	0.202253	3.84E-05	0.045956	0.001848	0.002974	0.038152	2.093014	0.020083	0.001137	8.55E-05	0.010903	0.001709	0.005267
363	348	0.000421	0.006103	8.79E-05	0.005191	4.99E-05	0.002025	0.053196	0.202834	4.45E-05	0.046424	0.002109	0.002938	0.035382	2.046219	0.018968	0.000924	0.000174	0.009346	0.001702	0.005153
365	351	0.000404	0.006117	4.21E-05	0.002952	1.82E-05	0.002625	0.054394	0.208181	1.14E-05	0.045829	0.002899	0.002857	0.038385	2.147032	0.020856	0.001062	9.33E-05	0.010114	0.001497	0.004912
367	353	0.000293	0.005869	7.56E-05	0.00133	1.37E-05	0.002115	0.054698	0.192568	6.87E-06	0.047459	0.002061	0.003265	0.041464	2.219632	0.020648	0.001139	6.3E-05	0.011567	0.002392	0.004889
369	356	0.000372	0.005546	0.000162	0.001243	0	0.001971	0.0546	0.136469	1.13E-05	0.048468	0.002047	0.003359	0.043438	2.326195	0.022493	0.001041	0.000155	0.010931	0.001979	0.004506
371	358	0.000272	0.005711	7.81E-05	0.001205	0	0.001987	0.055717	0.18555	0	0.048521	0.001996	0.003224	0.04564	2.271703	0.022108	0.00107	3.51E-05	0.011369	0.002059	0.005769
373	361	0.000259	0.006047	2.94E-05	0.00108	0	0.00211	0.056356	0.232629	0	0.04787	0.001904	0.003058	0.049508	2.117058	0.020907	0.001256	0	0.011466	0.001887	0.004728
375	363	0.000295	0.006491	0.000102	0.001093	0	0.002205	0.055018	0.234505	0	0.045381	0.002012	0.00281	0.043949	1.973297	0.020173	0.001074	2.05E-05	0.01057	0.002164	0.005276
377	365	0.000388	0.005916	1.36E-05	0.000995	0	0.002378	0.057125	0.189529	7.93E-06	0.049003	0.001973	0.003144	0.045558	2.121661	0.020101	0.001265	7.13E-05	0.011244	0.002328	0.004173
379	368	0.000351	0.005889	5.77E-05	0.001221	6.79E-06	0.001925	0.055476	0.124718	0	0.048553	0.001991	0.003383	0.058437	2.312465	0.021754	0.001152	0.000126	0.010329	0.001613	0.005033
381	370	0.000322	0.006663	8.53E-05	0.001206	5.61E-06	0.002166	0.056528	0.15923	0	0.049773	0.001939	0.003065	0.03848	2.207202	0.021797	0.001226	6.06E-05	0.010383	0.002645	0.004936
383	373	0.000354	0.006541	5.2E-05	0.001074	2.31E-05	0.001791	0.054919	0.233293	0	0.047056	0.002194	0.003027	0.037337	1.991233	0.021166	0.001746	3.35E-05	0.010513	0.002396	0.004713
385	375	0.000385	0.005761	5.49E-06	0.001101	0	0.001835	0.051882	0.24342	0	0.047409	0.001896	0.002854	0.040822	1.980441	0.020101	0.001265	7.13E-05	0.011244	0.001848	0.005311
387	378	0.000328	0.0061	6.45E-05	0.001051	9.05E-06	0.001461	0.055058	0.200344	0	0.04823	0.002082	0.003094	0.0459	2.187119	0.021309	0.001225	7.35E-05	0.011027	0.001839	0.005054
389	380	0.000282	0.005553	6.38E-05	0.001017	3.36E-05	0.001241	0.053431	0.247461	0	0.044959	0.001918	0.002938	0.077411	2.2619	0.0214	0.000979	1.16E-05	0.010843	0.002296	0.005052
391	383	0.000415	0.006706	1.85E-05	0.001076	0	0.001342	0.053158	0.238371	5.78E-05	0.044245	0.001895	0.002755	0.05539	1.952927	0.019667	0.001305	0	0.010872	0.001988	0.005245
393	385	0.000358	0.006433	4.13E-05	0.00097	0	0.001314	0.051735	0.255658	0	0.042927	0.001837	0.002694	0.065667	1.955924	0.019246	0.000865	0	0.010235	0.001995	0.004302
395	387	0.000297	0.005655	5.54E-05	0.000971	8.43E-06	0.00139	0.047691	0.233496	3.25E-05	0.039214	0.001642	0.002363	0.044856	1.786678	0.018144	0.000473	0	0.009846	0.001779	0.004861
397	390	0.000221	0.005508	8.43E-05	0.00206	0	0.001109	0.055611	0.202786	5.55E-06	0.047421	0.002433	0.00317	0.049098	2.157289	0.021367	0.001074	0.000182	0.010712	0.001887	0.004866
399	392	0.000267	0.005302	3.56E-05	0.00137	0	0.00126	0.052212	0.236157	2.29E-05	0.043646	0.001894	0.002797	0.054857	2.001506	0.02035	0.000826	0	0.010769	0.001621	0.004082
401	395	0.000235	0.005172	7.95E-05	0.00206	0	0.001185	0.052136	0.195658	1.12E-05	0.042327	0.001991	0.002907	0.039813	2.058546	0.020307	0.00075	5.93E-05	0.010341	0.00195	0.004332
403	397	0.00031	0.005002	5.69E-06	0.001042	9.1E-06	0.001029	0.047135	0.265461	0	0.041546	0.001619	0.002769	0.04691	1.972471	0.019927	0.000856	2.05E-05	0.010603	0.001763	0.004792
405	400	0.000253	0.004115	5.78E-05	0.001153	0	0.000831	0.043854	0.19862	1.31E-05	0.039472	0.001567	0.002522	0.048009	1.952996	0.019548	0.00053	1.96E-05	0.009762	0.001071	0.004186
407	402	0.000287	0.005115	3.45E-05	0.001114	5.7E-06	0.000881	0.049687	0.21221	0	0.043117	0.001594	0.002977	0.045793	2.040229	0.020501	0.000933	3.56E-05	0.010929	0.001377	0.005065
409	405	0.000244	0.004883	6.5E-05	0.001141	4.62E-06	0.000841	0.047917	0.272782	0	0.040727	0.001778	0.002473	0.077277	2.153371</						

Appendix 1- Bienen 4 - B

Depth	Real depth	%Clay	%Very Fine	%Fine Silt	%Coarse S	%Very Fine	%Fine San	%Middle C	%Coarse S	%Very Coarse	Sand	Clay	Silt	Sand	>8um	>16um	>32um	>64um	Original		Shifted Graph						
																			Zr/Rb	Si/Al	Zr/Rb	Si/Al	Ti/Al	Zr/Al	Zr/Ti		
267	241	42.04	20.29	20.77	12.9	3.76	0.24	0	0	0	42.04	53.95	4	57.96	37.67	16.9	4	1.606415	3.593333	43.74667	99.83333	2.282079	1.380133	13.46995	126.1366	150.7814	1.195382
269	244	42.79	21.68	22.12	11.09	2.21	0.1	0	0	0	42.79	54.89	2.32	57.2	35.52	13.4	2.32	1.380133	13.46995	126.1366	150.7814	1.195382	1.479459	6.717172	89.4697	140.7727	1.573412
271	246	39.03	20.77	23.35	13.27	3.06	0.51	0	0	0	39.03	57.4	3.57	60.96	40.19	16.84	3.57	1.479459	6.717172	89.4697	140.7727	1.573412	1.468896	19.03871	179.1677	194.9935	1.08833
273	249	48.54	22.41	18.5	8.61	1.86	0.07	0	0	0	48.54	49.53	1.94	51.45	29.04	10.54	1.94	1.468896	19.03871	179.1677	194.9935	1.08833	1.580784	11.11945	102.4608	123.0853	1.201292
275	252	48.36	22.24	18.92	8.23	1.84	0.41	0	0	0	48.36	49.38	2.25	51.64	29.4	10.48	2.25	1.580784	11.11945	102.4608	123.0853	1.201292	1.365692	14.38767	137.2159	139.9383	1.019841
277	255	46.91	22.45	19.4	8.72	2.06	0.46	0	0	0	46.91	50.57	2.52	53.09	30.64	11.24	2.52	1.365692	14.38767	137.2159	139.9383	1.019841	1.248697	11.06803	109.6735	104.2959	0.950968
279	257	46.92	22.21	19.2	8.91	2.52	0.25	0	0	0	46.92	50.32	2.77	53.09	30.88	11.68	2.77	1.248697	11.06803	109.6735	104.2959	0.950968	1.188192	29.37864	307.7184	292.699	0.951191
281	260	48.36	23.16	19.1	7.12	1.75	0.51	0	0	0	48.36	49.38	2.26	51.64	28.48	9.38	2.26	1.188192	29.37864	307.7184	292.699	0.951191	1.147691	10.64479	118.6641	113.1429	0.953472
283	263	50.79	21.87	17.05	7.19	2.57	0.54	0	0	0	50.79	46.1	3.11	49.22	27.35	10.3	3.11	1.147691	10.64479	118.6641	113.1429	0.953472	1.177483	12.5	133.5134	127	0.951215
285	266	49.97	20.18	15.47	8.36	4.58	1.46	0	0	0	49.97	44	6.03	50.05	29.87	14.4	6.03	1.177483	12.5	133.5134	127	0.951215	1.354623	12.9304	116.7436	123.0623	1.054124
287	268	55.57	21.65	14.97	6.16	1.56	0.08	0	0	0	55.57	42.78	1.64	44.42	22.77	7.8	1.64	1.354623	12.9304	116.7436	123.0623	1.054124	1.090083	17	159.608	139.3116	0.872835
289	271	56.01	21.91	14.89	5.04	1.6	0.56	0	0	0	56.01	41.83	2.16	44	22.09	7.2	2.16	1.090083	17	159.608	139.3116	0.872835	1.088847	14.27309	129.8795	117.2369	0.902659
291	274	54.6	22.15	15.37	5.06	2.16	0.67	0	0	0	54.6	42.58	2.83	45.41	23.26	7.89	2.83	1.088847	14.27309	129.8795	117.2369	0.902659	1.124359	17.90244	162.6878	146.4244	0.900033
293	276	47.47	19.34	13.31	6.19	7.68	5.94	0.06	0	0	47.47	38.84	13.69	52.52	33.18	19.87	13.69	1.124359	17.90244	162.6878	146.4244	0.900033	1.126776	12.49495	110.4916	97.70707	0.884294
295	279	51.17	22.31	16.97	7.19	1.93	0.43	0	0	0	51.17	46.47	2.36	48.83	26.52	9.55	2.36	1.126776	12.49495	110.4916	97.70707	0.884294	1.157386	16.89352	152.6806	140.3009	0.918918
297	282	47.57	22.17	17.94	8.23	2.8	1.27	0.03	0	0	47.57	48.33	4.09	52.44	30.27	12.33	4.09	1.157386	16.89352	152.6806	140.3009	0.918918	1.219799	17.71579	162.4421	164.2684	1.011243
299	285	51.2	22.34	17.14	7.41	1.77	0.13	0	0	0	51.2	46.89	1.9	48.79	26.45	9.31	1.9	1.219799	17.71579	162.4421	164.2684	1.011243	1.251441	16.92547	158.2112	182.1118	1.151068
301	287	50.82	22.6	17.29	6.93	2.08	0.29	0	0	0	50.82	46.81	2.37	49.19	26.59	9.3	2.37	1.251441	16.92547	158.2112	182.1118	1.151068	1.252251	18.74675	189.3701	198.7013	1.049275
303	290	50.78	22.49	17.29	7.38	1.88	0.19	0	0	0	50.78	47.16	2.06	49.23	26.74	9.45	2.06	1.252251	18.74675	189.3701	198.7013	1.049275	1.072459	16.8303	190.5576	171.6909	0.900992
305	293	52.81	21.94	16.64	6.79	1.49	0.33	0	0	0	52.81	45.37	1.82	47.19	25.25	8.61	1.82	1.22522	12.87755	128.9347	125.4776	0.973187	1.140241	10.53737	107.605	102.1388	0.949201
307	295	50.98	21.51	17.16	7.78	2.1	0.47	0	0	0	50.98	46.44	2.57	49.02	27.51	10.35	2.57	1.140241	10.53737	107.605	102.1388	0.949201	1.176808	12.21097	125.135	123.962	0.990626
309	298	52.84	21.78	16.31	6.58	2.13	0.36	0	0	0	52.84	44.67	2.49	47.16	25.38	9.07	2.49	1.176808	12.21097	125.135	123.962	0.990626	1.128471	10.66415	117.3585	107.9585	0.919904
311	301	54.25	22.05	15.78	5.85	1.46	0.61	0	0	0	54.25	43.68	2.07	45.75	23.7	7.92	2.07	1.128471	10.66415	117.3585	107.9585	0.919904	1.072459	16.8303	190.5576	171.6909	0.900992
313	304	54.25	22.39	15.72	5.67	1.46	0.5	0	0	0	54.25	43.79	1.96	45.74	23.35	7.63	1.96	1.072459	16.8303	190.5576	171.6909	0.900992	1.114485	19.92857	224.4571	202.9	0.903959
315	306	55.94	24.02	14.7	4.06	0.76	0.51	0	0	0	55.94	42.79	1.26	44.05	20.03	5.33	1.26	1.114485	19.92857	224.4571	202.9	0.903959	1.058657	11.66667	132.193	123.0921	0.931155
317	309	56.3	21.18	14.76	6.12	1.45	0.19	0	0	0	56.3	42.06	1.64	43.7	22.52	7.76	1.64	1.058657	11.66667	132.193	123.0921	0.931155	1.163431	17.48201	189.7194	204.8058	1.079519
319	312	55.69	21.02	14.88	6.58	1.69	0.13	0	0	0	55.69	42.48	1.82	44.3	23.28	8.4	1.82	1.163431	17.48201	189.7194	204.8058	1.079519	1.25563	10.96629	127.8371	152.5449	1.193276
321	315	53.57	20.82	15.91	7.11	2.23	0.36	0	0	0	53.57	43.84	2.59	46.43	25.61	9.7	2.59	1.25563	10.96629	127.8371	152.5449	1.193276	1.196213	11.3271	120.2196	130.1916	1.082948
323	317	53.78	21.04	15.19	6.87	2.49	0.64	0	0	0	53.78	43.09	3.13	46.23	25.19	10	3.13	1.196213	11.3271	120.2196	130.1916	1.082948	1.183179	22.49057	239.6509	252.0283	1.051647
325	320	53.66	21.09	15.35	6.97	2.39	0.54	0	0	0	53.66	43.4	2.94	46.34	25.25	9.9	2.94	1.183179	22.49057	239.6509	252.0283	1.051647	1.099335	9.311538	102.3462	95.30385	0.931191
327	323	55.95	21.35	14.99	5.6	1.63	0.49	0	0	0	55.95	41.94	2.11	44.06	22.71	7.72	2.11	1.099335	9.311538	102.3462	95.30385	0.931191	1.206817	11.28125	128.6406	139.4063	1.083688
329	325	54.99	24.2	13.05	5.28	2.22	0.25	0	0	0	54.99	42.53	2.47	45	20.8	7.75	2.47	1.206817	11.28125	128.6406	139.4063	1.083688	1.360539	16.15385	201.6077	237.4769	1.177916
331	328	49.62	20.6	16.41	9.34	3.61	0.43	0	0	0	49.62	46.34	4.04	50.39	29.79	13.38	4.04	1.360539	16.15385	201.6077	237.4769	1.177916	1.259185	13.1989	141.4586	160.1878	1.132401
333	331	49.98	20.31	16.29	9.12	3.9	0.4	0	0	0	49.98	45.72	4.3	50.02	29.71	13.42	4.3	1.259185	13.1989	141.4586	160.1878	1.132401	1.472492	13.45652	155.2826	215.6667	1.388866
335	334	44.67	19.05	17.15	11.72	6.42	1	0	0	0	44.67	47.92	7.41	55.34	36.29	19.14	7.41	1.472492	13.45652	155.2826	215.6667	1.388866	1.403233	11.56627	98.249	117.8434	1.199436
337	336	43.38	18.79	18.3	12.88	5.76	0.89	0	0	0	43.38	49.97	6.65	56.62	37.83	19.53	6.65	1.403233	11.56627	98.249	117.8434	1.199436	1.316693	14.31193	114.656	135.3899	1.180836
339	339	48.71	20.22	17.11	10.03	3.68	0.25	0	0	0	48.71	47.36	3.93	51.29	31.07	13.96	3.93	1.316693	14.31193	114.656	135.3899	1.180836					

		>8um	>16um	>32um	>64um
Original	Original	0.717176	0.700221	0.5530465	0.110655
Shifted	Shifted	0.638443	0.622511	0.5205392	0.138961

	Original					Shifted				
	Zr/Rb	Si/Al	Ti/Al	Zr/Al	Zr/Ti	Zr/Rb	Si/Al	Ti/Al	Zr/Al	Zr/Ti
>8um	0.717176	-0.22125	-0.26113	-0.00085	0.609866	0.638443	-0.03146	-0.17068	-0.02397	0.415501
>16um	0.700221	-0.27019	-0.30398	-0.02648	0.626561	0.622511	-0.06013	-0.2152	-0.05768	0.433535
>32um	0.553047	-0.24633	-0.27488	-0.0258	0.529087	0.520539	-0.08084	-0.24394	-0.09313	0.372565
>64um	0.110655	-0.03018	-0.07523	-0.00968	0.127846	0.138961	-0.0791	-0.21674	-0.18611	0.043038

Appendix 1- Biennen 4 - Raw data

Depth	Real depth	%Very Fine %Fine Silt %Coarse S %Very Fine %Fine San %Middle C %Coarse S %Very Coarse										AVG		P95
		< 8 µm	8-16 µm	16-32 µm	32-63 µm	63-125 µm	125-250 µm	250-500 µm	500-1000 µm	1000-2000 µm	Clay	Silt	STDEV Sand	
267	241	42.04	20.29	20.77	12.9	3.76	0.24	0	0	0	42.04	53.95	4	52.6
269	244	42.79	21.68	22.12	11.09	2.21	0.1	0	0	0	42.79	54.89	2.32	44.2
271	246	39.03	20.77	23.35	13.27	3.06	0.51	0	0	0	39.03	57.4	3.57	52.6
273	249	48.54	22.41	18.5	8.61	1.86	0.07	0	0	0	48.54	49.53	1.94	44.2
275	252	48.36	22.24	18.92	8.23	1.84	0.41	0	0	0	48.36	49.38	2.25	44.2
277	255	46.91	22.45	19.4	8.72	2.06	0.46	0	0	0	46.91	50.57	2.52	44.2
279	257	46.92	22.21	19.2	8.91	2.52	0.25	0	0	0	46.92	50.32	2.77	44.2
281	260	48.36	23.16	19.1	7.12	1.75	0.51	0	0	0	48.36	49.38	2.26	37.2
283	263	50.79	21.87	17.05	7.19	2.57	0.54	0	0	0	50.79	46.1	3.11	44.2
285	266	49.97	20.18	15.47	8.36	4.58	1.46	0	0	0	49.97	44	6.03	62.5
287	268	55.57	21.65	14.97	6.16	1.56	0.08	0	0	0	55.57	42.78	1.64	37.2
289	271	56.01	21.91	14.89	5.04	1.6	0.56	0	0	0	56.01	41.83	2.16	37.2
291	274	54.6	22.15	15.37	5.06	2.16	0.67	0	0	0	54.6	42.58	2.83	37.2
293	276	47.47	19.34	13.31	6.19	7.68	5.94	0.06	0	0	47.47	38.84	13.69	125
295	279	51.17	22.31	16.97	7.19	1.93	0.43	0	0	0	51.17	46.47	2.36	37.2
297	282	47.57	22.17	17.94	8.23	2.8	1.27	0.03	0	0	47.57	48.33	4.09	52.6
299	285	51.2	22.34	17.14	7.41	1.77	0.13	0	0	0	51.2	46.89	1.9	37.2
301	287	50.82	22.6	17.29	6.93	2.08	0.29	0	0	0	50.82	46.81	2.37	37.2
303	290	50.78	22.49	17.29	7.38	1.88	0.19	0	0	0	50.78	47.16	2.06	37.2
305	293	52.81	21.94	16.64	6.79	1.49	0.33	0	0	0	52.81	45.37	1.82	37.2
307	295	50.98	21.51	17.16	7.78	2.1	0.47	0	0	0	50.98	46.44	2.57	44.2
309	298	52.84	21.78	16.31	6.58	2.13	0.36	0	0	0	52.84	44.67	2.49	37.2
311	301	54.25	22.05	15.78	5.85	1.46	0.61	0	0	0	54.25	43.68	2.07	37.2
313	304	54.25	22.39	15.72	5.67	1.46	0.5	0	0	0	54.25	43.79	1.96	37.2
315	306	55.94	24.02	14.7	4.06	0.76	0.51	0	0	0	55.94	42.79	1.26	31.3
317	309	56.3	21.18	14.76	6.12	1.45	0.19	0	0	0	56.3	42.06	1.64	37.2
319	312	55.69	21.02	14.88	6.58	1.69	0.13	0	0	0	55.69	42.48	1.82	37.2
321	315	53.57	20.82	15.91	7.11	2.23	0.36	0	0	0	53.57	43.84	2.59	44.2
323	317	53.78	21.04	15.19	6.87	2.49	0.64	0	0	0	53.78	43.09	2.13	44.2
325	320	53.66	21.09	15.35	6.97	2.39	0.54	0	0	0	53.66	43.4	3.94	44.2
327	323	55.95	21.35	14.99	5.6	1.63	0.49	0	0	0	55.95	41.94	2.11	37.2
329	325	54.99	24.2	13.05	5.28	2.22	0.25	0	0	0	54.99	42.53	2.47	37.2
331	328	49.62	20.6	16.41	9.34	3.61	0.43	0	0	0	49.62	46.34	4.04	52.6
333	331	49.98	20.31	16.29	9.12	3.9	0.4	0	0	0	49.98	45.72	4.3	52.6
335	334	44.67	19.05	17.15	11.72	6.42	1	0	0	0	44.67	47.92	7.41	74.3
337	336	43.38	18.79	18.3	12.88	5.76	0.89	0	0	0	43.38	49.97	6.65	62.5
339	339	48.71	20.22	17.11	10.03	3.68	0.25	0	0	0	48.71	47.36	3.93	52.6

Al	Si	P	S	Cl	Ar	K	Ca	Sc	Ti	V	Cr	Mn	Fe	Co	Ni	Cu	Zn	Ga	As	Se		
267	241	0.0005	0.001797	0.00016	0.001154	0.00016	0.015633	0.023562	0.08944	0.000173	0.021878	0.000827	0.002034	0.022048	0.976278	0.010369	0.001057	0.000827	0.007778	0.001817	0.001694	0.003871
269	244	0.000325	0.004376	6.92E-05	0.002549	1.24E-05	0.006267	0.045735	0.189212	2.66E-05	0.040979	0.001584	0.002556	0.033156	1.723056	0.015351	0.000698	0.000486	0.011806	0.0025	0.003528	0.004381
271	246	0.000366	0.002462	0.0000117	0.001512	5.37E-05	0.006947	0.033467	0.126356	3.89E-05	0.03279	0.001136	0.002427	0.033843	1.509011	0.013521	0.000879	0.000652	0.011676	0.002673	0.003537	0.004779
273	249	0.000259	0.00493	9.86E-05	0.001201	1.5E-05	0.006193	0.04891	0.180713	1.34E-05	0.046396	0.001492	0.002728	0.060377	1.950086	0.017911	0.000952	0.000421	0.015002	0.002322	0.003229	0.004793
275	252	0.00047	0.005225	6.25E-05	0.001198	4.81E-05	0.006279	0.050677	0.166662	0	0.048147	0.001639	0.002803	0.051715	1.871563	0.01585	0.00093	0.000678	0.014735	0.002301	0.003342	0.005296
277	255	0.000363	0.005221	7.99E-05	0.001247	0	0.006422	0.055738	0.177138	0	0.049796	0.001434	0.003028	0.062447	2.248271	0.019776	0.000756	0.000496	0.014649	0.00317	0.00448	0.004998
279	257	0.000455	0.005031	0.000124	0.001067	6.63E-05	0.006214	0.05593	0.156249	9.2E-06	0.049854	0.001749	0.003092	0.049718	1.714358	0.019095	0.000719	0.000379	0.014542	0.002649	0.0052	0.004802
281	260	0.000158	0.004638	9.2E-05	0.000923	0.00025	0.006043	0.053252	0.133653	0.048584	0.001728	0.002935	0.041721	2.097581	0.01869	0.000406	0.000425	0.012986	0.002589	0.003631	0.005245	
283	263	0.000393	0.004179	0.0001024	0.001121	1.06E-05	0.005737	0.052121	0.134425	0.04685	0.001698	0.003071	0.037976	1.214903	0.01938	0.000662	0.000377	0.012635	0.002045	0.004158	0.005646	
285	266	0.000358	0.004472	0.000139	0.001115	6.39E-06	0.005448	0.053413	0.146028	2.08E-05	0.047771	0.001468	0.002763	0.036893	2.133111	0.019714	0.000749	0.000423	0.013467	0.002	0.004551	0.005054
287	268	0.000411	0.005318	6.18E-05	0.001286	1.66E-05	0.005731	0.054386	0.162478	0	0.048017	0.001709	0.002851	0.039146	2.028293	0.018513	0.001044	0.000431	0.012422	0.000212	0.004448	0.005124
289	271	0.000301	0.005109	2.42E-05	0.000976	3.02E-05	0.005389	0.056636	0.183147	0	0.047969	0.001723	0.002947	0.046981	2.303221	0.020988	0.00039	0.000414	0.01252	0.002179	0.003984	0.005278
291	274	0.000375	0.005325	8.28E-05	0.001009	1.05E-05	0.005967	0.058629	0.169743	2.56E-05	0.04868	0.001636	0.002813	0.045534	2.269989	0.020374	0.000531	0.000262	0.011505	0.002243	0.005294	0.005026
293	276	0.000308	0.005523	4.97E-05	0.001205	0	0.005344	0.059847	0.159419	0	0.050188	0.001646	0.002959	0.046188	2.337813	0.021608	0.000581	0.000488	0.011845	0.002423	0.005189	0.005944
295	279	0.000445	0.00556	0.000114	0.001166	1.65E-05	0.00544	0.058819	0.178698	0	0.049166	0.001625	0.003269	0.044989	2.265623	0.0209	0.000812	0.000556	0.011031	0.00233	0.004922	0.005344
297	282	0.000329	0.005551	6.24E-05	0.001334	2.59E-05	0.004944	0.057952	0.169818	0	0.050173	0.001608	0.003175	0.046563	2.225074	0.020476	0.000939	0.000173	0.011593	0.002509	0.003365	0.005039
299	285	0.00029	0.005143	3.82E-05	0.0039	0	0.005458	0.053752	0.212509	1.82E-05	0.047161	0.001595	0.002993	0.04211	2.013878	0.017945	0.00068	0.000593	0.010942	0.002457	0.005009	0.004957
301	287	0.000244	0.004122	0	0.014913	0	0.006041	0.044065	0.350755	0	0.038529	0.001466	0.00242	0.032894	1.774389	0.016638	0.000827	0.000316	0.009112	0.002345	0.00555	0.004836
303	290	0.000233	0.004365	4.69E-05	0.006922	3.02E-05	0.005348	0.050416	0.265083	3.63E-05	0.044098	0.001615	0.002548	0.034829	1.936139	0.018755	0.000541	0.000497	0.010308	0.00217	0.003777	0.005205
305	293	0.000367	0.004727	7.34E-05	0.001587	1.65E-05	0.005799	0.053964	0.176505	0	0.047324	0.001491	0.00274	0.043428	2.174478	0.019143	0.000502	0.000751	0.010428	0.002198	0.004066	0.00487
307	295	0.000416	0.004382	5.92E-05	0.003127	2.37E-05	0.004906	0.051041	0.210017	0.000118	0.044747	0.001672	0.002748	0.044207	2.096427	0.018752	0.000459	0.000265	0.009499	0.002053	0.00399	0.005234
309	298	0.000352	0.004298	4.01E-05	0.002587	0	0.005807	0.049854	0.1872	3.86E-05	0.044047	0.001606	0.002869	0.045412	1.256442	0.020389	0.00064	0.000434	0.010132	0.003048	0.004629	0.005385
311	301	0.000389	0.004151	0.000109	0.002047	4.99E-05	0.004388	0.052146	0.18334	8.81E-06	0.045687	0.001755	0.002909	0.044973	2.205407	0.019459	0.000524	0.000219	0.010191	0.003198	0.005086	0.004899
313	304	0.000242	0.004068	7.03E-05	0.002008	7.32E-06	0.005278	0.052315	0.15472	0	0.046061	0.001749	0.00286	0.037367	2.21915	0.019277	0.000435	7.47E-05	0.009776	0.002126	0.004972	0.005552
315	306	0.000208	0.00414	0.00011	0																	

Appendix 1 - Bienen 3 B

Depth	Real depth	%Clay	%Very Fine Silt	%Fine Silt	%Coarse S	%Very Fine	%Fine Sand	%Middle	%Coarse S	%Very Coarse	Sand	Original				Shifted graphs											
												Zr/Rb	Si/Al	Ti/Al	Zr/Al	Zr/Ti	Zr/Rb	Si/Al	Ti/Al	Zr/Al	Zr/Ti						
167	156	37.07	16.28	17.17	14.35	9.7	4.88	0.56	0	0	37.07	47.79	15.13	62.94	46.66	29.49	15.13	2.267076	1	0.42953	253.0604	589.1563	2.276946	0.919463	0.57047	273.6309	479.6588
169	158	40.71	16.92	16.82	13.68	8.67	3.16	0.05	0	0	40.71	47.42	11.87	59.3	42.38	25.56	11.87	2.276946	0.919463	0.57047	273.6309	479.6588	2.276946	0.658537	0.45935	150.626	327.9115
171	161	45.3	18.89	19.99	12.66	3.06	0.1	0	0	0	45.3	51.54	3.16	54.7	35.81	15.82	3.16	2.227606	0.658537	0.45935	150.626	327.9115	1.608038	5.677524	59.70358	151.5798	2.538873
173	163	44.92	20.45	18.81	9.96	3.5	2.1	0.25	0	0	44.92	49.23	5.85	55.07	34.62	15.81	5.85	1.608038	5.677524	59.70358	151.5798	2.538873	1.454148	15.88398	130.3591	165.1823	1.267133
175	165	41.83	19.88	19.3	11.19	4.31	2.84	0.65	0	0	41.83	50.36	7.8	58.17	38.29	18.99	7.8	1.454148	15.88398	130.3591	165.1823	1.267133	1.318156	16.39931	174.3194	196.7257	1.128536
177	168	48.87	22.76	18.69	7.24	1.77	0.67	0	0	0	48.87	48.69	2.44	51.13	28.37	9.68	2.44	1.318156	16.39931	174.3194	196.7257	1.128536	1.327495	12.91367	136.3621	151.5827	1.116169
179	170	47.6	22.05	19.36	9.24	1.72	0.05	0	0	0	47.6	50.64	1.76	52.42	30.37	11.01	1.76	1.327495	12.91367	136.3621	151.5827	1.116169	1.256725	21.22993	203.8796	215.0146	1.054616
181	172	47.7	22.45	19.44	7.87	1.79	0.75	0	0	0	47.7	49.76	2.54	52.3	29.85	10.41	2.54	1.256725	21.22993	203.8796	215.0146	1.054616	1.175155	17.18266	176.3313	177.5975	1.007181
183	174	47.87	23.4	19.9	7.65	1.15	0.03	0	0	0	47.87	50.95	1.18	52.13	28.73	8.83	1.18	1.175155	17.18266	176.3313	177.5975	1.007181	1.32949	18.24934	165.2175	175.2493	1.060719
185	177	33.47	17.29	21.83	19.09	7.71	0.6	0	0	0	33.47	58.22	8.31	66.52	49.23	27.4	8.31	1.32949	18.24934	165.2175	175.2493	1.060719	1.604662	18.31604	136.4481	171.7783	1.258928
187	179	51.24	23	17.36	7.05	1.32	0.03	0	0	0	51.24	47.4	1.36	48.76	25.76	8.4	1.36	1.604662	18.31604	136.4481	171.7783	1.258928	1.136858	16.83657	177.2548	170.9917	0.964666
189	181	44.69	21.2	19.27	11.62	3.17	0.06	0	0	0	44.69	52.09	3.22	55.32	34.12	14.85	3.22	1.136858	16.83657	177.2548	170.9917	0.964666	1.509341	20.79885	171.7443	208.0115	1.21117
191	184	43.68	19.04	19.55	13.65	3.98	0.1	0	0	0	43.68	52.24	4.08	56.32	37.28	17.73	4.08	1.509341	20.79885	171.7443	208.0115	1.21117	1.223319	16.54865	160.8297	161.4351	1.003764
193	186	47.5	21.62	19.33	9.68	1.84	0.03	0	0	0	47.5	50.63	1.87	52.5	30.88	11.55	1.87	1.223319	16.54865	160.8297	161.4351	1.003764	1.238907	14.20815	133.133	136.4313	1.024774
195	188	46.72	22.45	20.18	8.82	1.52	0.3	0	0	0	46.72	51.46	1.82	53.27	30.82	10.64	1.82	1.238907	14.20815	133.133	136.4313	1.024774	1.365843	19.02865	165.9115	174.1094	1.049411
197	191	46.57	22.52	19.83	8.92	1.84	0.32	0	0	0	46.57	51.27	2.16	53.43	30.91	11.08	2.16	1.365843	19.02865	165.9115	174.1094	1.049411	1.230675	18.07073	156.0659	154.7829	0.99178
199	193	49.22	22.16	18.45	8.79	1.38	0	0	0	0	49.22	49.4	1.39	50.78	28.62	10.17	1.39	1.230675	18.07073	156.0659	154.7829	0.99178	1.300381	16.95269	140.5957	145.886	1.037628
201	195	40.05	20.06	20.38	13.28	5.53	0.69	0	0	0	40.05	53.73	6.22	59.94	39.88	19.5	6.22	1.300381	16.95269	140.5957	145.886	1.037628	1.380082	17.67391	144.4565	153.5024	1.06262
203	198	43.15	21.41	20.62	11.23	3.24	0.35	0	0	0	43.15	53.26	3.59	56.85	35.44	14.82	3.59	1.380082	17.67391	144.4565	153.5024	1.06262	1.329841	14.80754	130.8313	135.248	1.033758
205	200	46.52	21.82	19.43	9.32	2.39	0.52	0	0	0	46.52	50.57	2.91	53.48	31.66	12.23	2.91	1.329841	14.80754	130.8313	135.248	1.033758	1.256648	16.70283	158.5024	161.1533	1.016725
207	202	51.66	23.15	17.19	6.28	1.4	0.31	0	0	0	51.66	46.63	1.71	48.33	25.18	7.99	1.71	1.256648	16.70283	158.5024	161.1533	1.016725	1.144192	17.683	154.9193	168.3314	1.086575
209	204	50.2	23.35	17.52	6.85	1.7	0.38	0	0	0	50.2	47.72	2.08	49.8	26.45	8.93	2.08	1.144192	17.683	154.9193	168.3314	1.086575	1.135542	18.16782	162.8897	147.0828	0.902959
211	207	49.12	22.38	18.67	7.89	1.6	0.34	0	0	0	49.12	48.94	1.94	50.88	28.5	9.83	1.94	1.135542	18.16782	162.8897	147.0828	0.902959	1.181963	17.24885	145.47	141.871	0.975259
213	209	50.67	23.44	18.23	6.17	1.17	0.33	0	0	0	50.67	47.84	1.49	49.34	25.9	7.67	1.49	1.181963	17.24885	145.47	141.871	0.975259	1.171474	15.067	152.6873	144.129	0.943949
215	211	53.28	22.66	16.69	6.29	1.05	0.04	0	0	0	53.28	45.63	1.09	46.73	24.07	7.38	1.09	1.171474	15.067	152.6873	144.129	0.943949	1.129714	14.5232	158.8866	146.3737	0.921246
217	214	51.39	21.98	17.28	7.61	1.68	0.06	0	0	0	51.39	46.87	1.74	48.61	26.63	9.35	1.74	1.129714	14.5232	158.8866	146.3737	0.921246	1.212236	21.36392	192.9684	193.6203	1.003378
219	216	45.31	19.66	17.15	11.11	5.95	0.82	0	0	0	45.31	47.93	6.77	54.69	35.03	17.88	6.77	1.212236	21.36392	192.9684	193.6203	1.003378	1.316982	17.91957	152.9303	167.7828	1.09712
221	218	49.38	23.36	19	7.08	1.13	0.04	0	0	0	49.38	49.44	1.18	50.61	27.25	8.25	1.18	1.316982	17.91957	152.9303	167.7828	1.09712	1.207283	16.87576	178.3788	178.2242	0.999134
223	221	45.09	22.43	20.4	10.04	2	0.04	0	0	0	45.09	52.87	2.04	54.91	32.48	12.08	2.04	1.207283	16.87576	178.3788	178.2242	0.999134	1.295924	20.64983	192.9461	206.0606	1.06797
225	223	52.91	23.19	16.74	6.08	1.04	0.04	0	0	0	52.91	46.01	1.08	47.09	23.9	7.16	1.08	1.295924	20.64983	192.9461	206.0606	1.06797	1.192314	15.79082	144.3316	147.926	1.024904
227	225	56.25	24.11	15.6	4.01	0.03	0	0	0	0	56.25	43.72	0.03	43.75	19.64	4.04	0.03	1.192314	15.79082	144.3316	147.926	1.024904	1.14197	12.29343	127.561	130.0023	1.019138
229	227	52.39	21.61	16.35	7.55	1.84	0.26	0	0	0	52.39	45.51	2.1	47.61	26	9.65	2.1	1.14197	12.29343	127.561	130.0023	1.019138	1.179101	16.85032	162.6561	177.6274	1.092043
231	230	56.06	21.87	15.18	6.11	1.61	0.17	0	0	0	56.06	43.16	1.78	44.94	23.07	7.89	1.78	1.179101	16.85032	162.6561	177.6274	1.092043	1.448841	15.92562	132.7052	170.3526	1.283692
233	232	56.07	21.92	14.94	5.82	1.2	0.05	0	0	0	56.07	42.68	1.24	43.93	22.01	7.07	1.24	1.448841	15.92562	132.7052	170.3526	1.283692	1.188961	16.09059	158.9373	181.1777	1.139932
235	234	55.64	21.55	14.48	5.8	2.17	0.36	0	0	0	55.64	41.83	2.53	44.36	22.81	8.33	2.53	1.188961	16.09059	158.9373	181.1777	1.139932	1.199894	11.17277	116.7173	135.6728	1.162405
237	237	48.28	20.09	15.53	7.79	3.77	3.44	1.1	0	0	48.28	43.41	8.31	51.72	31.63	16.1	8.31	1.199894	11.17277	116.7173	135.6728	1.162405	1.35873	13.15953	145.1518	218.2374	1.503512
239	239	42.04	17.41	14.62	10.17	7.14	6.68	1.94	0	0	42.04	42.2	15.75	57.96	40.55	25.93	15.75	1.35873	13.15953	145.1518	218.2374	1.503512					

		>8um	>16um	>32um	>64um
Original	Original	0.46	0.54	0.58	0.54
Shifted	Shifted	0.64	0.72	0.81	0.83
zonder bovenstuk:		0.631805	0.684728	0.691671	0.559718
/al + shift		0.427794	0.504796	0.625023	0.758034

	Original					Shifted				
	Zr/Rb	Si/Al	Ti/Al	Zr/Al	Zr/Ti	Zr/Rb	Si/Al	Ti/Al	Zr/Al	Zr/Ti
>8um	0.461224	-0.29373	-0.33379	0.361666	0.412453	0.644679	-0.19678	-0.34452	0.337021	0.427794
>16um	0.539429	-0.3863	-0.4211	0.425641	0.49444	0.723982	-0.30849	-0.45094	0.362854	0.504796
>32um	0.578639	-0.46452	-0.48621	0.519166	0.563077	0.805674	-0.44371	-0.57204	0.41232	0.625023
>64um	0.539442	-0.51009	-0.50386	0.575667	0.566567	0.834349	-0.58763	-0.66298	0.484758	0.758034

Appendix 1 - Bienen 3 A

Table with columns: Biennial Depth, Real depth %Clay, %Very Fine, %Fine Silt, %Coarse Silt, %Very Fine Sand, %Fine Sand, %Coarse Sand, %Very Coarse Sand, Silt, Sand, Silt + Sand, P95. Rows 167-239.

Bienenll

Table with columns: Biennial Depth, Real depth Normalized counts, and various elements (Al, Si, P, S, Cl, Ar, K, Ca, Sc, Ti, V, Cr, Mn, Fe, Co, Ni, Cu, Zn, Ga, As, Se, Br, Rb, Sr, Zr, Ag, Cd, Sn, Sb, Cs, Ba, Ta, W, Ir, Au, Hg, Pb, D1, Mo inc, Mo coh, Zr/Rb). Rows 167-239.

Appendix 11  
XRF settings

XRF settings					Biens X is missing! (no document.txt)									
Base path:	Sample name:	Section name	User ID		Base path:	Sample name:	Section name	User ID		Base path:	Sample name:	Section name	User ID	
Year	Month	Day	Time		Year	Month	Day	Time		Year	Month	Day	Time	
C:\Data\Utrecht\Bien	Bien I 0-100	Bien I 0-100	sif		C:\Data\Utrecht\Bien	Bien VI 4.3-5.30	Bien VI 4.30-5.30	sif		C:\Data\Utrecht\Bien	Bien VII 5.3-6.2	Bien VII 5.30-6.20	sif	
2012		3	6	6	2012		4	3	23	2012		1	24	23
Voltage		60 kV			Voltage		60 kV			Voltage		60 kV		
Current		42 mA			Current		40 mA			Current		40 mA		
Exposure time		200 ms			Exposure time		200 ms			Exposure time		200 ms		
line camera signal leve		117521 at 25 ms			line camera signal leve		110027 at 25 ms			line camera signal leve		105795 at 25 ms		
Step size		500 microns			Step size		1000 microns			Step size		1000 microns		
XRF	ON				XRF	ON				XRF	ON			
XRF exp. time		30 seconds			XRF exp. time		30 seconds			XRF exp. time		30 seconds		
Start coordinate		3 Stop coordinate		770	Start coordinate		1 Stop coordinate		786	Start coordinate		2 Stop coordinate		765
XRF voltage and currei		30		30	XRF voltage and currei		30		30	XRF voltage and currei		30		30
Tube	Mo				Tube	Mo				Tube	Mo			
Optical Start		0.5 Optical End		789.5	Optical Start		0.6 Optical End		805.6	Optical Start		0.5 Optical End		784.5
C:\Data\Utrecht\Bien	Bien II 0.80-1.55	Bien II 0.80-1.55	sif		C:\Data\Utrecht\Bien	Bien IV 2.4-3.4	Bien IV 2.4-3.4	sif3		C:\Data\Utrecht\Bien	Bien VIII	Bien VIII 6.2-7.2	sif	
2012		1	25	23	2012		4	12	23	2012		1	17	1
Voltage		60 kV			Voltage		60 kV			Voltage		60 kV		
Current		50 mA			Current		41 mA			Current		50 mA		
Exposure time		200 ms			Exposure time		200 ms			Exposure time		200 ms		
line camera signal leve		125256 at 25 ms			line camera signal leve		112126 at 25 ms			line camera signal leve		127963 at 25 ms		
Step size		1000 microns			Step size		1000 microns			Step size		1000 microns		
XRF	ON				XRF	ON				XRF	ON			
XRF exp. time		30 seconds			XRF exp. time		30 seconds			XRF exp. time		30 seconds		
Start coordinate		3 Stop coordinate		713	Start coordinate		1 Stop coordinate		777	Start coordinate		5 Stop coordinate		950
XRF voltage and currei		30		30	XRF voltage and currei		30		30	XRF voltage and currei		30		30
Tube	Mo				Tube	Mo				Tube	Mo			
Optical Start		0.6 Optical End		732.6	Optical Start		0.5 Optical End		796.5	Optical Start		0.5 Optical End		966.5
C:\Data\Utrecht\Bien	Bien III 155-240	Bien III 155-240	sif		C:\Data\Utrecht\Bien	Bien V3.4-4.3	Bien V 3.4-4.3	sif		C:\Data\Utrecht\Bien	Bien IX 7.2-8.2	Bien IX 7.2-8.2	sif	
2012		3	2	5	2012		1	18	16	2012		1	18	0
Voltage		60 kV			Voltage		60 kV			Voltage		60 kV		
Current		50 mA			Current		40 mA			Current		50 mA		
Exposure time		200 ms			Exposure time		200 ms			Exposure time		200 ms		
line camera signal leve		136750 at 25 ms			line camera signal leve		104902 at 25 ms			line camera signal leve		127789 at 25 ms		
Step size		500 microns			Step size		1000 microns			Step size		1000 microns		
XRF	ON				XRF	ON				XRF	ON			
XRF exp. time		30 seconds			XRF exp. time		30 seconds			XRF exp. time		30 seconds		
Start coordinate		4 Stop coordinate		730	Start coordinate		3 Stop coordinate		751	Start coordinate		3 Stop coordinate		940
XRF voltage and currei		30		30	XRF voltage and currei		30		30	XRF voltage and currei		30		30
Tube	Mo				Tube	Mo				Tube	Mo			
Optical Start		0.5 Optical End		749.5	Optical Start		0.6 Optical End		770.6	Optical Start		0.6 Optical End		959.6



Appendix D

Table with columns: Depth, SI, Al-Standardized, Ca, Ti, Mn, Fe, Rb, Sr, Zr, Pb. Contains 1000 rows of data.

Biogen III - Biogen X

Table with columns: Depth, SI, Al-Standardized, Ca, Ti, Mn, Fe, Rb, Sr, Zr, Pb. Contains 1000 rows of data.

Correlation of grain size with Zr/Rb ratio (Subcathodic cores)

Table with columns: Depth [cm], %Fine Silt, %Coarse Silt, %Very Fine, %Middle, %Coarse, %Very Coarse, Sand, and various grain size fractions (>8um, >16um, >32um, >64um).

Table for Klein Krotzenburg with columns: Depth [cm], %Fine Silt, %Coarse Silt, %Very Fine, %Middle, %Coarse, %Very Coarse, Sand, and various grain size fractions.

Table for Lauffen with columns: Depth [cm], %Fine Silt, %Coarse Silt, %Very Fine, %Middle, %Coarse, %Very Coarse, Sand, and various grain size fractions.

Table for Romerberg with columns: Depth [cm], %Fine Silt, %Coarse Silt, %Very Fine, %Middle, %Coarse, %Very Coarse, Sand, and various grain size fractions.

Table for Sindlingen with columns: Depth [cm], %Fine Silt, %Coarse Silt, %Very Fine, %Middle, %Coarse, %Very Coarse, Sand, and various grain size fractions.

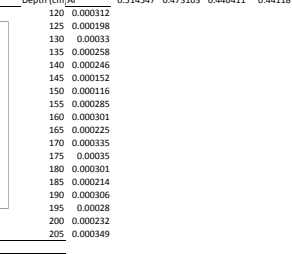
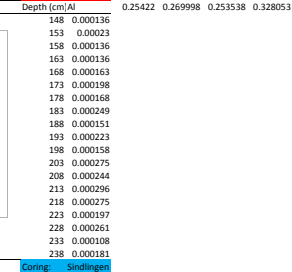
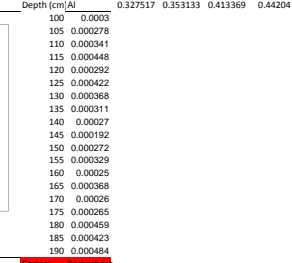
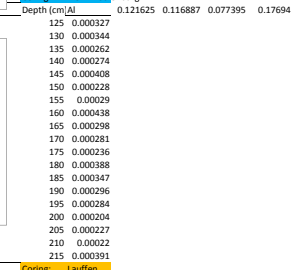
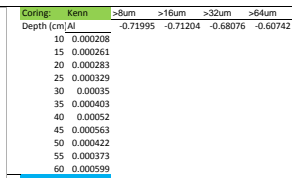


Table for Kenn with columns: Depth [cm], Al, >8um, >16um, >32um, >64um.

Table for Klein Krotzenburg with columns: Depth [cm], Al, >8um, >16um, >32um, >64um.

Table for Lauffen with columns: Depth [cm], Al, >8um, >16um, >32um, >64um.

Table for Romerberg with columns: Depth [cm], Al, >8um, >16um, >32um, >64um.

Table for Sindlingen with columns: Depth [cm], Al, >8um, >16um, >32um, >64um.

Appendix 8 B

Correlation of grain size with Zr/Rb ratio (Bienen)

Depth	Revidipth	Clay	Silt	Sand	Silt+Sand	Zr/Rb	Comments	Winkels (gebaseerd op foto's)
B7	545 531	43.03	52.03	4.95	56.98	1.47632		
	547 533.3784	48.06	47.59	4.35	51.94	1.18898		
	549 535.7568	51.14	45.17	3.69	48.86	1.15313		
	551 538.1351	49.46	46.77	3.77	50.54	1.195206		
	553 540.5135	54.84	43.61	1.55	46.15	1.1552165		
	555 542.8919	52.79	45.72	1.48	47.2	1.036847		
	557 545.2703	51.51	46.3	2.18	48.48	1.110693		
	559 547.6486	52.81	45.28	1.91	47.19	1.103164		
	561 550.027	51.85	46.35	1.8	48.15	1.109722		
	563 552.4054	50.88	47.24	1.87	49.11	1.115649		
	565 554.7838	52.96	44.82	2.22	47.04	1.121668		
	567 557.1622	46.65	50.65	2.71	53.36	1.146752		
	569 <b>559.5405</b>	34.95	57.21	7.83	<b>65.04</b>	<b>1.42952</b>		
	571 561.9189	37.85	56.16	5.99	62.15	1.318132		
	573 <b>564.2973</b>	29.43	62.1	8.48	<b>70.58</b>	<b>1.675998</b>		
	575 566.6757	42.6	54.7	2.71	57.41	1.460346		
	577 569.0541	45.23	50.66	4.11	54.77	1.236536		
	579 571.4324	48.21	49.62	2.17	51.79	1.10522	lam	
	583 573.8108	49.83	48.07	2.09	50.15	1.033475		
	583 576.1892	47.69	49.7	2.62	<b>52.32</b>	<b>1.121313</b>	zandbandje	
	585 578.5676	51.61	46.07	2.32	48.39	1.121932		
	587 580.9459	55.57	42.46	1.97	44.43	1.081368		
	589 583.3243	50.07	48.65	1.28	49.93	1.073478		
	591 585.7027	50.63	47.15	2.12	49.11	1.128898		
	593 588.0811	53.17	45.12	1.72	46.84	1.103875		
	595 590.4595	51.48	46.19	2.33	48.52	1.095042		
	597 592.8378	51.33	45.58	3.09	48.67	1.16029		
	599 595.2162	54.7	43.05	2.24	45.29	1.132616		
	601 597.5946	54.48	42.5	3.02	45.52	1.062155		
	603 599.973	49.11	47.58	3.31	<b>50.89</b>	<b>1.170151</b>		
	605 602.3514	54.03	44.14	1.82	45.96	1.100756		
	607 604.7297	51.18	46.57	2.25	48.82	1.100713		
	609 607.1081	51.85	45.43	2.72	48.15	1.153869		
	611 609.4865	54.86	44.1	1.04	45.14	1.036061		
	613 611.8649	55.41	43.09	1.51	44.6	1.039903		
	615 614.2432	52.78	45.49	1.73	47.22	1.113963		
	617 616.6216	54.5	43.22	2.28	45.5	1.070454		
	619 619	54.75	43.26	1.99	45.25	1.083737		
B8	631 621	46.06	49.59	4.35	53.94	1.432824		
	633 623.2273	50.25	46.02	3.73	49.75	1.222747		
	635 625.4545	54.39	43.27	2.34	45.61	1.14217		
	637 627.6818	54.41	43.43	2.17	45.6	1.275461		
	639 629.9091	54.07	44.21	1.72	45.93	1.148888		
	641 632.1364	53.82	44.61	1.57	46.18	1.107221		
	643 634.3636	51.32	46.91	1.77	48.68	1.058321		
	645 636.5909	50.88	46.16	2.96	49.12	1.049053		
	647 638.8182	49.59	47.47	2.94	50.41	1.07133		
	649 641.0455	45.84	50.15	3.6	54.16	1.16889		
	651 643.2727	48.64	49.2	2.16	51.36	1.211112		
	653 645.5	42.4	53.02	4.57	<b>57.58</b>	1.22814	zandbandje	
	655 647.7273	49.23	46.65	4.12	50.77	1.219428		
	657 649.9545	43.09	50.37	6.94	<b>59.99</b>	<b>1.384888</b>	zandbandje	
	659 652.1818	49.03	47.44	3.54	<b>55.91</b>	<b>1.218109</b>	zandbandje	
	661 654.4091	45.39	51.55	3.06	54.61	1.276869		
	663 656.6364	33.47	41.75	24.78	66.53	1.151337	zandband	
	665 <b>658.8636</b>	20.3	29.32	50.39	<b>79.78</b>	<b>1.246405</b>		
	667 661.0909	56.91	40.94	2.15	43.09	1.055379		
	669 663.3182	55.48	44.03	0.5	45.15	1.452224		
	671 665.5455	53.95	45.38	0.67	46.05	1.082503		
	673 667.7727	49.75	47.93	2.32	50.25	1.018846		
	675 670	46.18	52.02	1.8	53.82	1.089905	zandbandje	
	677 672.2273	44.72	50.81	4.47	55.28	1.207121		
	679 674.4545	45.51	50.18	4.31	54.49	1.279903		
	681 676.6818	46	50.32	3.68	54	1.247161		
	683 678.9091	40.17	52.24	7.59	59.83	1.26191		
	685 681.1364	39.68	55.97	4.35	60.22	1.307168		
	687 <b>683.3636</b>	36.96	46.71	16.2	<b>63.09</b>	<b>1.391572</b>	zandbandje	
	689 685.5909	56.49	41.45	2.06	43.51	1.400364		
	691 687.8182	50.17	46.94	2.89	49.83	1.002652		
	693 690.0455	47.48	50.85	1.67	52.52	1.165337		
	695 692.2727	47.17	49.8	3.04	52.84	1.054073		
	697 694.5	52.63	45.44	1.94	47.38	1.052821		
	699 696.7273	52.49	46.3	1.22	47.52	1.091862		
	701 698.9545	53.49	44.62	1.89	46.51	1.168335		
	703 701.1818	52.15	45.5	2.35	47.85	1.063624		
	705 703.4091	51.13	46.36	2.52	48.88	1.093411		
	707 705.6364	54.85	43.23	1.92	45.15	1.193906		
	709 707.8636	54.63	43.14	2.22	45.36	1.050253		
	711 710.0909	56.36	41.87	1.78	43.65	0.974071		
	713 712.3182	52.57	44.88	2.55	47.43	0.968535		
	715 714.5455	51.46	45.56	2.97	48.33	1.140937		
	717 716.7727	53.93	44.2	1.87	46.07	1.156166		
	719 719	49.69	47.26	3.04	50.3	1.173033		
B9	737 721	49.88	46.7	3.42	50.12	1.271767		
	739 723.4	49.55	46.84	3.61	50.45	1.090349		
	741 725.8	50.19	47.19	2.62	49.81	1.080732		
	743 728.2	50.22	46.44	3.34	49.78	1.055215		
	745 730.6	53.66	44.79	1.55	46.34	1.056821		
	747 733	52.12	47.1	0.78	47.88	1.058496		
	749 735.4	51.36	47.02	1.62	48.94	0.947748		
	751 737.8	56.27	41.83	1.9	43.12	0.961294		
	753 740.2	52.74	45.25	2.01	47.26	0.969979		
	755 742.6	52.98	45.79	1.22	47.01	0.964051		
	757 745	47.97	50.36	1.67	<b>52.08</b>	<b>0.958844</b>		
	759 747.4	55.16	43.03	1.81	44.81	1.022077		
	761 749.8	66.83	33.13	0.04	33.17	<b>1.046001</b>		
	763 752.2	67.1	31.9	1	32.9	0.739905		
	765 754.6	58.79	39.39	1.82	41.21	0.848911		
	767 757	56.38	41.88	1.74	43.62	0.918139		
	769 759.4	59.9	38.79	1.31	40.1	0.861406		
	771 761.8	55.28	43.49	1.23	44.72	0.908895		
	773 764.2	52.44	45.62	1.94	47.56	0.901318		
	775 766.6	55.48	43.02	1.5	44.52	0.97168		
	777 769	55.11	43.13	1.77	44.9	0.89982		
	779 771.4	41.21	54.07	4.72	<b>58.28</b>	<b>1.352218</b>	fijn zand bandje	
	781 773.8	60.98	37.53	1.49	39.02	0.863146		
	783 776.2	55.93	41.94	2.14	44.08	0.961182		
	785 778.6	52.67	44.92	2.42	47.34	0.922463		
	787 781	57.26	41.85	0.89	42.74	0.856417		
	789 783.4	59.66	40.29	0.95	40.34	1.070348		
	791 785.8	54.76	42.91	2.33	45.24	0.940608		
	793 788.2	56.53	41.94	1.53	43.47	0.923965		
	795 790.6	48.64	50.03	1.33	53.36	0.911503		
	797 793	54.75	43.49	1.76	45.25	<b>0.895628</b>		
	799 795.4	55.75	42.32	1.93	44.25	0.973973		
	801 797.8	51.55	46.56	1.89	48.45	0.93043		
	803 800.2	52.37	45.65	1.97	47.62	0.873183		
	805 802.6	60.5	38.95	0.55	39.5	0.996296		
	807 805	56.59	42.79	0.62	43.41	1.067939		
	809 807.4	49.77	48.39	1.85	50.24	1.112171		
	811 809.8	43.95	53.57	2.48	<b>56.05</b>	<b>1.314516</b>		
	813 812.2	45.8	52.05	2.16	54.21	1.141407		
	815 814.6	44.01	52.94	3.05	55.99	1.155002		
	817 817	42.47	54.08	3.45	57.99	1.24242		
B10	819 819	47.93	49.62	2.45	52.07	1.298183		
	821 821	47.37	49.01	3.62	52.63	1.276342		
	823 823							

Appendix 8  
Correlation of grain size with Zr/Rb ratio (Bienen)

Depth	Revised depth	Clay	Silt	Sand	Silt+Sand	Zr/Rb	Comments/Winkels (gebaseerd op foto's)
167	156	37.07	47.79	15.13	62.92	2.267076	naal
169	158.3056	40.71	47.42	11.87	59.29	2.276946	
171	160.6111	45.3	51.54	3.16	54.77	2.227606	
173	162.9167	44.92	49.23	5.85	55.08	1.608038	
175	165.2222	41.8	50.16	7.8	56.92	1.451448	
177	167.5278	48.87	48.69	2.44	51.13	1.318156	gelamineerd, (zand)laagjes
179	169.8333	47.6	50.64	1.76	52.4	1.327495	
181	172.1389	47.7	49.76	2.54	52.3	1.256725	
183	174.4444	47.87	50.95	1.38	52.19	1.175155	zandbandjes
185	176.75	33.47	58.22	8.31	66.37	1.132940	
187	179.0556	51.24	47.4	1.36	48.76	1.604662	
189	181.3611	44.69	52.09	3.22	55.31	1.136858	
191	183.6667	43.68	52.24	4.08	56.32	1.509341	zandbandjes
193	185.9722	47.5	50.63	1.87	52.5	1.223159	
195	188.2778	46.72	51.46	1.82	53.26	1.238907	
197	190.5833	46.57	51.27	2.16	53.43	1.365843	
199	192.8889	49.22	49.4	1.39	50.79	1.230675	
201	195.1944	40.05	53.73	6.22	59.96	1.300381	zandbandje
203	197.5	43.15	53.26	3.59	56.95	1.268982	
205	199.8056	46.52	50.57	2.91	53.48	1.329841	
207	202.1111	51.66	46.63	1.71	48.34	1.256648	
209	204.4167	50.2	47.72	2.08	49.8	1.144192	
211	206.7222	49.12	48.94	1.94	50.88	1.135542	
213	209.0278	50.67	47.84	1.69	49.3	1.181965	
215	211.3333	53.28	45.63	1.09	46.72	1.171474	
217	213.6389	51.39	46.87	1.74	48.61	1.129714	
219	215.9444	45.31	47.93	6.77	54.7	1.212326	zandbandje
221	218.25	49.38	49.44	1.38	50.62	1.319828	
223	220.5556	45.09	52.87	4.09	56.48	1.207185	
225	222.8611	52.91	46.01	1.08	47.00	1.25924	
227	225.1667	56.25	43.72	0.03	43.75	1.192314	
229	227.4722	52.39	45.51	2.1	47.61	1.14197	gelamineerd, z bandjes
231	229.7778	55.06	43.16	1.78	48.94	1.170102	
233	232.0833	50.67	42.68	1.24	43.92	1.448841	ml/fk laagje
235	234.3889	55.64	41.83	2.53	44.36	1.188961	
237	236.6944	48.28	43.41	8.31	51.72	1.199894	
239	239	42.04	42.2	15.75	57.96	1.25875	
241	241.95	42.04	53.95	42.04	65.99	1.606442	bioturbatie hele kern
243	244.2222	42.79	54.89	2.32	57.21	1.380133	
245	246.4444	39.03	57.4	3.57	60.97	1.479459	
247	248.6667	48.54	49.53	1.94	51.47	1.468896	
249	250.8889	48.36	49.38	2.25	51.63	1.589784	
251	253.1111	46.91	50.57	2.52	53.01	1.396561	
253	255.3333	46.92	50.32	2.77	53.09	1.248697	
255	257.5556	48.36	49.38	2.26	51.64	1.188192	
257	259.7778	50.79	46.1	3.11	49.21	1.147691	
259	262.0000	49.97	44	6.03	50.00	1.177483	
261	264.2222	55.17	42.78	1.64	44.4	1.263638	
263	266.4444	56.01	41.83	2.16	43.99	1.090083	
265	268.6667	54.6	42.58	2.83	45.41	1.088847	
267	270.8889	47.47	38.84	13.69	52.58	1.124359	
269	273.1111	51.17	46.47	2.36	48.83	1.129776	
271	275.3333	47.57	48.33	4.09	56.48	1.157386	
273	277.5556	51.2	46.89	1.19	48.79	1.219799	
275	279.7778	50.82	46.81	2.37	49.18	1.251441	
277	282.0000	50.78	47.16	2.06	49.22	1.252925	
279	284.2222	52.81	45.37	1.82	47.19	1.225242	
281	286.4444	50.98	46.44	2.57	49.01	1.140247	
283	288.6667	52.84	44.67	2.49	47.16	1.176808	
285	290.8889	54.25	43.68	2.07	45.75	1.128471	
287	293.1111	54.25	43.79	1.96	45.78	1.072459	
289	295.3333	55.94	42.79	1.26	44.05	1.114865	
291	297.5556	56.3	42.06	1.64	43.7	1.058657	
293	299.7778	55.69	42.48	1.82	44.3	1.163431	lichter laagje
295	302.0000	53.57	43.84	2.59	46.43	1.25563	
297	304.2222	53.78	43.09	3.13	46.22	1.196211	
299	306.4444	52.5	41.4	2.94	46.62	1.183179	schelp
301	308.6667	55.95	41.94	2.11	44.05	1.099335	zandig laagje
303	310.8889	54.99	42.53	2.47	45	1.206817	
305	313.1111	49.62	46.34	4.04	50.38	1.360539	
307	315.3333	53.30	45.72	4.3	50.02	1.259185	
309	317.5556	44.67	47.92	7.41	55.3	1.472968	
311	319.7778	43.38	49.97	6.65	56.62	1.403233	
313	322.0000	48.71	47.36	3.93	51.29	1.316693	
315	324.2222	50.74	46.06	3.2	49.26	1.209674	
317	326.4444	49.06	47.42	3.52	50.94	1.207495	
319	328.6667	52.89	45.07	2.04	47.11	1.214384	
321	330.8889	52.34	44.95	2.7	47.65	1.159693	
323	333.1111	50.56	46.02	3.41	49.43	1.135805	
325	335.3333	50.74	46.6	2.66	49.26	1.089273	
327	337.5556	49.7	46.8	3.5	50.29	1.115834	
329	339.7778	45.82	46.98	7.19	54.17	1.237924	
331	342.0000	48.99	45.87	5.14	51.01	1.264256	
333	344.2222	47.64	46.43	5.92	52.35	1.158997	
335	346.4444	45.02	49.84	5.14	54.98	1.206359	
337	348.6667	47.69	48.27	4.04	52.3	1.214395	
339	350.8889	40.71	52.31	6.98	59.28	1.343456	
341	353.1111	47.48	48.91	3.61	52.52	1.390087	
343	355.3333	52.11	46.34	1.55	47.89	1.15601	
345	357.5556	51.62	45.44	2.94	48.38	1.187209	
347	359.7778	46.72	48.12	5.17	52.95	1.202646	
349	362.0000	40.71	52.31	6.98	59.28	1.343456	
351	364.2222	47.48	48.91	3.61	52.52	1.390087	
353	366.4444	52.11	46.34	1.55	47.89	1.15601	
355	368.6667	51.62	45.44	2.94	48.38	1.187209	
357	370.8889	46.72	48.12	5.17	52.95	1.202646	
359	373.1111	40.71	52.31	6.98	59.28	1.343456	
361	375.3333	47.48	48.91	3.61	52.52	1.390087	
363	377.5556	52.11	46.34	1.55	47.89	1.15601	
365	379.7778	51.62	45.44	2.94	48.38	1.187209	
367	382.0000	46.72	48.12	5.17	52.95	1.202646	
369	384.2222	40.71	52.31	6.98	59.28	1.343456	
371	386.4444	47.48	48.91	3.61	52.52	1.390087	
373	388.6667	52.11	46.34	1.55	47.89	1.15601	
375	390.8889	51.62	45.44	2.94	48.38	1.187209	
377	393.1111	46.72	48.12	5.17	52.95	1.202646	
379	395.3333	40.71	52.31	6.98	59.28	1.343456	
381	397.5556	47.48	48.91	3.61	52.52	1.390087	
383	399.7778	52.11	46.34	1.55	47.89	1.15601	
385	402.0000	51.62	45.44	2.94	48.38	1.187209	
387	404.2222	46.72	48.12	5.17	52.95	1.202646	
389	406.4444	40.71	52.31	6.98	59.28	1.343456	
391	408.6667	47.48	48.91	3.61	52.52	1.390087	
393	410.8889	52.11	46.34	1.55	47.89	1.15601	
395	413.1111	51.62	45.44	2.94	48.38	1.187209	
397	415.3333	46.72	48.12	5.17	52.95	1.202646	
399	417.5556	40.71	52.31	6.98	59.28	1.343456	
401	419.7778	47.48	48.91	3.61	52.52	1.390087	
403	422.0000	52.11	46.34	1.55	47.89	1.15601	
405	424.2222	51.62	45.44	2.94	48.38	1.187209	
407	426.4444	46.72	48.12	5.17	52.95	1.202646	
409	428.6667	40.71	52.31	6.98	59.28	1.343456	
411	430.8889	47.48	48.91	3.61	52.52	1.390087	
413	433.1111	52.11	46.34	1.55	47.89	1.15601	
415	435.3333	51.62	45.44	2.94	48.38	1.187209	
417	437.5556	46.72	48.12	5.17	52.95	1.202646	
419	439.7778	40.71	52.31	6.98	59.28	1.343456	
421	442.0000	47.48	48.91	3.61	52.52	1.390087	
423	444.2222	52.11	46.34	1.55	47.89	1.15601	
425	446.4444	51.62	45.44	2.94	48.38	1.187209	
427	448.6667	46.72	48.12	5.17	52.95	1.202646	
429	450.8889	40.71	52.31	6.98	59.28	1.343456	
431	453.1111	47.48	48.91	3.61	52.52	1.390087	
433	455.3333	52.11	46.34	1.55	47.89	1.15601	
435	457.5556	51.62	45.44	2.94	48.38	1.187209	
437	459.7778	46.72	48.12	5.17	52.95	1.202646	
439	462.0000	40.71	52.31	6.98	59.28	1.343456	
441	464.2222	47.48	48.91	3.61	52.52	1.390087	
443	466.4444	52.11	46.34	1.55	47.89	1.15601	
445	468.6667	51.62	45.44	2.94	48.38	1.187209	
447	470.8889	46.72	48.12	5.17	52.95	1.202646	
449	473.1111	40.71	52.31	6.98	59.28	1.343456	
451	475.3333	47.48	48.91	3.61	52.52	1.390087	
453	477.5556	52.11	46.34	1.55	47.89	1.15601	
455	479.7778	51.62	45.44	2.94	48.38	1.187209	
457	482.0000	46.72	48.12	5.17	52.95	1.202646	
459	484.2222	40.71	52.31	6.98	59.28	1.343456	
461	486.4444	47.48	48.91	3.61	52.52	1.390087	
463	488.6667	52.11	46.34	1.55	47.89	1	

Appendix 7  
Flood event data

may 2014

Depth (cm) Core (#)	Flood event	Clay	Silt	Sand	Silt+Sand	Zr/Rb	
446 Bienen 6	1784	32.1	55.27	12.63	67.9	1.846883	
560 Bienen 7	1729	34.95	57.21	7.83	65.04	1.42952	
564 Bienen 7	1726	29.43	62.1	8.48	70.58	1.673995	
659 Bienen 8	1682	20.3	29.32	50.39	79.71	1.555375	<i>shifted</i>
683 Bienen 8	1671	36.96	46.71	16.32	63.03	1.400364	<i>shifted</i>

Normalized (elemental count / (Mo inc count + Mo coh count))

Depth (cm)	Flood event	Si	K	Ca	Ti	Mn	Fe	Rb	Sr	Zr	Pb	Zn
446	1784	0.003033	0.033441	0.129732	0.035742	0.022297	1.390508	0.031834	0.044756	0.058793	0.003545	0.008559
560	1729	0.007159	0.058218	0.240734	0.051701	0.042128	2.016871	0.036929	0.055031	0.052791	0.003311	0.011441
564	1726	0.008979	0.0569	0.298224	0.051381	0.047759	1.82751	0.034626	0.061358	0.057963	0.001994	0.010124
659	1682	0.004726	0.050135	0.243651	0.042107	0.049185	1.691992	0.033292	0.058041	0.051781	0.003551	0.008654
683	1671	0.004305	0.050033	0.204551	0.04408	0.057711	1.995458	0.035354	0.056074	0.049508	0.003071	0.009377

Al-Standardized (normalized count/ Al count)

Depth (cm)	Flood event	Si	K	Ca	Ti	Mn	Fe	Rb	Sr	Zr	Pb	Zn
446	1784	12.9	142.7	553.5	152.5	95.1	5932.1	135.8	190.9	250.8	15.1	36.5
560	1729	12.6	117.7	314.5	100.7	128.3	4819.8	77.2	87.1	84.5	5.7	21.0
564	1726	19.1	174.0	318.5	159.9	157.9	6868.8	118.1	121.7	133.3	11.2	35.6
659	1682	28.0	296.9	1443.0	249.4	291.3	10020.9	197.2	343.8	306.7	21.0	51.3
683	1671	23.8	276.5	1130.4	243.6	318.9	11027.5	195.4	309.9	273.6	17.0	51.8



Appendix 5C

Table with columns for Depth (m), Longitude, Latitude, and various chemical elements (C, S, Cl, K, Ca, Ti, Cr, Mn, Fe, Co, Ni, Cu, Zn, Sr, Zr, Ag, Cd, In, Sn, Pb, Cs, Ba, Tl, W, V, Ir, Au, Hg, Pt, D1, Mo, In, Mn, Co) for normalized counts. Includes a 'Total' row at the bottom.

Table with columns for Depth (m) and various chemical elements (C, S, Cl, K, Ca, Ti, Cr, Mn, Fe, Co, Ni, Cu, Zn, Sr, Zr, Ag, Cd, In, Sn, Pb, Cs, Ba, Tl, W, V, Ir, Au, Hg, Pt, D1, Mo, In, Mn, Co) for normalized counts + Al standard. Includes a 'Total' row at the bottom.

Table with columns for Sample ID, Longitude, Latitude, and various chemical elements (C, S, Cl, K, Ca, Ti, Cr, Mn, Fe, Co, Ni, Cu, Zn, Sr, Zr, Ag, Cd, In, Sn, Pb, Cs, Ba, Tl, W, V, Ir, Au, Hg, Pt, D1, Mo, In, Mn, Co) for normalized counts.

Table with columns for Depth (m) and various chemical elements (C, S, Cl, K, Ca, Ti, Cr, Mn, Fe, Co, Ni, Cu, Zn, Sr, Zr, Ag, Cd, In, Sn, Pb, Cs, Ba, Tl, W, V, Ir, Au, Hg, Pt, D1, Mo, In, Mn, Co) for normalized counts. Includes a 'Total' row at the bottom.

Table with columns for Depth (m) and various chemical elements (C, S, Cl, K, Ca, Ti, Cr, Mn, Fe, Co, Ni, Cu, Zn, Sr, Zr, Ag, Cd, In, Sn, Pb, Cs, Ba, Tl, W, V, Ir, Au, Hg, Pt, D1, Mo, In, Mn, Co) for normalized counts + Al standard. Includes a 'Total' row at the bottom.

Table with columns for Sample ID, Longitude, Latitude, and various chemical elements (C, S, Cl, K, Ca, Ti, Cr, Mn, Fe, Co, Ni, Cu, Zn, Sr, Zr, Ag, Cd, In, Sn, Pb, Cs, Ba, Tl, W, V, Ir, Au, Hg, Pt, D1, Mo, In, Mn, Co) for normalized counts.

Table with columns for Depth (m) and various chemical elements (C, S, Cl, K, Ca, Ti, Cr, Mn, Fe, Co, Ni, Cu, Zn, Sr, Zr, Ag, Cd, In, Sn, Pb, Cs, Ba, Tl, W, V, Ir, Au, Hg, Pt, D1, Mo, In, Mn, Co) for normalized counts + Al standard. Includes a 'Total' row at the bottom.

Table with columns for Sample ID, Longitude, Latitude, and various chemical elements (C, S, Cl, K, Ca, Ti, Cr, Mn, Fe, Co, Ni, Cu, Zn, Sr, Zr, Ag, Cd, In, Sn, Pb, Cs, Ba, Tl, W, V, Ir, Au, Hg, Pt, D1, Mo, In, Mn, Co) for normalized counts.

Appendix 5B

Main Core (normalized counts) table with columns for Depth (cm), SI, P, S, Cl, Ar, K, Ca, Sc, Ti, V, Cr, Mn, Fe, Co, Ni, Cu, Zn, Ga, As, Se, Br, Rb, Sb, Sr, Zr, Ag, Cd, Sn, Sb, Cs, Ba, Ta, W, Ir, Au, Hg, Pb, D1, Mo inc, Mo coh.

Coring - Steinhilber (normalized counts + Al standardized) table with columns for Depth (cm), SI, P, S, Cl, Ar, K, Ca, Sc, Ti, V, Cr, Mn, Fe, Co, Ni, Cu, Zn, Ga, As, Se, Br, Rb, Sb, Sr, Zr, Ag, Cd, Sn, Sb, Cs, Ba, Ta, W, Ir, Au, Hg, Pb, D1, Mo inc, Mo coh.

Coring - Stein Krutz (normalized counts) table with columns for Depth (cm), SI, P, S, Cl, Ar, K, Ca, Sc, Ti, V, Cr, Mn, Fe, Co, Ni, Cu, Zn, Ga, As, Se, Br, Rb, Sb, Sr, Zr, Ag, Cd, Sn, Sb, Cs, Ba, Ta, W, Ir, Au, Hg, Pb, D1, Mo inc, Mo coh.

Coring - Stein Krutz (normalized counts + Al standardized) table with columns for Depth (cm), SI, P, S, Cl, Ar, K, Ca, Sc, Ti, V, Cr, Mn, Fe, Co, Ni, Cu, Zn, Ga, As, Se, Br, Rb, Sb, Sr, Zr, Ag, Cd, Sn, Sb, Cs, Ba, Ta, W, Ir, Au, Hg, Pb, D1, Mo inc, Mo coh.

Surface Samples (ppm) table with columns for SAMPLE, Sr, Rb, Pb, Zn, Fe, Mn.



Appendix 5A

Moselle		(normalized counts)																																						
Depth (cm)	Kenn	Si	P	S	Cl	Ar	K	Ca	Sc	Ti	V	Cr	Mn	Fe	Co	Ni	Cu	Zn	Ga	As	Se	Br	Rb	Sr	Zr	Ag	Cd	Sn	Sb	Cs	Ba	Ta	W	Ir	Au	Hg	Pb	D1	Mo inc	Mo coh
10	0.000208	0.002231	0.000168	0.000905	0	0.000654	0.032573	0.014141	0	0.03412	0.001496	0.002548	0.018427	1.523494	0.015727	0.000182	0.0001408	0.047371	0.000915	0.00397	0.004433	0.002064	0.033343	0.02578	0.042039	0.000211	9.62E-05	8.37E-05	1.02E-05	0	0.000664	0.00502	0.006501	0.00135	0.004717	0.00271	0.007612	0.00096	0.782105	0.217895
15	0.000261	0.003861	0.000211	0.000998	2.55E-06	0.000954	0.046159	0.012509	0	0.045012	0.000192	0.002374	0.025942	1.829588	0.01829	0.005099	0.000796	0.039602	0.001827	0.005508	0.005084	0.001997	0.039662	0.028712	0.046954	0.00031	0.000112	7.77E-05	0	0.000699	0.005392	0.009769	0.00166	0.005053	0.003612	0.006699	0.00401	0.771014	0.228896	
20	0.000283	0.004344	0.000183	0.000868	0	0.001502	0.053366	0.012508	0	0.050316	0.002104	0.003174	0.026995	2.033477	0.018742	0.000814	0.00068	0.03332	0.00209	0.005436	0.004858	0.001677	0.042317	0.029878	0.049187	0.000534	0.000122	0.000106	0	0.000109	0.006058	0.008674	0.001315	0.00479	0.003796	0.006856	0.004736	0.76545	0.23455	
25	0.000329	0.005903	0.000182	0.000923	0	0.001801	0.063669	0.012859	0	0.054689	0.002297	0.003341	0.024867	2.043517	0.018689	0.000866	0.000742	0.02674	0.003259	0.005752	0.004914	0.000762	0.044433	0.030889	0.051496	0.000596	0.000138	8.37E-05	0	0.000111	0.005363	0.010165	0.001067	0.004974	0.004626	0.006283	0.003774	0.75738	0.24262	
30	0.00035	0.006788	0.000227	0.001021	4.25E-06	0.002295	0.072883	0.011133	0	0.062754	0.002277	0.003761	0.027571	2.322807	0.021732	0.001247	0.001111	0.024894	0.003439	0.006501	0.005289	0.000921	0.049185	0.032778	0.051151	0.000573	0.000297	8.49E-05	0	0.001582	0.005925	0.010885	0.001463	0.005765	0.004484	0.005699	0.005389	0.75436	0.24564	
35	0.000403	0.006907	0.000157	0.000942	6.47E-06	0.002355	0.076743	0.01095	0	0.067953	0.002694	0.003824	0.027768	2.679204	0.024327	0.000741	0.000495	0.019828	0.00288	0.006892	0.005548	0.000671	0.052792	0.033641	0.057059	0.000765	0.000303	8.95E-05	0	0.001732	0.006116	0.009579	0.001879	0.005434	0.006542	0.00551	0.006528	0.750221	0.249779	
40	0.00052	0.007441	0.000222	0.001023	3.81E-06	0.002006	0.082839	0.010007	0	0.073331	0.002896	0.004226	0.024944	2.864377	0.025986	0.000648	2.06E-05	0.017122	0.003039	0.008689	0.005791	0.00556	0.056179	0.0346	0.057139	0.000551	0.000247	0.000107	0	0.001832	0.006148	0.009757	0.001684	0.005334	0.004515	0.00398	0.00723	0.747988	0.252012	
45	0.000563	0.008344	0.000149	0.000931	7.74E-06	0.002046	0.089463	0.009927	0	0.080084	0.003304	0.004394	0.021967	3.131638	0.028003	0.000741	1.7E-05	0.018168	0.003187	0.0074	0.006067	0.000759	0.06004	0.03654	0.056399	0.000501	0.000241	9.75E-05	0	0.001752	0.005987	0.009591	0.002116	0.005622	0.004693	0.004659	0.007764	0.744	0.256	
50	0.000422	0.007056	0.000135	0.000881	0	0.002168	0.085943	0.009927	0	0.07761	0.003249	0.004498	0.020821	3.210773	0.03047	0.001157	0	0.016675	0.003189	0.007462	0.006024	0.000657	0.060639	0.03685	0.055398	0.000494	0.000187	3.37E-05	0	0.001676	0.006051	0.00961	0.00219	0.00567	0.004469	0.004547	0.008546	0.743751	0.256429	
55	0.000373	0.006885	0.000185	0.000858	0	0.002272	0.084629	0.009291	0	0.077188	0.002978	0.004407	0.019932	3.148108	0.028189	0.000358	3.88E-06	0.017477	0.002588	0.007992	0.000789	0.000412	0.059414	0.036469	0.053028	0.000537	0.000287	9.94E-05	0	0.001765	0.006068	0.009551	0.002877	0.00567	0.004807	0.004091	0.008605	0.745045	0.254955	
60	0.000599	0.008687	0.000247	0.001015	0	0.001976	0.094887	0.011142	0	0.08313	0.003359	0.004827	0.022467	3.746324	0.033771	0.000326	0	0.017156	0.003477	0.010135	0.006485	0.000805	0.061741	0.038363	0.054082	0.000515	0.000233	1.65E-05	0	0.001996	0.006107	0.009715	0.001894	0.005723	0.00454	0.00492	0.010466	0.73867	0.26133	

Kern		(normalized counts + Al standardized)																																						
Depth (cm)	Al	Si	P	S	Cl	Ar	K	Ca	Sc	Ti	V	Cr	Mn	Fe	Co	Ni	Cu	Zn	Ga	As	Se	Br	Rb	Sr	Zr	Ag	Cd	Sn	Sb	Cs	Ba	Ta	W	Ir	Au	Hg	Pb	D1	Mo inc	Mo coh
10	1	10.71311	0.808743	4.346995	0	3.142077	156.3825	67.89344	0	163.8115	7.18306	12.21585	88.46995	7314.363	75.5082	0.874317	6.759563	227.429	4.393443	19.06011	21.28142	9.909836	160.082	123.7705	201.8333	1.010929	0.461749	0.401639	0.04918	0	3.185792	24.10109	31.21311	6.480874	22.64481	13.01093	36.54645	14.21038	3754.918	1046.126
15	1	14.78537	0.807317	3.75122	0.009756	3.653659	176.7756	47.90732	0	172.3829	6.860976	10.36585	98.20244	7006.805	70.04634	1.529268	6.997561	137.9927	6.997561	21.09268	19.47073	7.64878	151.8951	109.9585	179.8195	1.187805	0.429268	0.297561	0	0.2678049	20.64878	29.46829	6.356098	19.35122	13.83415	26.76829	15.35854	2952.766	876.9512	
20	1	15.34732	0.645608	3.067999	0	5.305361	188.5258	44.18648	0	177.7506	7.433566	11.21445	95.36597	7183.667	66.20979	2.876457	2.403263	117.7086	3.822284	19.20513	17.16317	5.925408	149.8942	105.5011	173.7622	1.885781	0.431235	0.375291	0	3.601399	21.40093	30.64103	4.645688	16.93208	13.41026	24.21911	16.73193	2704.107	828.5944	
25	1	17.95789	0.553684	2.808421	0	5.48	193.6884	39.11789	0	166.3705	6.987368	9.861053	75.64842	6216.653	56.85474	2.635789	2.256842	81.34737	9.915789	17.49684	14.94947	2.317895	135.1726	93.96842	156.6589	1.812632	0.418047	0.254737	0	3.378947	16.31368	30.92421	3.246316	15.13263	14.07968	19.11368	11.48	2304.053	738.0821	
30	1	19.41498	0.649798	2.921053	0.012146	6.564777	208.4615	32.40688	0	179.4899	6.512146	10.75709	78.8583	684.698	62.12955	3.566802	3.178138	71.17206	9.836032	18.59514	15.12753	2.635628	140.6802	93.75304	157.7429	1.637652	0.850202	0.242915	0	4.524201	16.94534	28.84413	4.184211	16.48785	12.82389	16.2996	15.41296	2157.621	702.581	
35	1	17.12478	0.390374	2.335116	0.016043	5.83779	190.2709	27.14973	0	168.4777	6.679144	9.481283	68.8492	6642.617	60.31551	1.836007	1.228164	49.4082	7.14082	17.08734	13.75579	1.663102	130.8913	82.96078	141.4688	1.896613	0.752228	0.199643	0	4.294118	15.16399	23.75045	4.657754	13.47237	11.26203	13.66132	16.18538	1860.041	619.2834	
40	1	14.30352	0.426886	1.966276	0.007331	3.856305	159.2302	19.2346	0	140.9531	5.565982	8.123167	47.94575	5505.774	49.94868	1.244868	0.039589	32.91056	5.841642	16.70088	11.1305	1.068915	107.9839	66.50587	109.8299	1.058651	0.475073	0.205279	0	3.520528	11.81672	18.75513	3.237537	10.25367	8.678886	7.64956	13.89736	1437.748	484.4062	
45	1	14.81181	0.26511	1.652473	0.013736	3.631888	158.8104	17.62225	0	142.1621	5.865385	7.800824	38.99451	5559.152	49.71016	1.31456	0.03022	32.25137	5.657967	13.13599	10.76923	1.347527	106.587	64.86401	100.1168	0.888736	0.427198	0.173077	0	3.10989	10.62775	17.02473	3.758864	9.980769	8.333044	8.270604	13.78297	1320.718	454.4396	
50	1	16.7119	0.319703	2.085502	0	5.132829	203.3539	21.99539	0	183.816	7.695167	10.65428	49.31413	7604.615	72.16729	2.379777	0	39.49442	5.53903	17.67386	14.26766	1.555762	143.6208	87.27881	131.2082	1.171004	0.442739	0.079926	0	3.97026	14.33086	22.76208	3.185874	13.87175	10.58264	10.76052	20.24164	1761.55	606.9182	
55	1	18.46875	0.495833	2.302083	0	6.09375	227.0167	24.92202	0	207.0563	7.989833	11.82292	53.46667	8444.827	75.61667	0.960417	0.010417	46.88333	6.941667	21.4375	19.01667	1.04167	159.3792	97.82708	142.2479	1.441667	0.76875	0.266667	0	4.735417	16.27708	25.62083	7.716667	15.21042	12.89375	10.975	23.08333	1998.59	683.9188	
60	1	14.50986	0.412615	1.754271	0	3.30092	158.4875	18.60972	0	138.8502	5.611038	8.061761	37.52562	6257.38	56.40604	0.545335	0	28.6544	5.806833	16.92773	10.8318	1.344284	103.1248	64.07622	90.33114	0.86071														



Appendix 3  
Exact coring and sampling locations

Name	Date	Position	N dd	E dd	Altitude	Boring	Kernen	Losse monsters	Opmerking
1	24-10-11 1:54 PM	N49 48 24.5 E6 44 26.9	49.8068	6.74079	123 m	voor boring: zie boorstaat			
2	24-10-11 1:54 PM	N49 48 24.5 E6 44 26.9	49.8068	6.74079	124 m	zie loc. 2 boring			Zelfde als 2 Palaeo restgeul van Moezel; Geen kern genomen vanwege veel inspoelingsmateriaal (bontzandsteen) vanaf nabijgelegen helling
3	24-10-11 4:50 PM	N49 48 26.3 E6 43 55.8	49.8073	6.73217	117 m	boring	KENN1 (0-0.6 m); KENN2-3-4; KENN13	KENN 5 (1.1-1.2 m); KENN6 (1.2-1.3 m); KENN7 (1.4-1.5 m); KENN8 (1.5-1.6 m); KENN9 (1.6-1.7 m); KENN10 (1.7-1.8 m); KENN11 (1.9-2.0 m); KENN12 (2.0-2.2 m)	Palaeo restgeul van Moezel; Losse monsters KENN5 - 12 zijn genomen omdat het door de hardheid van het bodemmateriaal niet mogelijk was de brede guts meer dan ca. 10 cm de bodem in te krijgen. KENN12 en KENN13 zijn met de smalle guts bemonsterd.
4	24-10-11 5:15 PM	N49 48 45.8 E6 44 27.3	49.81272	6.7409	120 m			KENN levee 1 (0.1-0.2 m); KENN levee 2 (0.2-0.3 m)	Overafzettingen in rietveld nabij oever van Moezel; alleen opp. Monster
5	24-10-11 5:34 PM	N49 48 47.4 E6 44 11.1	49.81316	6.7364	121 m			KENN pointbar 1 (0.1-0.2 m); KENN pointbar 2 (0.2-0.3 m)	Pointbarafzettingen op iets grotere afstand van de Moezel dan loc. 4; alleen opp. Monsters
6	25-10-11 11:51 AM	N50 03 34.2 E8 57 22.6	50.05951	8.95627	109 m	boring			Palaeo restgeul van de Main; Monsternamen afgebroken op bevel van boswachter (geen vergunning om in Naturschutzgebiet te boren)
7	25-10-11 12:43 PM	N50 03 43.4 E8 57 33.9	50.06204	8.95941	104 m	boring			Palaeo restgeul van de Main; Geen kern gestoken omdat de restgeulopvulling vrijwel uit niet-klastisch materiaal bestond (veen en gyttja)
8	25-10-11 3:28 PM	N50 04 32.1 E8 57 33.6	50.07557	8.95932	103 m	boring	KK1 (1.2-2.2 m); KK1 (2.2-3.2 m)		Palaeo restgeul van de Main bij Klein Krotzenburg;
9	25-10-11 3:56 PM	N50 04 41.3 E8 58 33.3	50.07813	8.97593	99 m			KK2 (0.1-0.2 m); KK2 (0.2-0.3 m)	Overafzetting van de Main bij Klein Krotzenburg; ca 30 m vanaf oever
10	26-10-11 11:43 AM	N49 03 45.0 E9 09 10.5	49.06251	9.15291	161 m	boring	Lauffen I (1.0-1.9 m)		Palaeo restgeul (Holocene) van de Neckar
11	26-10-11 1:57 PM	N49 05 44.4 E9 09 27.8	49.09566	9.15772	163 m			Neckar floodplain hoog (0.1-0.2 m) (0.2-0.3 m)	hooggelegen recente overbank/floodplain afzettingen langs de Neckar nabij Horkheim
12	26-10-11 2:05 PM	N49 05 43.4 E9 09 36.4	49.09538	9.16011	160 m			Neckar floodplain laag (0.1-0.2 m) (0.2-0.3 m)	laaggelegen recente overbank/floodplain afzettingen (geul langs de Neckar nabij Horkheim; in de Geul grondwaterputten (t.b.v. oeverinfiltratie?))
13	26-10-11 4:53 PM	N49 28 15.4 E8 35 54.7	49.47095	8.59852	93 m			Edingen (0.1-0.2 m) (0.2-0.3 m)	overbank afzettingen ca. 15 m vanaf oever Neckar bij Neckarhausen (naam Edingen zou eigenlijk Neckarhausen moeten zijn)
14	26-10-11 5:31 PM	N49 28 36.7 E8 32 45.0	49.47685	8.54582	90 m			Mannheim (0.1-0.2 m) (0.2-0.3 m)	floodplainafzetting van de Neckar bij Mannheim. Floodplain is hooggelegen (ca.4-5 m) boven waterniveau van Neckar/ rivier ligt diep t.o.v. floodplain
15	27-10-11 10:55 AM	N49 15 49.0 E8 23 12.2	49.2636	8.38674	90 m	boring	Römerberg1 (1.4-2.4 m) (2.4-3.1 m)		Palaeo restgeul van Oberrhein bij Mechttersheim/Römerberg
16	27-10-11 12:24 PM	N49 15 29.1 E8 25 33.5	49.2581	8.42596	98 m			Römerberg2 (0.1-0.2 m) (0.2-0.3 m)	recente floodplainafzetting langs de Oberrhein; relatief hooggelegen en zandig/zavelig sediment
17	27-10-11 12:28 PM	N49 15 29.3 E8 25 35.3	49.25814	8.42648	97 m			Römerberg3 (0.1-0.2 m) (0.2-0.3 m)	recente floodplainafzetting langs de Oberrhein; relatief laaggelegen en kleilig sediment uit moerasbosje langs waterkant
18	27-10-11 3:04 PM	N50 03 45.0 E8 31 11.6	50.06251	8.5199	85 m	boring	Sindlingen (1.2-1.8)	Sindlingen1 (0.1-0.2 m) (0.2-0.3 m)	Oude geul langs huidige loop Main op ca. 70 m van oever. Op ca. 80 cm -mv humeus materiaal ruikt olie-achtig (zie boorstaat). Op ca. 1 m -mv grindlaag (gestort of fluviaal afgezet?)
19	28-10-11 9:28 AM	N49 42 11.2 E8 21 58.6	49.70311	8.36628	85 m			Rheindürkheim1 (0.1-0.2 m) (0.2-0.3 m)	laagte op floodplain tussen levee en kade/terrasrand
20	28-10-11 9:32 AM	N49 42 12.3 E8 22 04.1	49.70342	8.3678	86 m			Rheindürkheim2 (0.1-0.2 m) (0.2-0.3 m)	levee
21	28-10-11 10:57 AM	N49 59 48.0 E8 01 46.6	49.99667	8.02961	75 m			Ingelheim1 (0.1-0.2 m) (0.2-0.3 m)	net over levee
22	28-10-11 11:05 AM	N49 59 39.5 E8 01 31.2	49.99429	8.02532	76 m			Ingelheim2 (0.1-0.2 m) (0.2-0.3 m)	zandiger sediment da Ingelheim1
23	28-10-11 12:35 PM	N50 16 47.6 E7 27 34.4	50.2799	7.45955	64 m			Alken1 (0.1-0.2 m) (0.2-0.3 m)	Smalle strook floodplain langs Moezel
24	28-10-11 12:40 PM	N50 16 57.2 E7 27 29.3	50.28256	7.45814	63 m			Alken2 (0.1-0.2 m) (0.2-0.3 m)	Smalle strook floodplain langs Moezel
25	28-10-11 12:43 PM	N50 16 58.0 E7 27 28.6	50.28279	7.45796	63 m			Alken3 (0.1-0.2 m) (0.2-0.3 m)	Smalle strook floodplain langs Moezel; op ca 10 m van oever; maaveld ca. 3 m dan waterpeil Moezel
26	28-10-11 1:35 PM	N50 26 18.6 E7 26 23.1	50.4385	7.43974	56 m			Andernach1 (0.1-0.2 m) (0.2-0.3 m)	Locatie aan het einde van smalle floodplain langs Rijn
27	28-10-11 1:41 PM	N50 26 10.4 E7 26 31.6	50.43623	7.44211	55 m			Andernach2 (0.1-0.2 m) (0.2-0.3 m)	Laagte (ca. 20 cm lager dan omgeving) midden in smalle strook floodplain
28	28-10-11 4:10 PM	N50 46 10.6 E7 03 52.8	50.76962	7.06468	43 m			Bonn1 (0.1-0.2 m) (0.2-0.3 m)	Levee ca. 5 m boven waterpeil Rijn
29	28-10-11 4:14 PM	N50 46 09.2 E7 03 46.7	50.76923	7.06297	44 m			Bonn2 (0.1-0.2 m) (0.2-0.3 m)	Hoger gelegen distaler deel van floodplain halfweg tussen oever en dijk. Op 0.2-0.3 m duidelijk zandiger sediment dan toplaat.

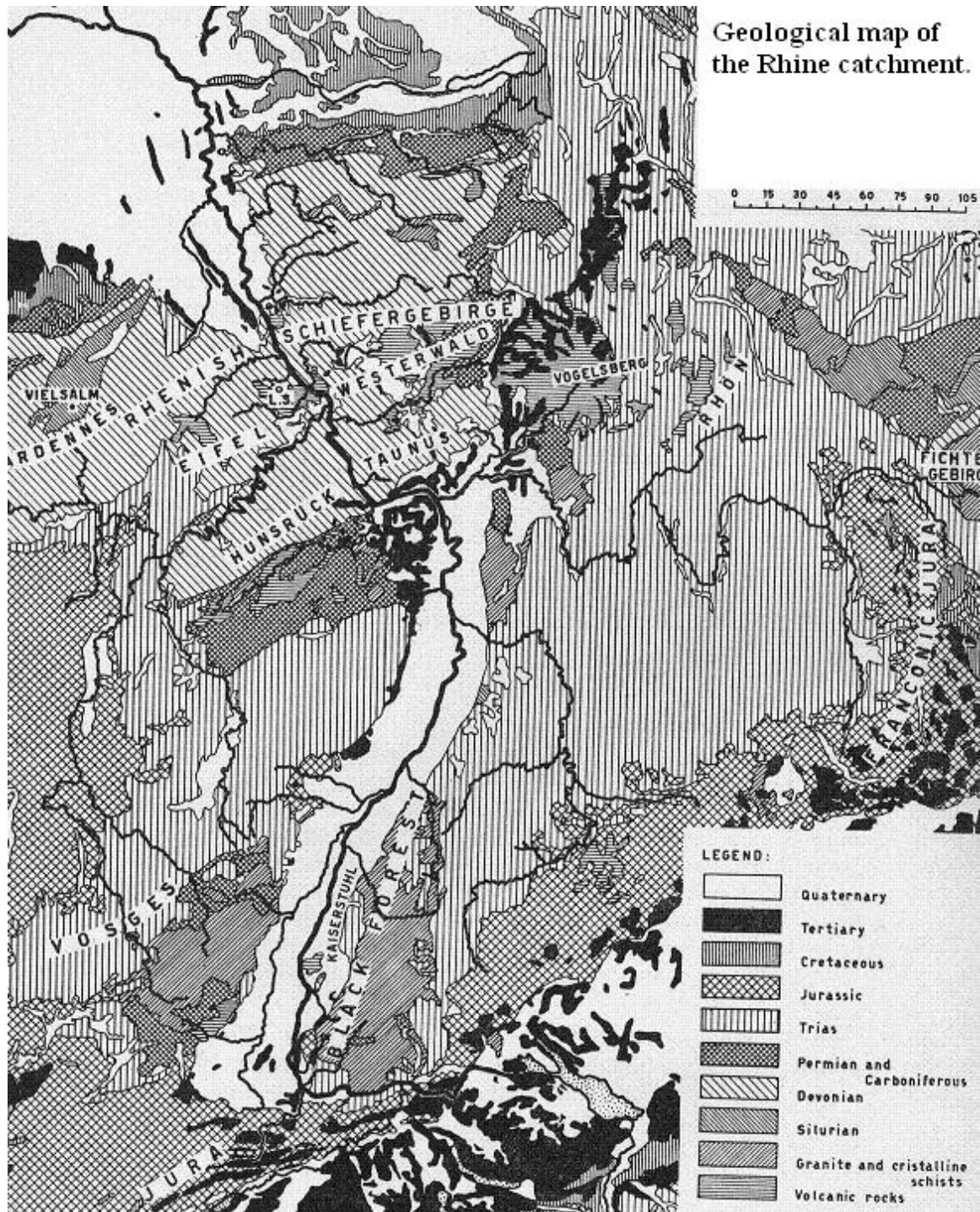
Appendix 2

Table 5: Normalized counts of selected elements (with plots)

Table with columns: Biennium X, Biennium X Depth, Biennium X Real Depth, Biennium Y, Biennium Y Depth, Biennium Y Real Depth, and 16 numerical columns for elements K, Ca, Ti, Mn, Fe, Rb, Zr, Pb, Zn, Al, Si, K, Ca, Ti, Mn, Fe, Rb, Zr, Pb, Zn, Al. The table contains a grid of data points for various elements across different bienniums and depths.

## Appendix 12 Geological map of the Rhine catchment

Geological map of the Rhine catchment. After Van Andel, 1950



### Appendix 13 Distributive regions of the Rhine catchment

Map of the distributive regions of mineral assemblages of the Rhine catchment. After Van Andel, 1950

